NATURE AND CHARACTERISTICS OF FRACTURE SYSTEM WITHIN WAJID SANDSTONE GROUP, SW SAUDI ARABIA

BY

MOHAMMED HASAN BARRAN BENAAFI

A Dissertation Presented to the

DEANSHIP OF GRADUATE STUDIES

KING FAHD UNIVERSITY OF PETROLEUM & MINERALS

DHAHRAN, SAUDI ARABIA

In Partial Fulfillment of the
Requirements for the Degree of

DOCTOR OF PHILOSOPHY

In

GEOLOGY

April 2017

KING FAHD UNIVERSITY OF PETROLEUM & MINERALS

DHAHRAN- 31261, SAUDI ARABIA

DEANSHIP OF GRADUATE STUDIES

This thesis, written by **MOHAMMED HASAN BARRAN BENAAFI** under the direction his thesis advisor and approved by his thesis committee, has been presented and accepted by the Dean of Graduate Studies, in partial fulfillment of the requirements for the degree of **DOCTOR OF PHILOSOPHY IN GEOLOGY.**

Dr. Mustafa Hariri
(Advisor)

Dr. Abdulaziz Al-Shaibani
Department Chairman

Dr. Osman Abdullatif
(Co-Advisor)

Dr. Salam A. Zummo
Dean of Graduate Studies

Dr. Mohammed Makkawi
(Member)

6/6/17
Date

Dr. Abdulaziz Al-Shaibani
(Member)

Prof. Giovanni Bertotti
(Member)

Mohammed Hasan Barran Benaafi

2017

Dedicated to

My Father (May Allah be merciful to him)

My Mother

My wife

And

My Sons (Hasan and Salah) and my Daughter (Asma)

ACKNOWLEDGMENTS

Great appreciations are due to my thesis advisor Dr. Mustafa Hariri for his enormous contributions to the success of this dissertation. The guidance and assistance received from him during the data collection, laboratory and final production of this dissertation are indeed appreciated. Great thanks also due to my co-advisor Dr. Osman Abdullatif for his help and guidance during all stage of this dissertation. The contributions from other members of my dissertation committee, Dr. Mohammed Makkawi, Dr. Abdulaziz Al-Shaibani, Prof.Giovanni Bertotti (External member from Delft University) are also thankfully acknowledged. I wish to express my deep appreciation to Dr. Abdulaziz Al-Shaibani (departmental chairman) who facilitated all the administrative needs in the course of my studentship. All my course instructors, other faculty members and all staff of geosciences department include Ahmed Al-Bahrani, Elias Arif, Adnan Al-Mubarak, Mohammed Al-Otaibi and Ahmed Al-Saif are thanked for their individual and collective assistance. I wish to express my deep appreciation to research institute(RI) and civil engineering department for assisting me with the XRD and SEM analyses, and UCS analysis, respectively. Great thanks for the petroleum engineering department and for Mr. Ahmed Moosa for assisting me with the porosity and permeability measurements. Mr. Azizulla Khan is thanked for helping me in the preparation of the thin section slides. Mr. Mushabbab Q. Yahya and Mr. Shahul Hameed are thankfully acknowledged for assisting me with laboratory analyses and other facilities. Great thanks are due to King Abdul Aziz City for Science and Technology (KACST) for providing me with satellite images.

I appreciate and thank the university authorities (KFUPM) for granting me the Ph.D studentship. The financial assistance from the Deanship of Research (KFUPM)(Project#FT141013) is gratefully acknowledged. All my family members are thanked for their moral support and endurance during the period of this study. Great thanks also due to Mr. Abdullah Alqubalee, Mr. Ammar Abdlmutalib, and Mr. Jarrah Mohammed for field work help. Great thanks for Mr. Mohammed Maghwer for his assistance and support during the period of my PhD program. Great thanks due to Turky Ben-Shejaa for his help during field work. Above all, my greatest gratitude is due to Allah for granting me the patience and knowledge to successfully pass this Ph.D. stage.

Table of Content

List of tables

List of Figures

ABSTRACT

Full Name : Mohammed Hasan Barran Benaafi

Thesis Title : Nature and Characteristics of Fracture System within Wajid Sandstone Group, SW Saudi Arabia

Major Field : Geology

Date of Degree : April 30, 2017

The Wajid Group is a Cambro-Permian sedimentary succession(sandstone) in southwest Saudi Arabia. It forms a groundwater aquifer in the Wadi Al-Dawasir and Najran Areas (Wajid Graben), and it is a potential hydrocarbon reservoir in the Rub' Al-Khali Basin. It exposed in an area extending from Wadi Al-Dawasir southward to Najran city, with isolated outcrops in Abha area. This dissertation aims to map and characterize the regional and outcrop-scale fracture system within the Wajid Group outcrops and to define its possible tectonic origin. A further objective is to characterize the fracture-hosting sandstone properties (included sedimentological, stratigraphical, and petrophysical) to define the main factors controlling the geomechanical and fracture characteristics (e.g. fracture spacing) of the studied sandstone. The fracture system within Wajid Group was investigated in multi-scale approach. The regional-scale fractures (lineaments) were obtained using multi-resolution satellite images (Landsat, Spot, and STRM(DEM)). At the outcrop scale, the fracture characteristics include orientation, type, infilling materials, spacing, height, termination, and cross-cutting relationships were directly characterized from the outcrops. The northerly (N-S, NNW-SSE, and NNE-SSW), easterly (E-W, ENE-WSW, and ESE-WNW), NW-SE, and NE-SW trending lineaments are observed within Wajid Group. The eastern Outcrops are dominated by northerly (N-S, NNW-SSE,

and NNE-SSW) and NW-SE trending lineament; however, the western outcrops are dominated by NE-SW trending lineaments. At the outcrop scale, three main fracture sets were identified as predominant include NNW-SSE, NNE-SSW, and ENE-WSW; however, the NW-SE and NE-SW were also observed. The lineaments and fractures within Wajid Group are much possible inherited from the Precambrian basement structures. The fractures within Wajid Group outcrops are mainly vertical to sub-vertical, Mode 1 type of fracture (joints). They are open fractures; however, in some outcrops, they are infilled either by calcite or iron oxide. Fracture swarms were also observed in the studied outcrops, and they oriented NNE-SSW.

Four main geological factors control the fracture distribution (average fracture spacing) within Wajid Group include bed thickness, diagenetic features (cementation and dissolution), lithofacies type, and matrix porosity. Besides, the geomechanical characteristics of Wajid Group are mainly controlled by sandstone texture, cement content and type, matrix porosity, and matrix permeability. Hierarchal fracture conceptual models were established to define fracture distribution within Wajid Group sandstone and its lithological and stratigraphic controls. The outcomes of this dissertation provide insight into the tectonic origin of the Wajid Group fracture system, and understanding of the fracture distribution which can help to enhance the groundwater production from fractured aquifers in Wajid Graben and gas production from the hydrocarbon reservoirs in Rub' Al-Khali Basin.

الاسم الكامل: محمد حسن بران بن عفي

عنوان الرسالة: طبيعة وخصائص نظام صدوع مجموعة احجار رمل الوجيد، جنوب غرب المملكة العربية السعودية

التخصص: جيولوجيا

تاريخ الدرجة العلمية: ابريل 2017

ملخص الرسالة

مجموعة الوجيد في جنوب غرب المملكة العربية السعودية عبارة عن تتابع طبقي من احجار الرمل التي ترسبت من العصر الكامبري الى البيرمي. هي عبارة عن خزانات للمياة الجوفية في منطقتي وادي الدواسر ونجران(حوض الوجيد), وهي ايضاً تعتبر خزانات للنفط في حوض الربع الخالي. تنكشف احجار رمل مجموعة الوجيد في منطقة تمتد من وادي الدواسر جنوبا الى نجران مع وجود بعض المنكشفات الصغيرة في منطقة ابها. هذه الاطروحة تهدف الى تخريط ووصف نظام الصدوع الاقليمية لمجموعة الوجيد لتحديد اصلها التكويني. ايضا تهدف هذه الاطروحة الى وصف الخصائص الرسوبية والطباقية لاحجار رمل مجموعة الوجيد لتحديد العوامل الرئيسية التي تتحكم في الخصائص الجيوميكانيكية و خصائص نظام الصدوع في مجموعة الوجيد. وقد تم دراسة نظام الصدوع لمجموعة الوجيد باستخدام منهج متعدد المستويات. نظام الصدوع الاقليمي تم دراستة باستخدام صور اقمار صناعية بدقة متنوعه(لاندسات و سبوت). على مستوى المنكشفات الصخرية فان خصائص نظام الصدوع (الاتجاة, النوع, المادة الاحمة, المسافة بين الصدوع, الطول, نوع النهائة, وعلاقة التقاطع) تم وصفها مباشرة من المنكشف الصخري.

لقد تم ملاحظة وجود الصدوع الاقليمية ذات الاتجاة الشمالي والشرقي والشمالي غربي والشمالي الشرقي في مجموعة الوجيد. المنكشفات الصخرية الشرقية من مجموعة الوجيد تتميز بوجود الصدوع الاقليمية ذات الاتجاة الشمالي والشمالي الغربي ; غير ان المنكشفات الصخرية الغربية من مجموعة الوجيد تتميز بوجود الصدوع الاقليمية ذات الاتجاة الشمالي الشرقي.على مستوى المنكشف الصخري هناك ثلاثة اتجاهات رئيسية للصدوع وهي الشمالية شمالية شرقية و الشمالية شمالية غربية والشرقية شمالية شرقية, ومع ذلك فان الصدوع الشمالية غربية والشمالية شرقية تم ملاحظتها في المنكشف الصخري باعداد قليلة. الصدوع الموجودة في مجموعة الوجيد من المحتمل انها موروثة من البنيات الجيولوجية التركيبة لصخور ما قبل الكامبري في الدرع العربي. صدوع مجموعة الوجيد هي صدوع راسية وهي Mode 1 من انواع الصدوع. هذه الصدوع هي مفتوحة ولاكن في بعض المنكشفات الصخرية تبين انها مملؤة او مغلفة باكاسيد الحديد او معدن الكالسيت. كذلك تمت ملاحظة وجود اسراب من الصدوع ذات الاتجاة الشمالي شمالي شرقي في منطقة الدراسة.

أربعه عوامل جيولوجية رئيسية تتحكم في توزيع النظام صدوع مجموعة الوجيد وهي سماكة الطبقة الصخرية, خصائص النشاة المابعدية للصخور, نوع السحنات الصخرية و مسامية الصخور. بالاضافة الى ذلك فان الخصائص الجيوميكانيكة لصخور مجموعة الوجيد تعتمد بشكل اساسي على النسيج الصخري لاحجار الرمل و نوعية وكمية

المادة الاحمة ومسامية ونفاذية الحجر الرملي. قد تم بناء نموذج بنائي هرمي لاظهار انتشار الصدوع في مجموعة الوجيد وعلاقتها بالخصائص الرسوبية والطباقية.

نتائج هذه الاطروحة تقدم نظرة تفصيلية للتكوين التكتوني لنظام صدوع مجموعة الوجيد وتعطي فهم لتوزيع هذه الصدوع بمايساعد على تحسين الانتاج من المياة الجوفية من صخور مجموعة الوجيد في حوض الوجيد وكذلك تحسين استخراج النفط من تلك الصخور في حوض الربع الخالي.

Chapter 1

Introduction

1.1 Introduction

Great amount of Hydrocarbon reserves of the world hold in fractured reservoirs(Nelson, 2001). Fracture network has a major impact on the hydrocarbon exploration and production. Understanding of natural fractures system in such reservoirs is, therefore, necessary for increasing hydrocarbon exploration and production. Hydrocarbon production from tight sandstone reservoirs relies on induced hydraulic fractures. Understanding of the geometry and distribution of the natural fractures system is essential to get an effective treatment design of induced hydraulic fractures.

The natural fractures system in the reservoirs usually detected from core or borehole images (borehole images such as FMI). However, the ability to construct the fractures system from the core and the borehole images is very limited as it does not reveal the abundance of different fracture sets, the spacing between fractures, the fracture length and the vertical persistence of fracture pattern across the sedimentary layers. Thus, study fracture system from outcrop analog can be used to understand fractures distribution in three dimensional over the area of the interest. The outcrop analogs are widely used to study the fracture system of the fractured sandstone reservoirs(Olson et al., 2009; Nelson, 2001; Odling et al., 1999; Strijker et al., 2012; Bertotti et al. 2007; Sonntag et al. 2012; Hennings et al., 2000; Laubach and Ward 2006). Besides the economic importance of the fracture system, the analysis of the natural fracture system provides insight into the structural geology and tectonic history of the study area. Understanding the relationship between fracture geometry characteristics and host rock properties help to understand the

fracture pattern in the sedimentary rocks which were deposited in different depositional environments.

In this study, the fracture system of the Wajid Group sandstone was studied in regional and outcrops scale. Wajid Group is a Paleozoic sandstone succession in the southwestern part of Saudi Arabia. This group is a well-known groundwater aquifer in the Wadi Al-Dawasir and Najran Areas(Wajid Basin) (Al Alawi and Abdulrazzak 1994; Edgell 1997; GTZ/DCo 2009), and it represents siliciclastic hydrocarbon reservoirs in the Rub' Al-Khali Basin in Saudi Arabia, Oman, UAE, and Yemen (Alsharhan et al., 1991; Evans et al. 1991; Konert et al., 2001; Pollastro 2003; Lange 2006; Bu-khamseen et al. 2010)

Although Wajid Group has a significant economic importance and its outcrops are extending to the subsurface of Rub' Al-Khali basin, there is no detailed earlier study conducted on the natural fractures systems of Wajid Group in the outcrops. Accordingly, this dissertation investigated the fracture system characteristics of the Wajid Group sandstone outcrop in the southwestern part of Saudi Arabia as analog of the groundwater aquifers and hydrocarbon reservoirs in the Wajid and the Rub' Al-Khali Basins.

The principal objective of this dissertation is to characterize the fracture systems of Wajid Group outcrop in multi-scale approach, and understanding the controls on the fracture geometry characteristics and distribution

1.2 Problem Statement

Wajid Group is a groundwater aquifer and potential hydrocarbon reservoir in Rub' Al-Khali Basin. Its fracture system has an impact on the fluid flow behavior in the subsurface in Rub' Al-Khali Basin (Zeeb et al. 2010; Bu-khamseen et al. 2010), and its

outcrops display fracture system which can be observed from satellite images and outcrop scale. Despite the aforementioned importance of Wajid Group, there is no detailed study conducted on the fracture system of Wajid Group. Therefore, characterization of the natural fracture system within Wajid Group in multiscale will help to understand its impact on the fluid flow in the aquifer and reservoir in Rub' Al-Khali Basin. Moreover, understanding the natural fracture distribution within Wajid Group will help and improve the treatment design of induced hydraulic fractures in tight sandstone reservoir of the Rub' Al-Khali Basin.

1.3 Study Objectives

The main objective of this study is to provide detail characterization of the fracture system of the Wajid Group and define the possible origin in the light of tectonic framework. In addition to, this study provides a geomechanical, sedimentological, and petrophysical characterization of fracture-host rock to define main controls on the fracture distribution. Finally, to create a conceptual fracture model that define the fracture system and its relationship with host rock properties.

1.4 Area of Study

This study focuses on the Cambrian to Permian Wajid Group sandstone outcrops in the southwest part of Saudi Arabia. The area extends from Wadi Al-Dawasir to Najran city and includes several isolated outcrops in Abha area (**Figure** 1.1). Wajid Group outcrops in the study area bounded on the east by large sand dunes of Rub' Al-Khali desert and from the west by the Proterozoic basement rocks (Arabian Shield)(Figure 1.2). The characteristics of the outcrop-scale fractures and the fracture-hosting sandstone properties

were studied in details in Wadi Al-Dawasir area, where, the whole succession of Wajid Group exposed (Figure 1.2B).

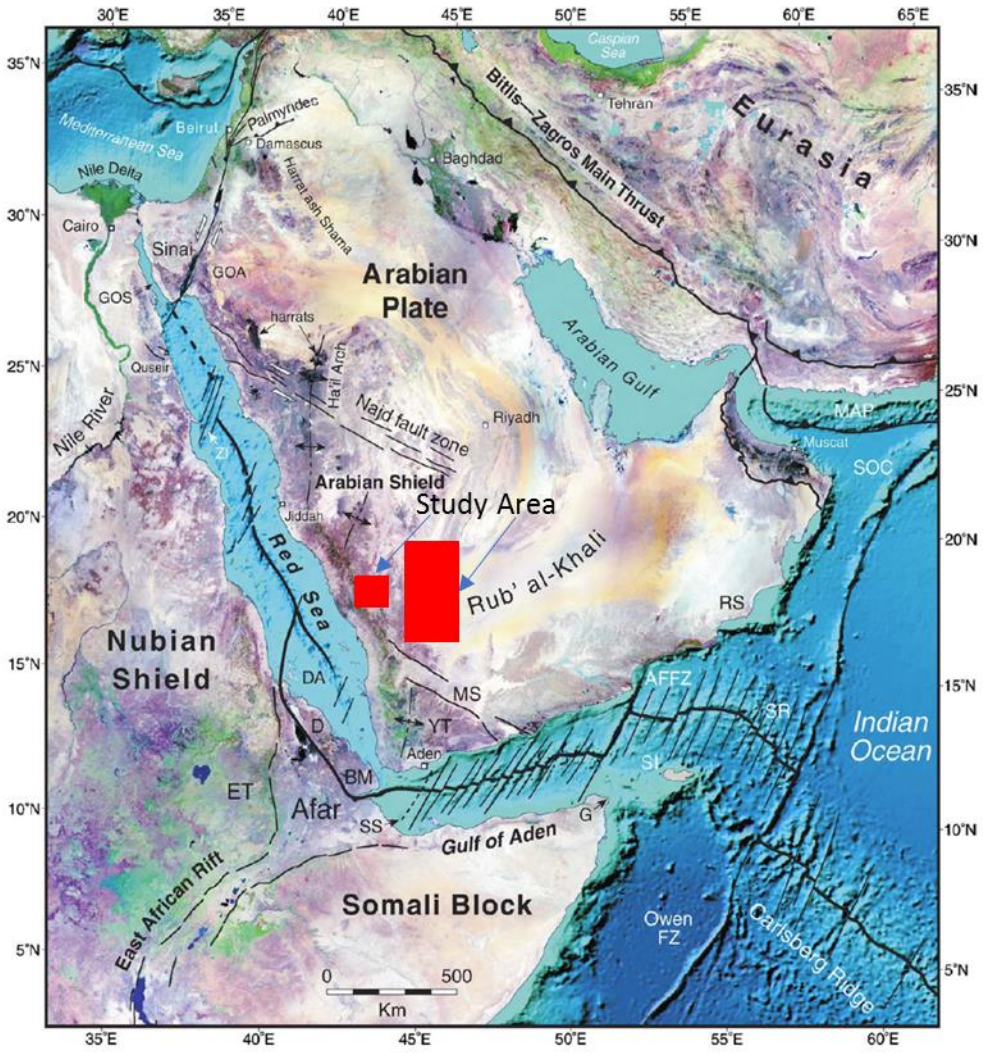

Figure 1.1: Location of Wajid Group outcrops (after Bosworth et al., 2005).

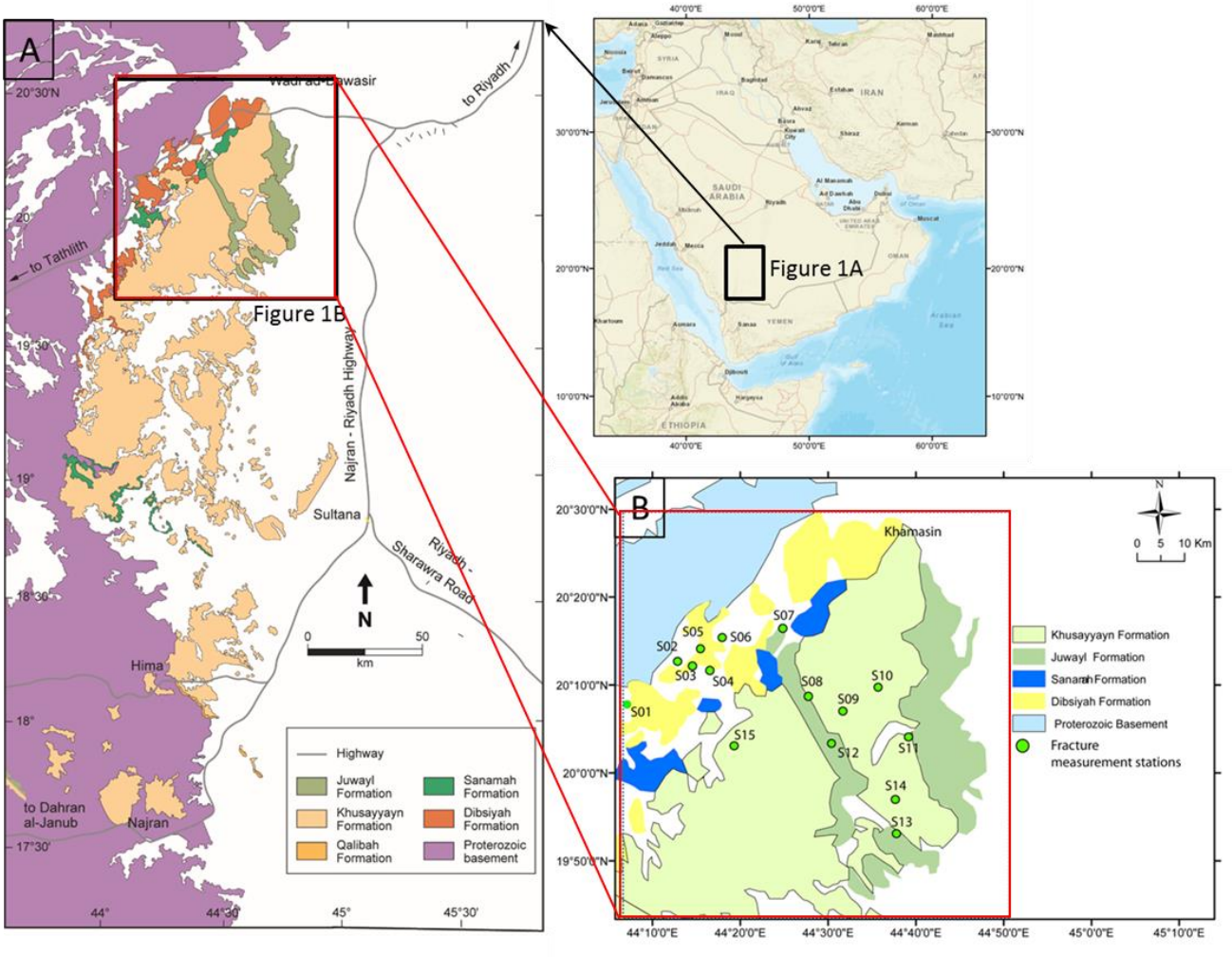

Figure 1.2: (A) Geological map of the Wajid Group sandstone in the southwestern part of Saudi Arabia, and (B) geological map Wadi Al-Dawasir area with locations of fracture measurement stations (S01-S15) (modified from Kellogg et al., 1986 and Al-Husseini, 2004; Knox et al., 2007).

1.5 Methodology

1.5.1 Introduction

The fracture system within Wajid Group was studied in a multiscale approach from satellite images to direct outcrop investigation. Moreover, laboratory analyses were conducted to measure the host rock properties included petrographic, petrophysical and geomechanical to define their controls on fracture distribution (Figure 1.3).

1.5.2 Remote Sensing (Satellite) Analysis

Landsat-8 OLI/TIRS satellite images of eleven multispectral bands with 30-m resolution, Spot-5 satellite images of four bands with 2.5-m resolution, and SRTM Digital Elevation Model (DEM) with 30-m resolution were used to delineate lineament traces of the Wajid Group. Additionally, the aeromagnetic lineament traces within the studied outcrop were detected from the reduced to pole magnetic anomaly map. The satellite images were provided by King Abdulaziz City for Science and Technology (KACST). The shortwave infrared-2 band of the Landsat-8 satellite images was used in band combination at all channels (i.e., red, green, and blue) to detect lineament traces, whereas a 4/3/2 band combination of the Spot-5 images was employed for lineament detection. Following the band combination, the satellite images were composited, enhanced, and filtered using Erdas Imagine 2014 and ArcMap 10.2.1 software. Two types of enhancement were used to detect lineaments, including radiometric and spatial enhancements. The percentage LUT stretch type with cubic convolution re-sampling technique was used to enhance the images. Edge enhancement and low pass filtering were also used to enhance the images for lineament detection. Lineament traces were digitized and interpreted from the

enhanced images using Arc Map 10.2.1 software (ArcGIS). The Shaded reliefs of SRTM DEM were generated to achieve better detection of lineaments. The orientations of the lineament traces extracted from the digitized lineament trace maps were statistically analyzed to define the major lineament trends and their possible stress regime

1.5.3 Field Investigation

Field studies included two folds; outcrops fractures characterization, and sedimentological and stratigraphic descriptions.

1.5.3.1 Fracture characterization

The characteristics of the natural fractures included orientation, type, infilling materials, cross-cutting relationships were defined in 15 outcrop stations in Wadi Al-Dawasir area. In this area all formations of Wajid Group are present, and the outcrops located on the western flank of Rub' Al-Khali Basin (Figure 1.2). Four stations were in Dibsiyah Formation, three in Sanamah Formation, five in Khusayyayn Formation (one only with fracture swarms, station S14), and three in Juwayl Formation. The average fracture spacing, height, and termination were quantified in five outcrop stations (included S01, S03, S04, S10, and S13 in Figure 1.2) using the scanline method.

1.5.3.2 Sedimentological and stratigraphic Study

Sedimentological and stratigraphic properties (included lithofacies type, lithology, texture, sedimentary structure, and bed thickness) of the fracture-hosting sandstone were described and measured in five outcrop stations (included S01, S03, S04, S10, and S13 in Figure 1.2)(the same outcrop stations where the fracture spacing was measured) to define their controls on the fractures spacing and distribution. Vertical sedimentological log was

established for each outcrop station, and 82 representative sandstone samples were collected for the petrographic, petrophysical, and geomechanical laboratory analyses to correlate the rock properties with fractures properties.

1.5.4 Laboratory Analyses

Three types of laboratory analyses were conducted for the collected sandstone samples; petrographic, petrophysical, and geomechanical to define the relationship between fracture characteristics and host rock properties.

1.5.4.1 Petrographic analysis

Thin sections were prepared for the all collected sandstone samples from Wajid Group outcrops to define their texture, mineral composition, and diagenesis features. 20 sandstone samples were selected for X-Ray Diffractometer(XRD) analysis to define their mineral composition in a semi-quantitative way. 10 sandstone samples were selected for Scanning Electron microscopy analysis (SEM-EDX) to identify the cement and clay type of the studied sandstone.

1.5.4.2 Petrophysical analysis

Petrophysical properties included matrix porosity, grain density, and matrix permeability were measured for 63 sandstone samples from Wajid Group outcrops to define their control on the sandstone geomechanical behavior and fractures distribution. Cylindrical core plug (1.5 cc diameter, 5cm length) prepared for the petrophysical properties analyses. Helium-porosimeter device was used to measuring gas porosity and grain density of the sandstone samples. Mini-permeameter device was used to measure the gas permeability. In addition, grain size analysis was carried out on 79 sandstone samples

using the sieve analysis machine to measure the mean grain size and sorting parameters and define their controls on fracture spacing.

1.5.4.3 Geomechanical analysis

Geomechanical measurements were conducted in both field and laboratory to obtained the geomechanical properties (included Schmidt Reading Numbers(RN), Static Young's Modulus(E), and unconfined compressive strength(UCS)) of the Wajid Group sandstones. In the field, the rock strength (Schmidt Reading Numbers(RN)) measurements were conducted using the portable Schmidt hammer device. The static Young's modulus(E), and unconfined compressive strength(UCS) were measured for 82 sandstone samples in the laboratory using uniaxial compression test equipment. This test conducted on cubic rock samples with dimension (5.2 cm length, 3.4 cm width, and 3.4 cm height). The uniaxial compression test was conducted to define the strength and elasticity properties (brittleness) of the studied sandstone.

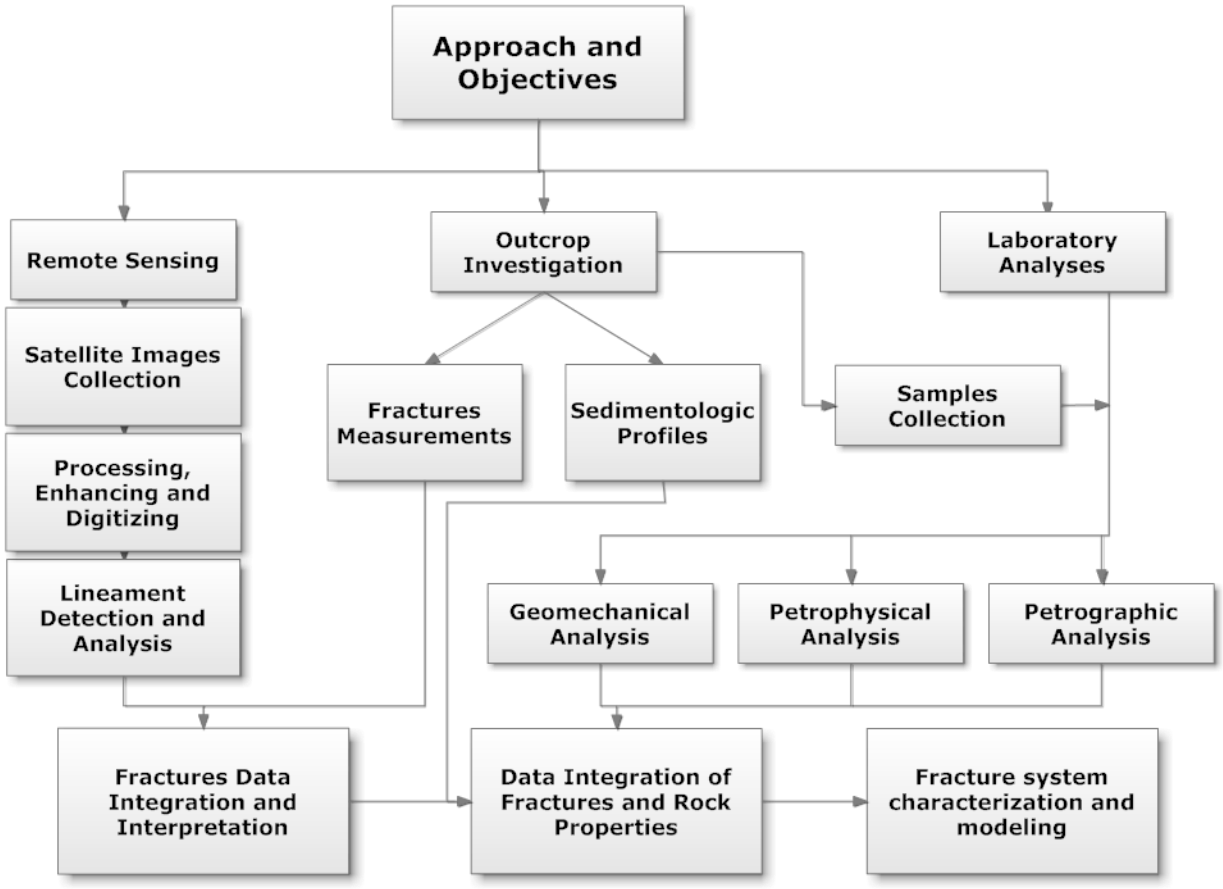

Figure 1.3: Flowchart shows the systematic flow of study tasks

Chapter 2

Geological and Tectonic Setting of Wajid Group

2.1 Previous studies

2.1.1 Sedimentology and Stratigraphy

Wajid Group Sandstone (Wajid sandstone) was named after Jabal Al-Wajid (South of Wadi Al-Dawasir area) by Jackson, Gierhardt and Owens in 1948 (Jackson et al., 1963). The Group located in the southwestern part of Saudi Arabia as continuous exposure extends from Wadi Al-Dawasir southward to Najran city with smaller isolated outcrops in the southwest (in Abha, and Khumis Musheet) and extend into northern part of Yemen (Powers et al., 1966). The base of Wajid Group sandstone overlies the basement rock (igneous and metamorphic rock) with nonconformity contact, and the upper part of Wajid sandstone overlain by basal Khuff carbonate with disconformity contact (Powers et al., 1966). The age of Wajid Group sandstone is early Paleozoic as suggested by Alabouvette and Villemur , (1973); However, a Cambro-Ordovician age was suggested by Dabbagh and Rogers, (1983) and Moshrif and El-Hiti, (1989). The latest age assignment for Wajid Group was Cambrian to Permian by Evans et al.,1991; Stump & Van der Eem, (1995) and Keller et al., (2011). The Wajid sandstone was considered as one formation until 1982 when Pallister subdivided it into two; Ilman and Shum Formations (Pallister, 1982). Kellogg et al., (1986) mapped the Tathlith quadrangle and divided the Wajid Formation into four members from base to top; Dibsiyah, Sanamah, Khusayyayn, and Juwayl. According to Kellogg et al (1986), each member separated by distinct discontinuity with the thin conglomeratic layer. Evan et al., (1991) upgraded the Wajid

Formation into a group and its members into formations and they have also identified Qusaiba shale in the southern Wajid outcrop belt.

Dabbagh and Roger (1983) carried out a detailed sedimentological study of Wajid sandstone. This study included the depositional environments, where, they suggested a braided-stream depositional environment for southern part of Wajid belt and a shallow marine depositional environment for the northern part. Moshrif and El-Hitt (1989) recognized six lithofacies in Wajid sandstone. A comparative study in term of sedimentology between Wajid Sandstone and the Paleozoic succession in Egypt was conducted by Wanas and Abdel-Maguid, 2006. Babalola, (1999) studied the depositional environment and provenance of the isolated remnant of Wajid in Khamis Mushait area. Mahgoub, (2007) studied the Juwayl Formation of Wajid sandstone in term of facies, depositional environment, and reservoir quality. Khusayyayn Formation studied by Siddiqi, (2007) in term of facies, depositional environment, and reservoir quality. Abdulkadir, (2007) studied in details Dibsiyah Formation in term of sedimentology and reservoir quality. The heavy minerals distribution within Wajid sandstone was also studied for provenance implication and tectonic setting by Babalola, 1999 and Hussain et al., 2004. Moreover, Wanas and Abdel-Maguid, (2006) studied the provenance and tectonic setting of Wajid Formation based on the petrographic and geochemical investigation. Knox et al., (2007) studied the distribution of heavy minerals within Wajid sandstone for stratigraphic evolution implication. Abdulkadir, et al., (2010) studied the distribution of petrophysical parameters within the lower formation of Wajid sandstone (Dibsiyah Formation). Abdulkadir and Abdullatif, (2013) studied the facies of Dibsiyah Formation to interpret the depositional environment and the reservoir quality. Detailed

sedimentological study for all Wajid formations conducted by Al Ajmi, (2013) and Al-Ajmi et al., (2015). Recently, Yassin & Abdullatif, (2017) studied the geochemical characteristics of the Wajid Group sandstone.

Glacial deposits in Sanamah and Juwayl formations of Wajid Group sandstone were studied by several researchers. McClure et al., (1988) recognized the glacial deposits in the uppermost part of Wajid sandstone (Juwayl Formation) and they assigned Carboniferous to early Permian age for those deposits. Vaslet, (1990) recognized the late Ordovician glacial deposits in Wajid sandstone (Sanamah Formation). Glacial environments assigned to Sanamah and Juwayl Formations by (McClure et al., 1988; Vaslet, 1990). However, Dabbagh and Rogers, (1983) assigned glaciofluvial environment for these formations and glacial/periglacial interpreted by Evans et al., (1991). Furthermore, purely fluvial processes interpreted by (Hadley and Schmidt, 1975; Alsharhan et al.,1991; Alsharhan, et al., 1993). Recently, the paleoenvironments of glacial deposits in SW Saudi Arabia have been studied by (Keller et al., 2011). The non-glacial conglomeratic beds within Wajid sandstone studied by Hadley and Schmidt, (1975).

Al-Laboun, (1986) suggested Saq and Lower Tabuk formations in central and northern Arabia equivalent to the Wajid Sandstone. Evans et al, (1991) considered Wajid Sandstone an equivalent to Saq, Qassim, Zarga, Sarah, Qalibah and Unayzah Formations. Moreover, Vaslet (1990) correlated the Wajid Sandstone to Qassim and Zarqa Formations in the central and northwest Arabia and Dibsiyah Member of Kellogg et al. (1986) with the Saq Formation. He also assigned an Ordovician age to other Members and correlated them with the Sarah and Zarqa Formations of the central Arabia.

2.1.2 Structure Geology

The structure geology of the western part of Rub' Al-Khali Basin where the equivalent sandstone of Wajid Group occurred studied by Dyer & Husseini, (1991) and Lange, (2006). They identified several kilometer NW-SE trending graben system. Stewart, (2016) studied the Precambrian basement structures within Rub' Al-Khali Basin based on regional magnetic and gravity data and reflection seismic data. He detected two major trends of basement structure which are N-S and NW-SE.

There is only two studies consider the fracture orientation within Wajid Group which are Zeeb et al., (2010) and Al Ajmi et al., (2014). Zeeb et al., (2010) studied the fracture fluid flow in the Wajid sandstone aquifers using Google satellite images of some outcrops and found that the fracture system has an influence on flow behavior in the studied aquifers. They concluded that the NW-SE trending fracture set strongly controls the fractures fluid flow in the Wajid sandstone aquifer. Al Ajmi et al., (2014) studied the fracture conductivity of the Wajid sandstone aquifers in southwest Saudi Arabia and concluded that the fracture conductivity has an effect on the groundwater flow in the studied aquifers.

2.1.3 Petroleum System

It is well known that the Qusaiba petroleum system in Paleozoic succession in Saudi Arabia is the main petroleum system. The primary hydrocarbon reservoirs are the Permian Unayzah sandstone (Juwayl Formation of Wajid Group is the equivalent of Unayzah member B and C) and Devonian Jauf sandstone (Khusayyayn Formation of Wajid Group is the equivalent). Besides that, the other reservoirs of Qusaiba Paleozoic

total petroleum system are the Cambrian-Ordovician Saq Sandstone(Dibsiyah Formation of Wajid Group is the equivalent), shallow-marine sandstones of the Ordovician Qasim Formation(missing in Wajid Group) , and the late Ordovician glacial and periglacial clastics of the Zarqa and Sarah Formations(Sanamah Formation of Wajid Group is the equivalent) (McGillivray and Husseini, 1992; Konert et al., 2001;Stump & Van der Eem, 1995; Pollastro, 2003; Abu-Ali and Littke 2005; Al-Mahmoud and Al-Ghamdi, 2010; Bu-Khamseen et al., 2010).

2.2 Tectonic and structural framework

2.2.1 Arabian Plate Tectonic

Tectonically, the Arabian Shield was part of a larger geologic unit known as the Arabian-Nubian Shield(ANS). The Arabian-Nubian Shield is a juvenile crust, which welded west and east Gondwana. It formed during the Pan-African cratonization by accretion of interoceanic island-arc between about 900 and 550 Ma when closing of the Mozambique Ocean(Nehlig et al., 2002)(Figure 2.1, Figure 2.2, Figure 2.3). Thus, tectonostratigraphic terranes (namely; The Ad-Dawadimi, Afif, Hijaz, Midyan, Asir, Jeddah, Hail, Hijaz and Ar Ryan) have been formed (Figure 2.1). Those terranes are separated by major NW-trending faults and by N, NW and NE-oriented suture zones lined by serpentinized ultramafic rocks (ophiolites) (Stoeser and Camp, 1985; Brown et al., 1989; Nehlig et al., 2002; Al-Husseini, 2000; Husseini 2000) (Figure 2.1).

Final cratonization of the terranes between 680 and 610 Ma induced a network of strike-slip faults consisting of the N-trending Nabitah belt, the major NW striking left-lateral faults (early Najd faults), lined by gneiss domes and associated with sedimentary basins,

and N to NE-trending right-lateral faults. The latest collision orogeny was the Al Amar-Idsas Orogeny between the Afif terrane and the Ar Rayn terrane. This took place along the N-trending Al Amar- Idsas Suture that is here referred to as the Amar Suture (Al-Husseini, 2000)(Figure 2.1, Figure 2.2, Figure 2.3).

The accretion was followed by widespread extensional tectonics and crustal thinning between approximately 620 and 530 Ma (Edgell, 1992; Al-Husseini, 2000). During the extensional stage, N-trending structures (e.g. Ghawar anticline and Qatar Arch) were formed (Figure 2.2, Figure 2.4) (Edgell, 1992; Al-Husseini, 2000). In the final stage of the extensional tectonics, the NW-trending left-lateral Najd fault system was developed (details in Najd fault system section) (Figure 2.3, Figure 2.4). This stage was followed by peneplanation of the Arabian Shield and the onset of deposition of the Paleozoic sedimentary succession (e.g., the Wajid Group located southwest of Saudi Arabia) (Sharland et al., 2001). During the Carboniferous period, the Hercynian Orogeny affected the whole region and reactivated the pre-existing basement structures(Sharland et al., 2001; Faqira et al., 2009; Konert et al., 2001). In the Late Oligocene, the Arabian plate separated from the African plate due to the opening up of the Red Sea and the Gulf of Aden (Johnson, 1998; Beydoun, 1991; Bosworth et al., 2005)(Figure 2.2).

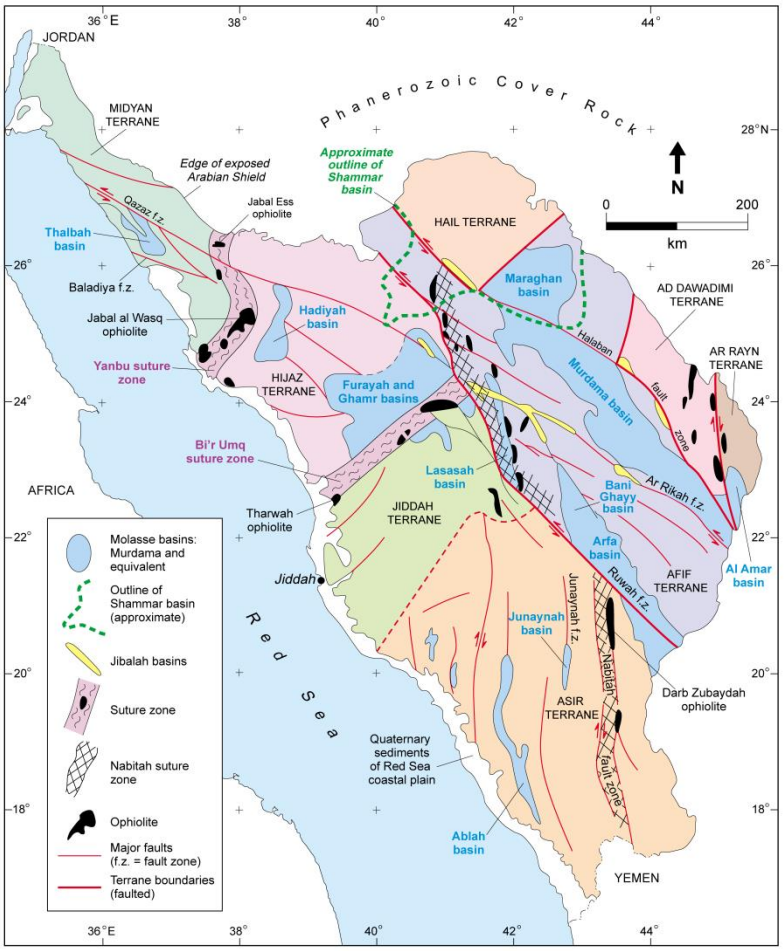

Figure 2.1: Simplified geologic sketch map of the Arabian Shield showing the terranes and their boundaries, and the main Pan-African structural features and sedimentary basins. Major fault zones, such as Ruwah, Ar Rikah, Halaban, and Qazaz, belong to the Najd fault system(Nehlig et al., 2002).

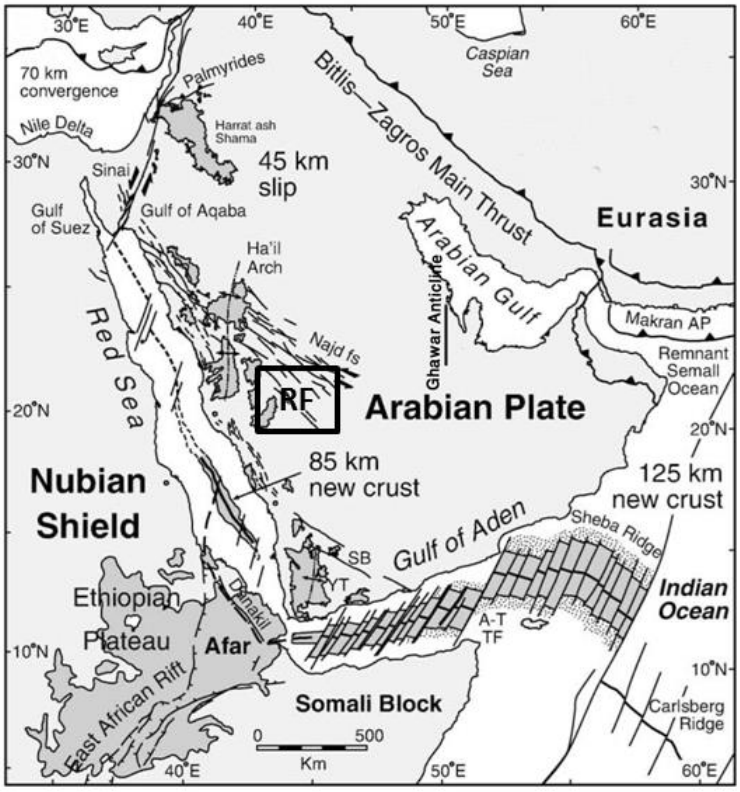

Figure 2.2: Tectonic map of the Arabian Plate (RF=Ruwah fault zone) (Bosworth et al., 2005).

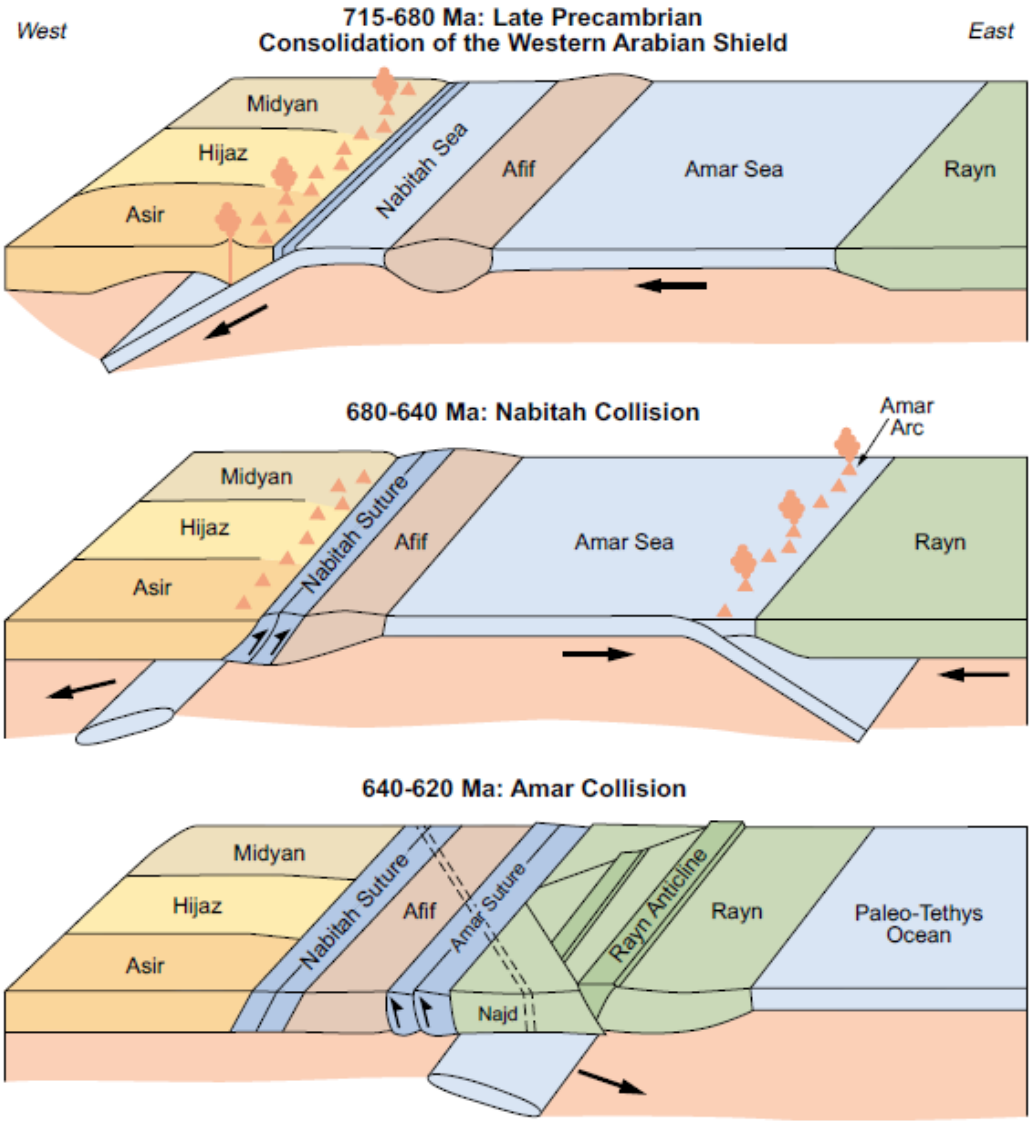

Figure 2.3: Reconstruction of the tectonic evolution of Arabian shield (Al-Husseini, 2000)

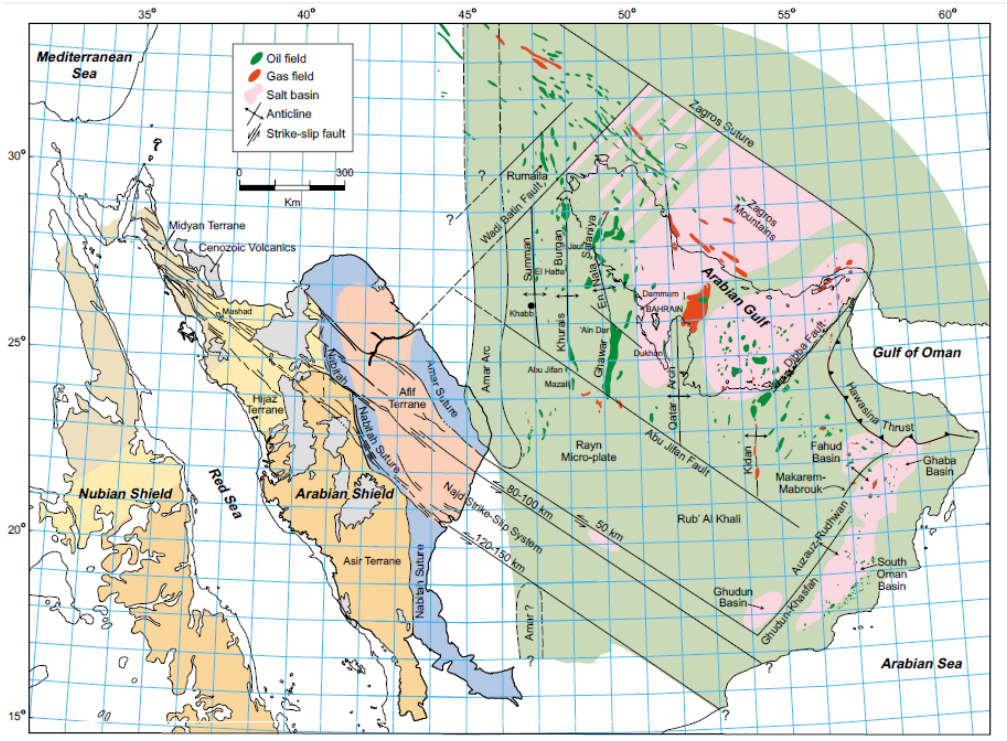

Figure 2.4: Geological map of the Arabian shield with basement grains and the propagation of Najd fault system in the Rayn micro-plate (Stoser and Camp, 1985; Al-Husseini, 2000).

2.2.2 Najd Fault System

Najd fault system is a major left-lateral wrench fault system developed in the latest stages of the Arabian-Arabian Shield accretion (Al-Husseini, 2000) (Figure 2.2, Figure 2.4). Najd fault system recognized throughout the magnetic anomalies lineament in Arabian Shield(Johnson and Stewart, 1995). Its present-day orientation is northwest - southeast as indicated by major faults and elongation of several accompanying sedimentary basins such as the Najd Rift Basins and the Rub' Al Khali half-graben (Dyer & Husseini, 1991) (Figure 2.4, Figure 2.5).

Najd fault system is the most predominant tectonic event occurred in the period from Late Precambrian to early Cambrian (Figure 2.4)(Brown and Jackson, 1960). It exposed over 1100 km over Arabian Shield with 300 km left-lateral dislocation(Brown, 1972; Moore and Al-Shanti 1979; Davies, 1984) and it extended under the Phanerozoic sediment across the western part of Rub' Al-Khali where it coincides with faults in southern Yemen and the deep subsea valley which separates Socotra from Somalia (Figure 2.4)(Brown, 1972; Husseini, 2000). Considering the extension of Najd fault system under a Phanerozoic rock in western part of Rub' Al-Khali, the total length of Najd fault is about 2000km (Brown, 1972; Husseini, 2000).

The episode of Najd fault tectonic occurred in two phases of tectonics. The early phase of Najd fault system was dextral, and it may have occurred from about 640 to 600 Ma(Husseini, 2000). The final phase of Najd fault system tectonic was a sinistral strike-slip fault, and it may have lasted from about 600 to 540 Ma (Husseini, 2000).

Several pull-apart basins developed in the Arabian Shield during the early stage of Najd fault system tectonics(dextral phase), such as Bani Ghayy Basins where Bani Ghayy group deposited, Murdama basin, and Arfa basin (Agar, 1987; Johnson, 2003; Nehlig et al., 2002)(Figure 2.4, Figure 2.5, Figure 2.6).

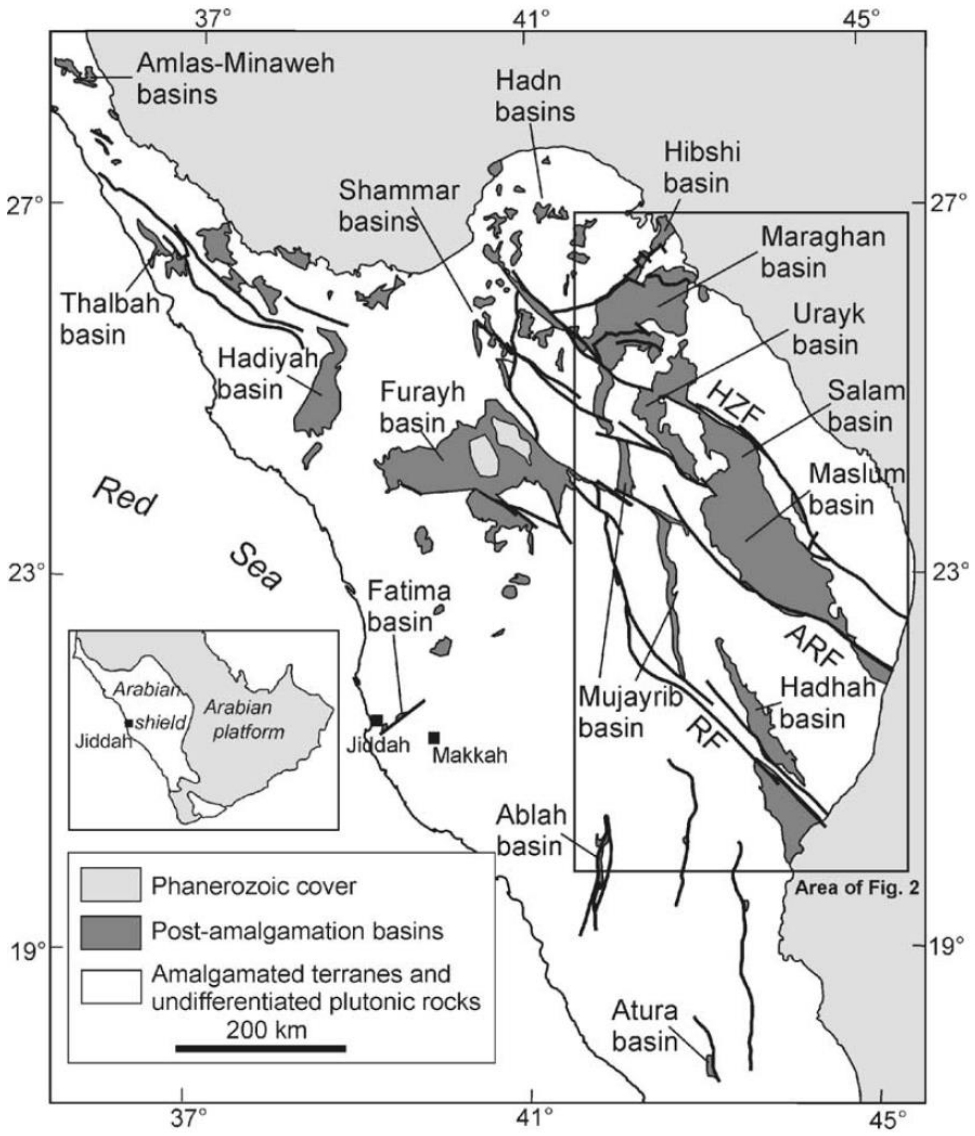

Figure 2.5: Map shows the Arabian Shield Basins and Najd fault zones. RF=Ruwah fault zone, ARF=Ar Rika fault zone, and HZF: Halaban-Zarghat fault zone(Johnson, 2003).

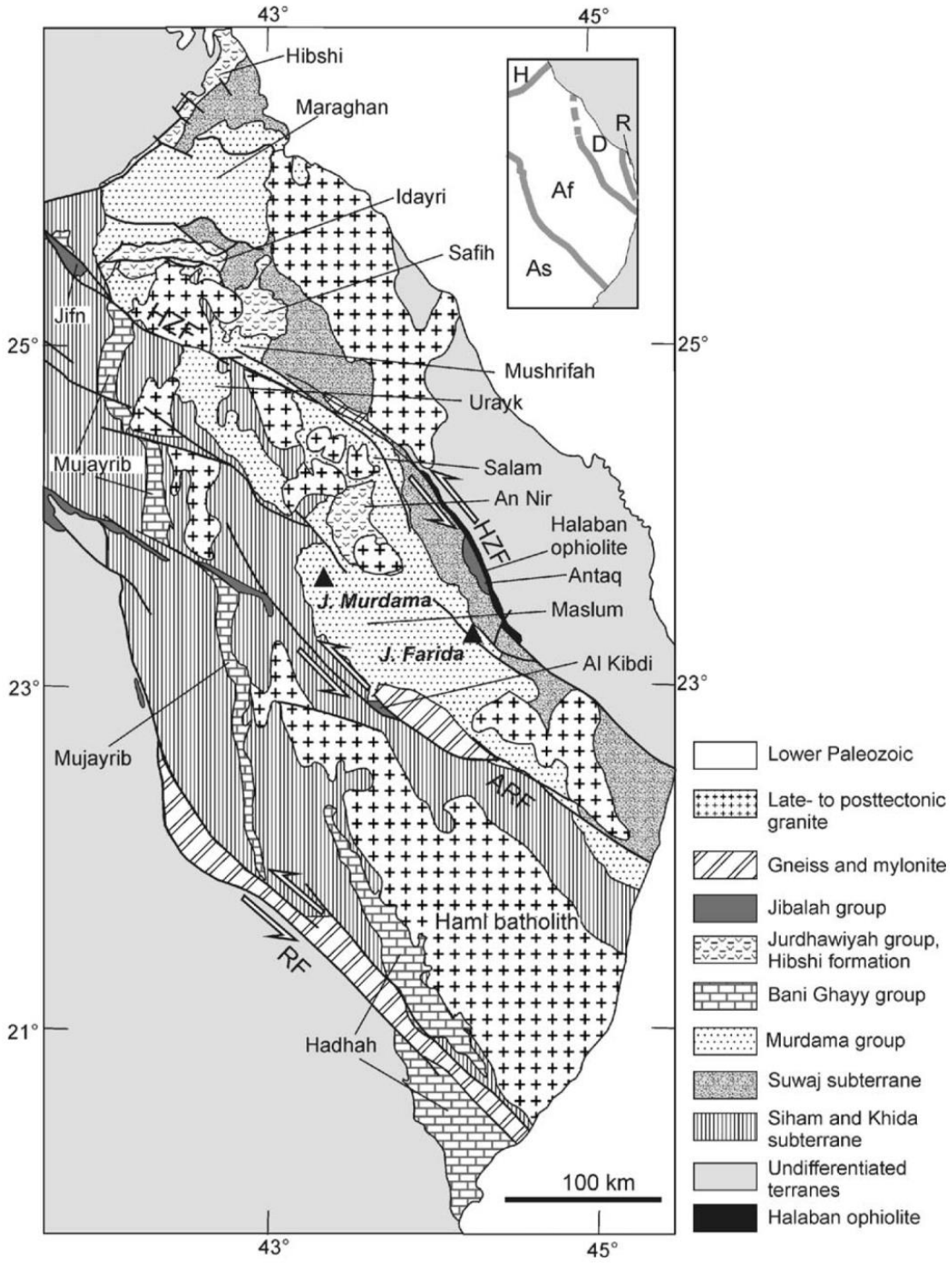

Figure 2.6: Geological map of NE Arabian Shield shows basins and Najd fault zones. RF=Ruwah fault zone, ARF=Ar Rika fault zone, and HZF: Halaban-Zarghat fault zone(Johnson, 2003).

2.2.3 Tectonic Evolution of Wajid Group

The Wajid Group sandstone is located within the Wajid Graben(Wajid Basin), one of the graben structures located in the western Rub' Al Khali Basin(Dyer and Husseini, 1991; Lange, 2006). The Rub' Al-Khali Basin, southwest the Arabian Plate characterized by several hundred kilometers long trending northwest-southeast graben systems with a depth of approximately six kilometers (Dyer and Husseini, 1991; Lange, 2006).These grabens were formed coincidentally with the development of Najd fault system (the last tectonic event of the evolution of the Precambrian Arabian Shield). Reactivation history of the Wajid Graben reflected five major tectonic events; Two tectonic events occurred before 520 Ma, a middle/upper Cambrian event, a base Devonian event` and Carboniferous event (Lange, 2006).

During the Paleozoic Era, the Arabian plate was subjected to a series of major uplifts and subsequent erosion that were marked by pronounced unconformities and incised paleovalleys. The Paleozoic sedimentary succession in Saudi Arabia was divided into four mega-depositional cycles; Middle Cambrian to Early Ordovician, Late Ordovician to Early Silurian, Middle Devonian, and Middle Carboniferous to Late Permian(Stump & Van der Eem, 1995) (Figure 2.7).

The Cambrian age regional uplift was inferred from the angular unconformity relationship between Yatib/Siq and Saq formation in central and northern part of Saudi Arabia. This period of uplift coincides with late Pan-African orogeny deformation period. Yatib/Siq strata were eroded from the Wajid plateau(Stump & Van der Eem, 1995). In

the southern part, the Dibsiyah Formation of Wajid sandstone overlain by Sanamah formation with unconformity relationship, which reveals a period of uplift and erosion that probably removed Qassim formation in southwestern Arabia section. This period of uplift coincides with the Taconic period of deformation which has been documented in other areas of northern Gondwanaland. The Sanamah Formation overlain by Qusaisba Member of Qalibah Formation with unconformity relationship which reveals a period of uplift and erosion. This period of uplift also coincides with the Taconic period of deformation. The Qalibah Formation of Wajid Group overlain by Khusayyayn Formation with unconformity relationship which reveals a period of uplift and erosion. This period of uplift coincides with the Acadian period of deformation. The Khusayyayn Formation overlain by Juwayl Formation with unconformity relationship which reveals a period of uplift and erosion coincides with the Hercynian period of deformation (Stump & Van der Eem, 1995).

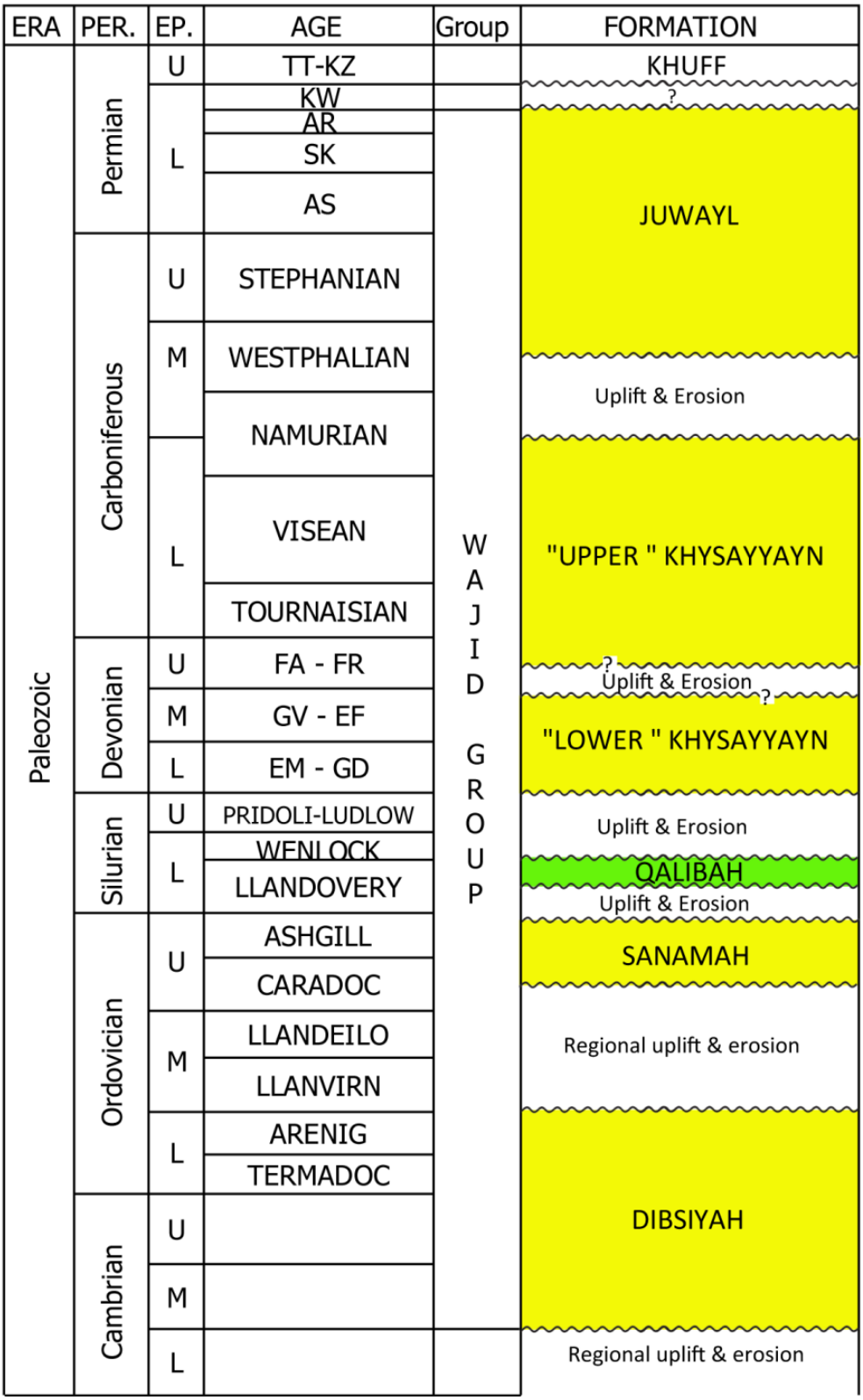

Figure 2.7: Major tectonic events in the Paleozoic succession of southwestern Arabia (Stump & Van der Eem, 1995).

The progressive erosion of the Sharawra and Qusaiba Members of Qalibah Formation of Wajid Group documented the uplift that occurred During the Acadian deformation phase. In addition, the presence of Juwayl Formation valleys in the outcrop and in subsurface was probably formed in response to the uplift by the Hercynian orogeny which occurred during the Middle Carboniferous.

2.2.4 Najd Fault System control on Wajid Group

Three main parallel fault zones formed the Najd fault system in Arabian Shield namely Ruwah, Ar Rikah, Halaban-Zarghat (Nehlig et al., 2002; Al-Husseini, 2000; Husseini, 1988; and Johnson, 2003) (Figure 2.4, Figure 2.5, Figure 2.6). The displacement along Ruwah fault zone range is about 120-150 km (Figure 2.3)(Nehlig et al., 2002; and Mogren et al., 2008). This fault zone marks the suture zone between Asir and Afif terranes and dislocates the northerly trending Nabitah suture zone(Johnson, 2003) (Figure 2.4).

The Ruwah fault zone formed the southern segment of Najd Fault System and extends to the subsurface beneath the Phanerozoic sedimentary succession in the western part of Rub' Al-Khali Basin crossing the Wajid Group outcrops in Wadi Al-Dawasir and Tathlith (areas of this study)(Dyer & Husseini, 1991).Thus, this fault zone considered the most control on the Wajid Group sandstone in the study area.

2.3 Geological setting of Wajid Group

The sedimentary succession of Wajid Group sandstone is dipping gently (around 3^{o}) towards east to Rub' Al-Khali Basin(Alsharhan et al., 1991). The sandstone of Wajid Group in the outcrop is subdivided into five formations which are in ascending order;

Dibsiyah, Sanamah, Qalibah, Khusayyayn, and Juwayl formations (Evan et al, 1991; Kellogg et al. 1986) (Figure 2.8, Figure 2.9).

2.3.1 Dibsiyah Formation

The Dibsiyah Formation is the lower formation of Wajid sandstone which overlies the basement rocks (Arabian shield) with Non-conformable contact and overlain by Sanamah Formation or younger units with unconformable contact (Stump & Van der Eem, 1995). Middle (?) Cambrian to late Ordovician age assigned to Dibsiyah Formation(Figure 2.8, Figure 2.9).

Dibsiyah Formation is 145-m thick at the reference section on the west flank of Jabal Dibsiyah and subdivided informally into lower Dibsiyah and upper Dibsiyah (Kellogg et al, 1986). The lower Dibsiyah consist at the base of paleosol overlain by cobble to pebble conglomerates with variable thickness containing rounded quartz boulders in a quartzose matrix cemented by calcite and hematite. Conglomerates overlain by mature sandstone with conglomeratic beds intercalation. The lower part of Dibsiyah characterized by intense cross-bedding with imbricated clasts within channels of medium-grained to conglomeratic sandstones (AlSharhan and Nairn ,1997).The upper part of the Dibsiyah Formation consists of quartz-arenite with cross-bedded and intense skolithos sandstone.

The Paleoenvironment of the lower part of Dibsiyah formation is interpreted as a braided stream. The upper part of Dibsiyah formation was deposited in shoreface to tidal flat/tidal channel depositional setting (Stump and Van Der Eem, 1995).

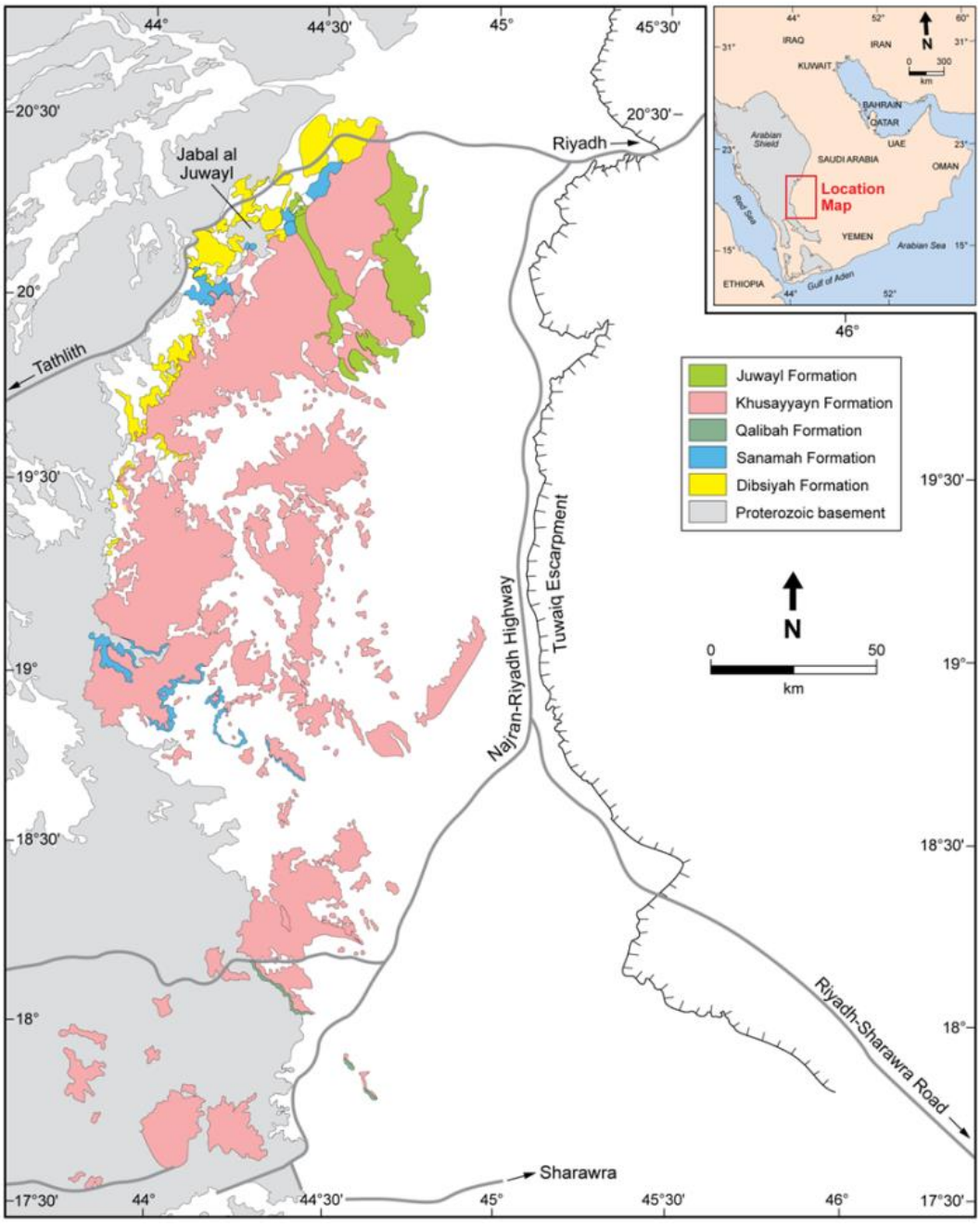

Figure 2.8: Geological map of Wajid Group sandstone(after Al-Husseini, 2004 and Knox et al., 2007).

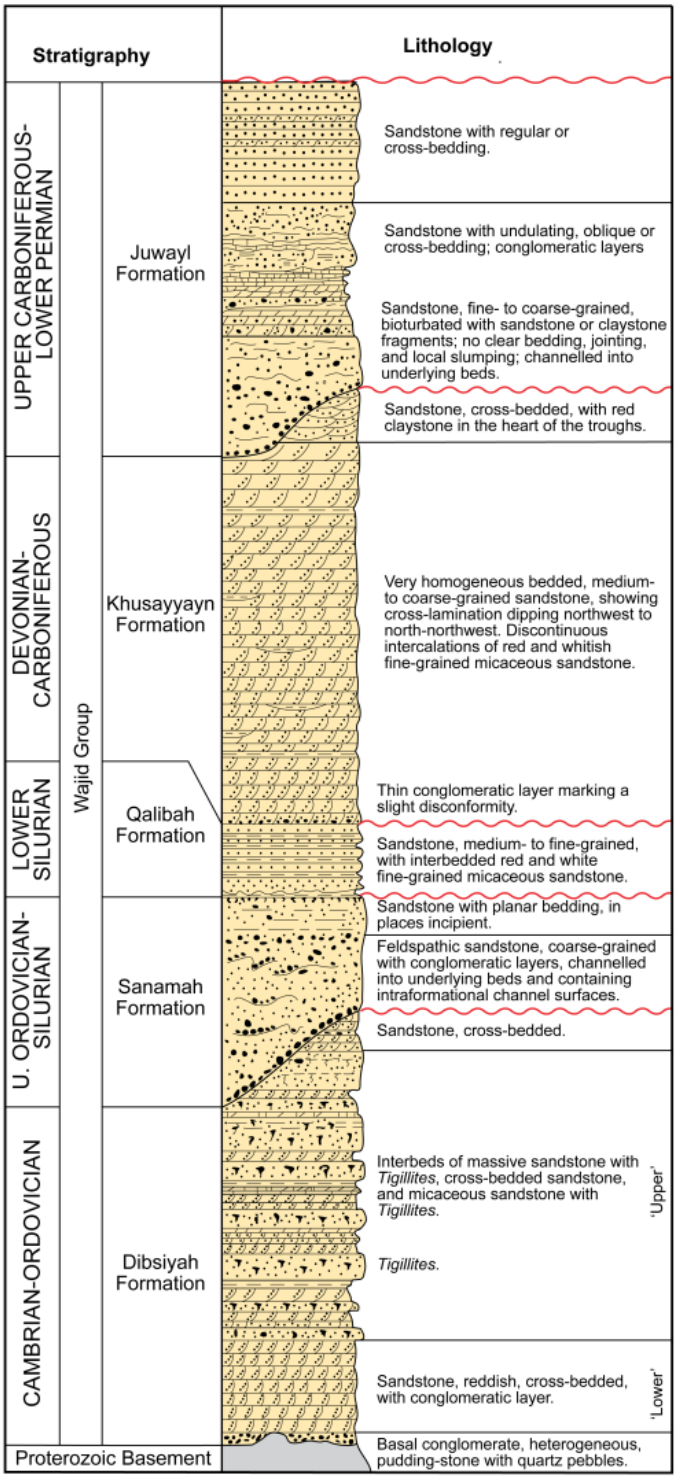

Figure 2.9: Stratigraphic Column of the Wajid Group, lithology, and environments (after Evan et al, 1991; Al-Husseini, 2004; and Knox et al., 2007).

2.3.2 Sanamah Formation

Sanamah formation is 55 m thick in the reference section in Jabal Sanamah. It rests with unconformable contact on the tigillite-bearing sandstone of Dibsiyah Formation (Kellogg et al, 1986) and overlain with disconformable contact by Qusiaba member of Qulibah Formation or by Khusayyayn Formation (Stump & Van Der Eem, 1995)(Figure 2.8, Figure 2.9). In term of lithology, the Sanamah Formation mainly consists of basal conglomerate overlain by massive coarse-grained conglomeratic sandstone. Laterally, Sanamah Formation is a discontinuous sedimentary body which wedges out between Dibsiyah and Khusayyayn Formations (Kellogg et al, 1986).

2.3.3 Qalibah formation

Qalibah formation consists of two members; Qusaiba and Sharawra member. The Qusaiba member is mainly mudstone whereas, Sharawra member is sandstone. In Wajid outcrop in SW Saudi Arabia, Qusaiba crop out and it is about 61 m. it rests unconformably on Sanamah Formation and overlain by Khusayyayn Formation with very sharp and unconformable contact (Figure 2.8, Figure 2.9). It mainly consists of a succession of siltstone and flaggy, silty sandstone (Evans et al. 1991).

In the subsurface, the Qalibah Formation consists of two members: the lower Qusaiba Member and the upper Sharawra Member. The Qusaiba Member is a succession of dominant shale with minor siltstones and sandstones; the Sharawra member is dominantly sandstones with subordinate siltstones, (Evans et al. 1991).

2.3.4 Khusayyayn Formation

In the type section, Khusayyayn Formation is about 200m (Kellogg et al, 1986). It has unconformable contact with Qusaiba member of Qalibah formation in Hima area. However, it also rests nonconformity on the Precambrian basement near Najran area and with unconformable contact with Sanamah Formation south of Wadi Al-Dawasir. Khusayyayn Formation is overlain by Juwayl Formation with unconformable contact (Stump & Van Der Eem, 1995). Khusayyayn Formation consists mainly of homogenous bedded, medium to coarse-grained sandstone with cross-lamination dipping NW (Figure 2.8, Figure 2.9)(Kellogg et al, 1986).

2.3.5 Juwayl Formation

Juwayl Formation is about 125 m thick in the composite section for the northern area of Wajid outcrop belt and similar thickness determined by(McClure, 1980) in Bani Khatmah area. However, 50 m to a 135-m thickness of Juwayl Formation determined from the same area by Hadley and Schmidt (1975). Juwayl Formation overlies Khusayyayn Formation with unconformable contact and overlain by carbonate of the Khuff Formation with unconformable contact (Figure 2.8, Figure 2.9).

In term of lithology, Juwayl Formation consists of stacked channel sandstone and debris flows. At the base, Juwayl Formation consists of medium to coarse-grained, massive sandstone with regular bedding and varves with dropstones. This unit is overlain by sandstone unit with undulating, oblique or cross-bedding conglomeratic layers. The upper unit is sandstone with regular or cross-bedding (Figure 2.8) (Evans et al, 1991). The bulk lithology range between sublitharenite/subarkosic to guartzarenite. The Juwayl formation

crop out in two distinct belts within Wadi Tathlith quadrangle (Kellogg et al, 1986), one of these belts trend north and the other trend NNE.

Chapter 3

Lineament Study and Analysis

3.1 Introduction

Lineaments are defined as straight or slightly curved surface features of natural origin, interpreted from images (O'leary et al., 1976; Koike et al., 1998). They may consist of geomorphic (relief), tonal (contrast differences) and straight valleys, contrasting tone, straight ridges, and alignment of vegetation (Roy et al. 1993; Ross and Frohlich, 1993; Cepeda, 1994; Hatcher, 1995; Sabin 1997). Lineaments may represent fracture traces and relate to a zone of weakness in the Earth's crust (Sabin, 1997). They are essential for the regional-scale study of fracture traces due to their cost- and time-efficiency, and better interpretations. Moreover, lineaments provide basic knowledge and information about stress and tectonic setting(Hariri, 2008).

Lineaments analysis and interpretation were conducted on Wajid Group using Landsat-8 OLI/TIRS satellite images with 30-m resolution, Spot-5 satellite images with 2.5-m resolution and SRTM Digital Elevation Models (DEM) with 30-m resolution. Those images were processed and enhanced using ArcGIS 10.2 and Erdas Imagine software to obtain better traces of lineaments. Lineaments were delineated and traced on computer screen manually using ArcMap 10.2. Nine lineament traces maps were constructed covering the northern, central, southern, and western parts of the study area (Figure 3.1). Lineaments attributes and properties such as orientation and length were determined and statistically analyzed to define the major lineament trends and their length distribution.

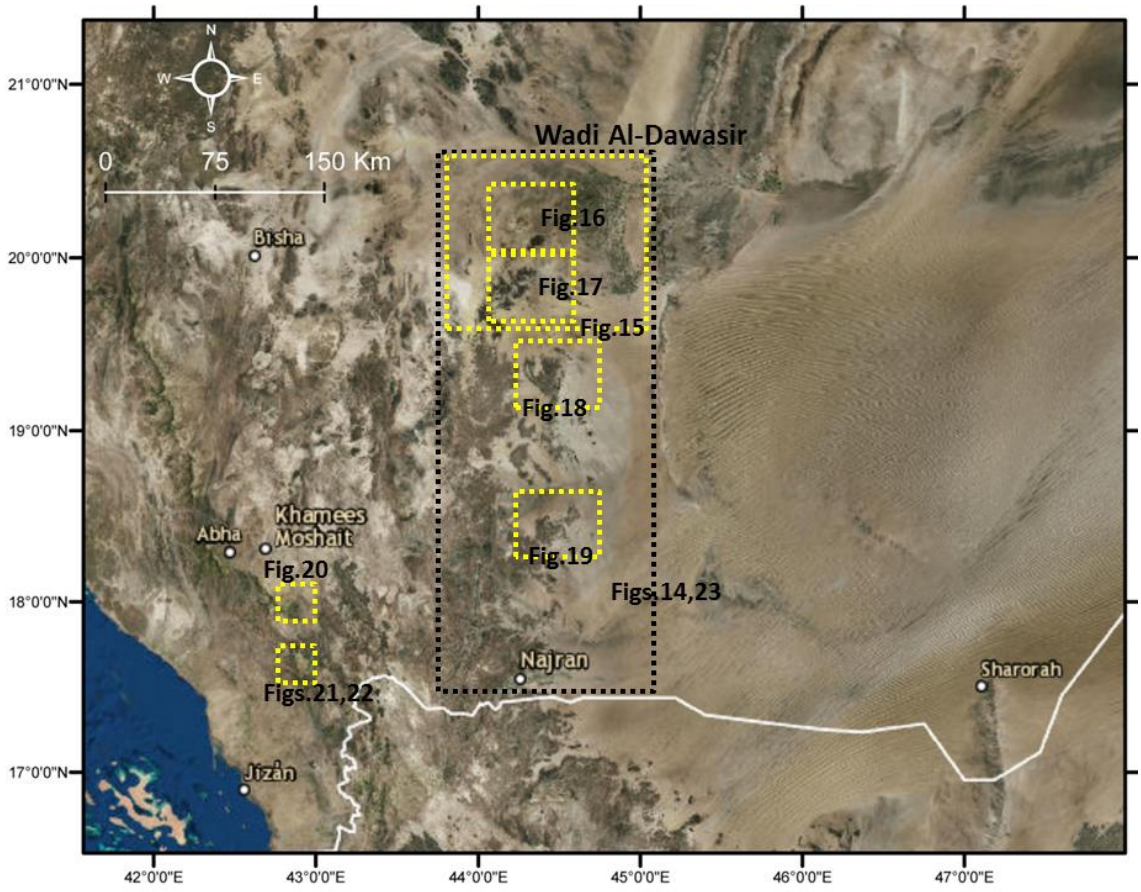

Figure 3.1: Location map of lineaments study. The dash line boxes define the outline of lineament maps.

3.2 Lineament Traces Maps

Lineament traces within Wajid Group outcrop were delineated and mapped in multi-scale maps (1:1500000, 1:500000, 1:200000, 1:125000, 1:12000, and 1:6000) based on the visual interpretation of lineaments from satellite images and shaded-DEM images(Figure 3.1), and nine lineament trace maps were generated. The large lineament traces within northern, central and southern parts of Wajid Group outcrop were mapped with a scale of 1:1500000 and two major trends of lineament were dominant: NNE-SSW (015^0) and NW-SE (145^0) (Figure 3.2). The satellite images and DEM-shaded derived lineament traces in the northern part of the studied area, where the Dibsiyah, Sanamah, Khusyyayn

and Juwayl formations are exposed (Wadi Al-Dawasir and Tathlith areas) have been mapped with a scales of 1:500000 and 1:200000 in three maps (Figure 3.3)(Figure 3.4)(Figure 3.5). Lineament traces map with a scale of 1:500000 has been established with 382 lineament traces and five major lineament trends were identified NW-SE (135^0), NW-SE (150^0) NNE-SSW(015^0), NE-SW(045^0), and E-W(090^0)(Figure 3.3). In Wadi Al-Dawasir area, a lineament trace map with a scale of 1:200000 has been established with 96 lineament traces and four major lineament trends were identified NW-SE(135^0), NNW-SSE(165^0), ENE-WSW(075^0), and E-W(090^0)(Figure 3.4). In Tathalith area, a lineament trace map with a scale of 1:200000 has been established with 102 lineament traces and four major lineament trends were identified NW-SE (135^0), NW-SE (150^0), NNE-SSW(010^0), and E-W(090^0) (Figure 3.5).

In the central part of the studied area, where the Khusayyayn Formation is exposed, satellite images and DEM-shaded derived lineament trace map with a scale of 1:200000 was constructed, and 197 lineament traces were defined (Figure 3.6). In this area, six lineament trends were identified: NW-SE (135^0), NNW-SSE (165^0), N-S (000^0), NNE-SSW (015^0), NE-SW (030^0) and WNW-ESE (105^0) (Figure 3.6). A satellite images and DEM-shaded derived lineament trace map with a scale of 1:200000 and 676 lineament traces was generated for the southern part of the studied area, where the Khussyayan formation outcrop overlay the basement rocks, and six trends of lineament traces were defined: NW-SE (140^0), N-S(000^0), NNE-SSW(015^0), NE-SW(030^0), NE-SW(050^0) and WNW-ESE (120^0)(Figure 3.7).

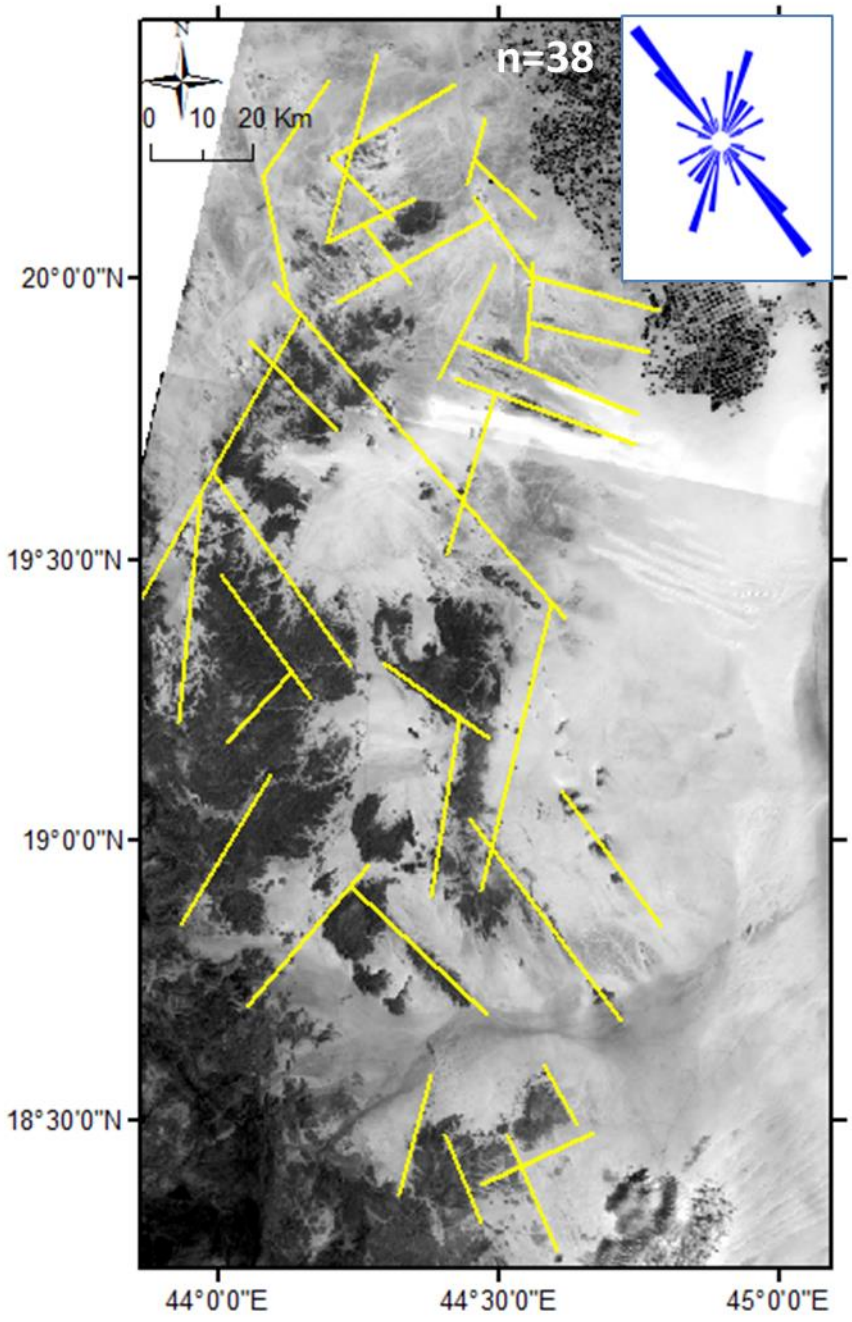

Figure 3.2: Map and rose diagram of the Major lineaments within the whole outcrop of Wajid Group traced on the Landsat satellite image. Rose diagram shows NW-SE and NNE-SSW lineament trends.

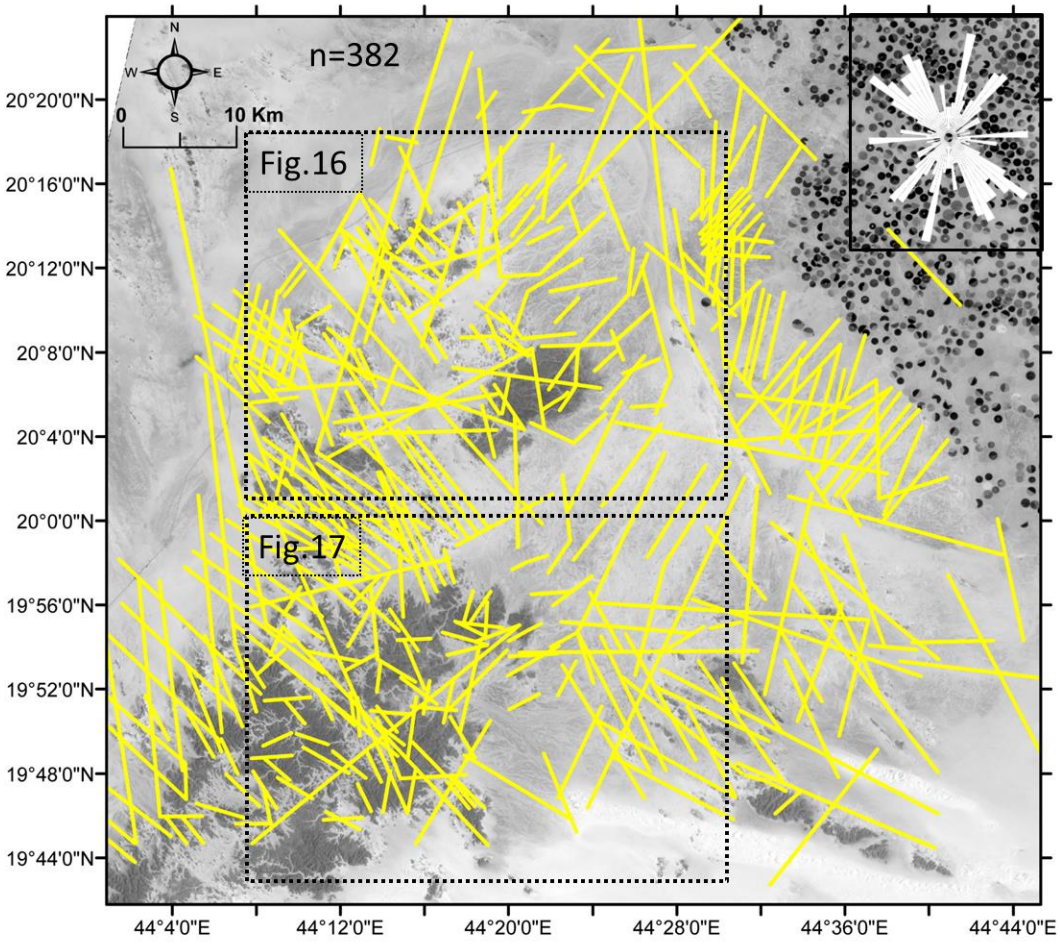

Figure 3.3: Landsat Satellite-derived Lineament traces map with a scale of 1:500000 of the northern part of Wajid Group outcrops (Wadi Al-Dawasir & Tathlith areas). Rose diagram shows NW-SE, NNE-SSW, E-W, and NE-SW lineament trends.

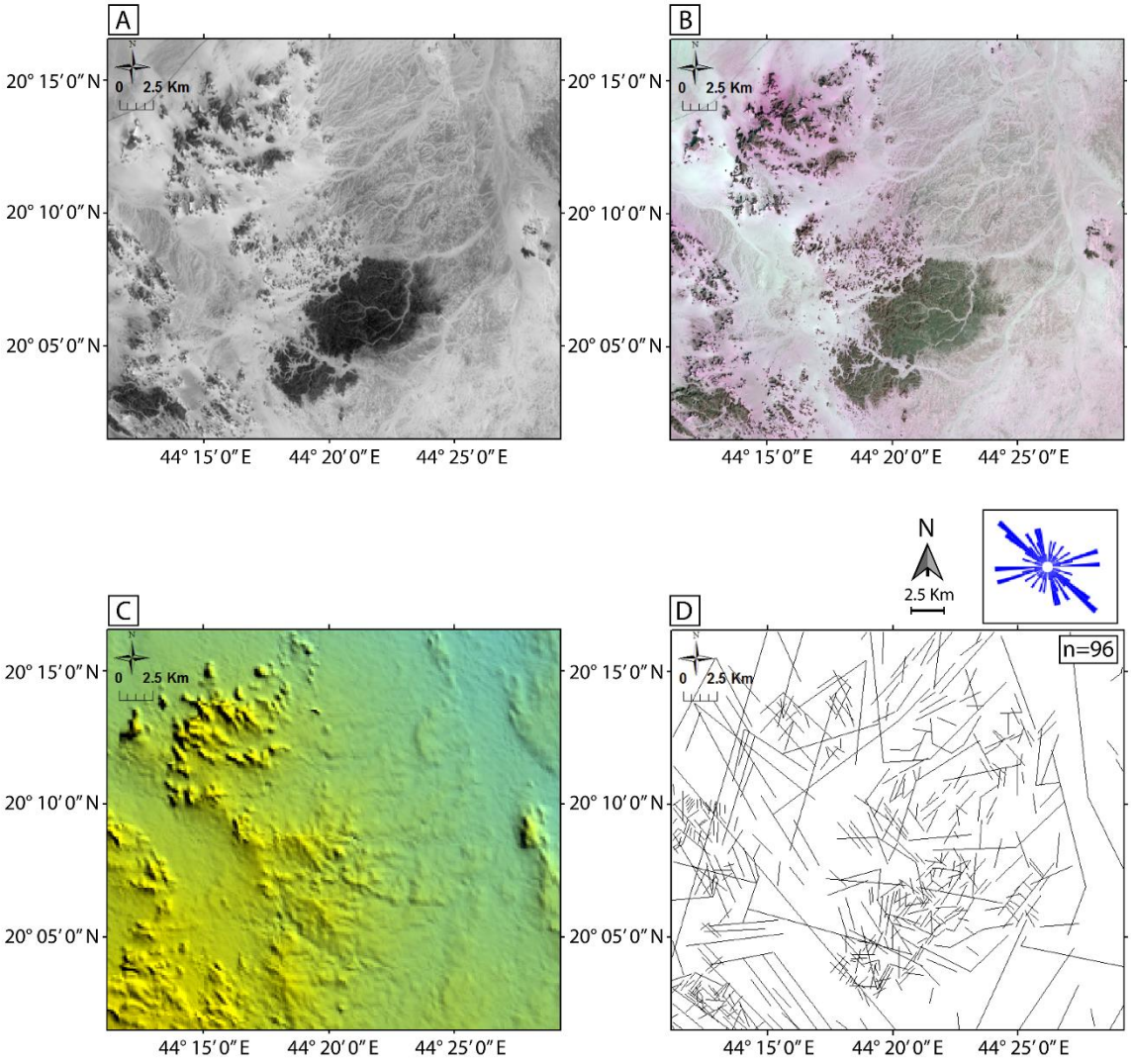

Figure 3.4: A) Landsat-8 satellite image, B) Spot-5 satellite image, C) Shielded relief digital elevation model (SRTM DEM), and D) Interpreted lineament trace map with the combination of lineaments from A, B, and C of the northern part of Wajid Group outcrop (Wadi Al-Dawasir), and rose diagram shows NW-SE, E-W, and NNW-SSE lineament trends.

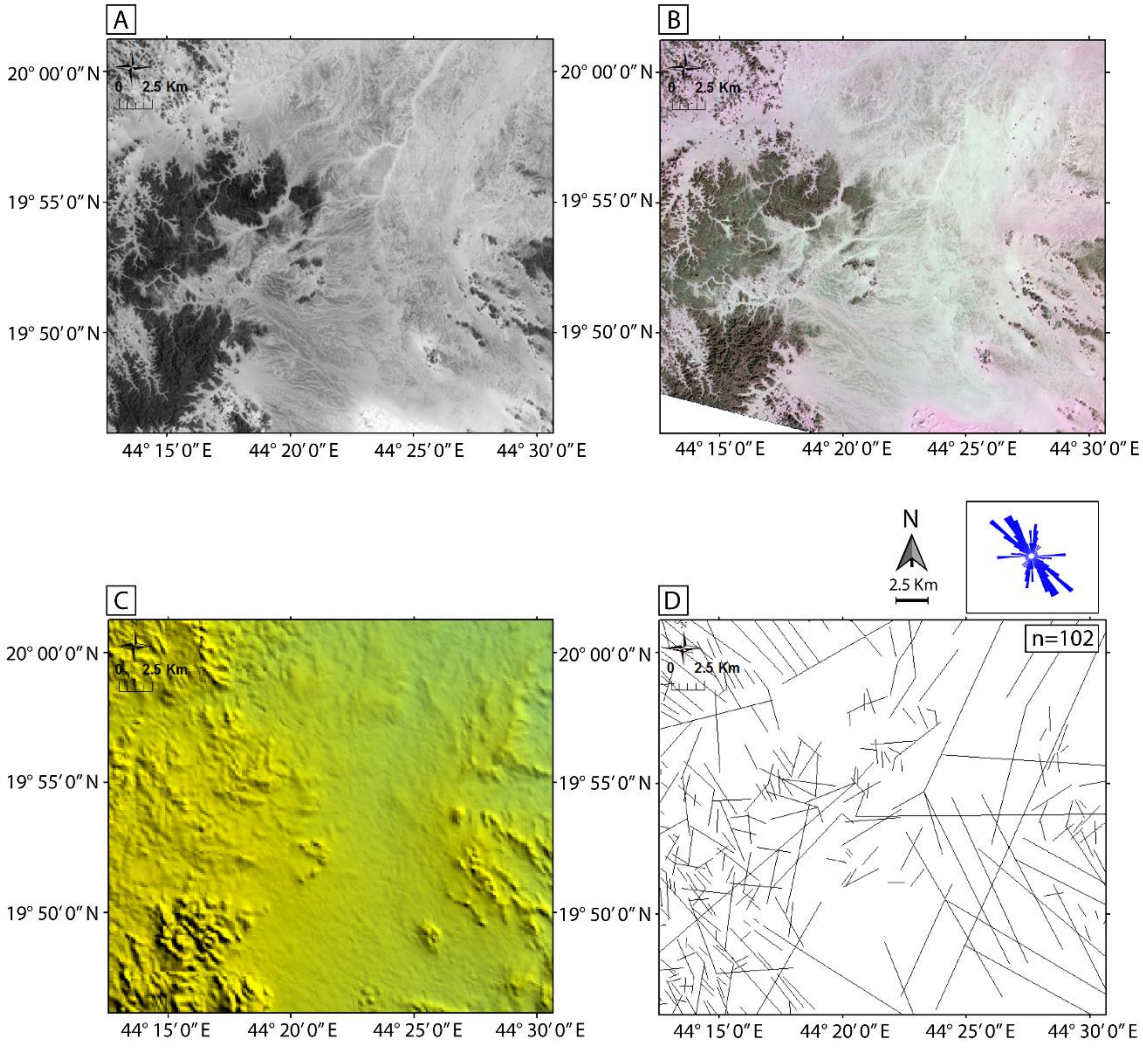

Figure 3.5: A) Landsat-8 satellite image, B) Spot-5 satellite image, C) Shielded relief digital elevation model (SRTM DEM), and D) Interpreted lineament trace map with the combination of lineaments from A, B, and C of the northern part of Wajid Group outcrop (Tathlith area), and rose diagram shows NW-SE, E-W, and NNE-SSW lineament trends.

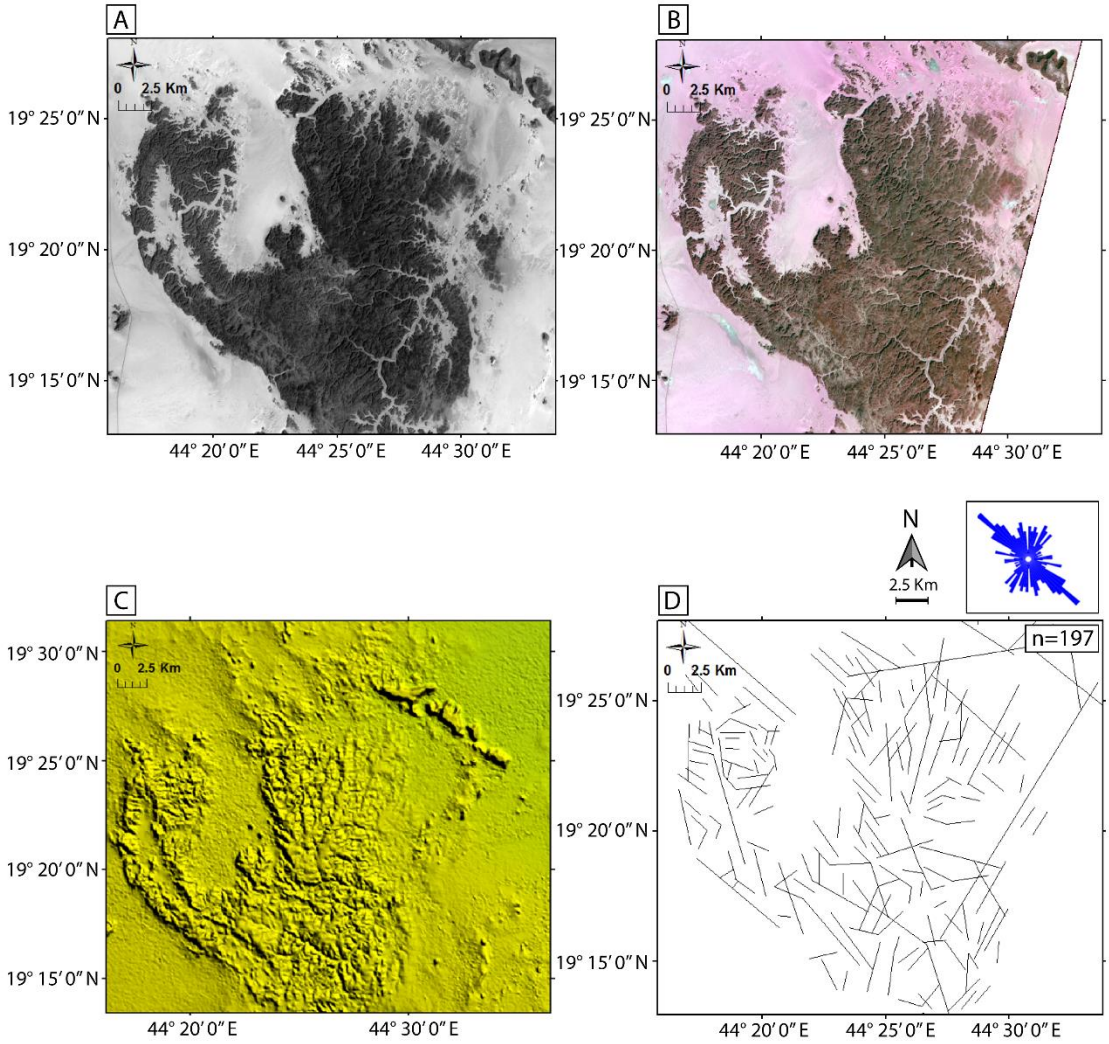

Figure 3.6: A) Landsat-8 satellite image, B) Spot-5 satellite image, C) Shielded relief digital elevation model (SRTM DEM), and D) Interpreted lineament trace map with the combination of lineaments from A, B, and C of the central part of Wajid Group outcrop, and rose diagram shows NW-SE lineament trend.

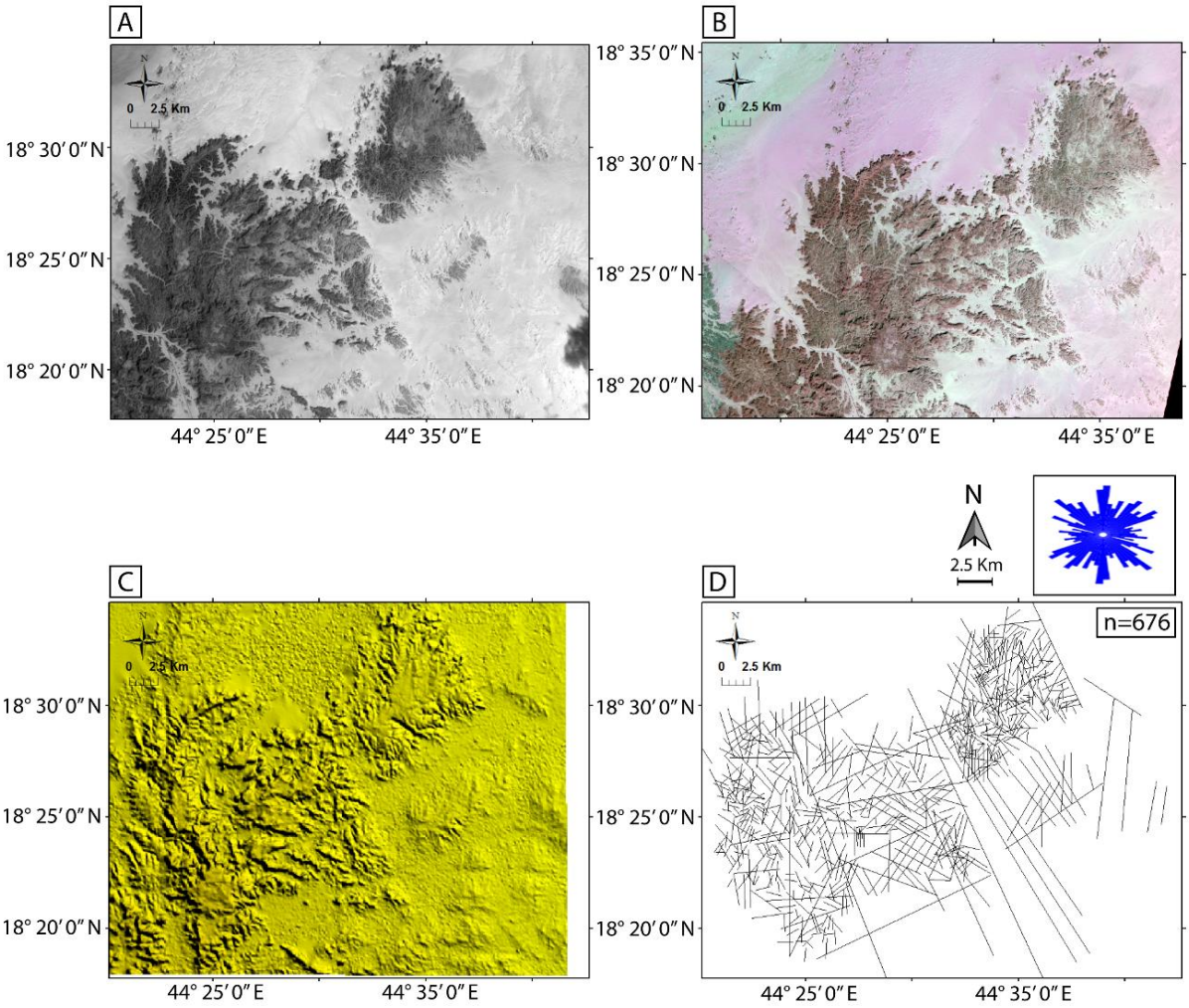

Figure 3.7: Landsat-8 satellite image, B) Spot-5 satellite image, C) Shielded relief digital elevation model (SRTM DEM), and D) Interpreted lineament trace map with the combination of lineaments from A, B, and C of the southern part of Wajid Group outcrop (Najran area), and rose diagram shows NW-SE, N-S, and NE-SW lineament trends..

Lineament trace map with a scale of 1:12000 was constructed to account for the western outcrops of the Wajid Group in Abha city (Figure 3.1), where the lower part of Wajid Group exposed, and 342 lineament traces were defined (Figure 3.8). In this area, four lineament trends were identified: NE-SW (035^0), NW-SE (140^0), N-S (005^0), and E-W (095^0); however, the NE-SW (035^0) is the most dominant lineament trend (Figure 3.8). The lineament traces within Wajid Group outcrop in Jabal Al-Gahar, SW of Abha city were mapped with a scales of 1:125000 and 1:6000 to define the major trends of lineament on a different scale. 1559 lineament trace were detected from the lineament trace map with a scale of 1:125000 and two lineament trends were also delineated included NE-SW(030^0) and WNW-ESE(110^0); where the NE-SW(030^0) is the most dominant (Figure 3.9). In Jabal Al-Gahar, the lineament traces within Wajid Group outcrop also were mapped with a scale of 1:6000, and 73 lineament traces were delineated and two orthogonal lineament trends were observed included NE-SW(030^0) and WNW-ESE(110^0) (Figure 3.10).

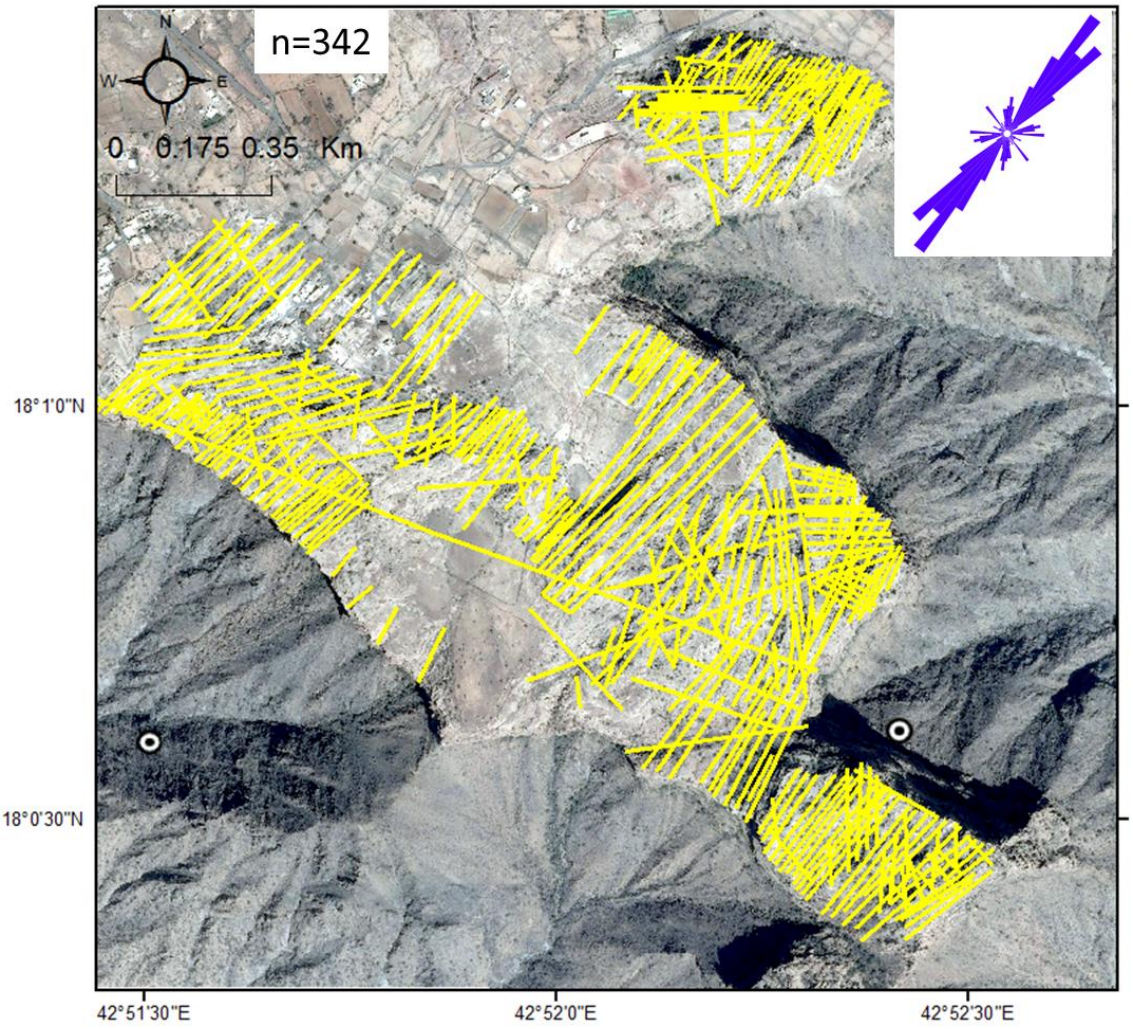

Figure 3.8: Satellite-derived Lineament trace map of Wajid Group outcrop in Abha area and the rose diagram shows NE-SW lineament trend.

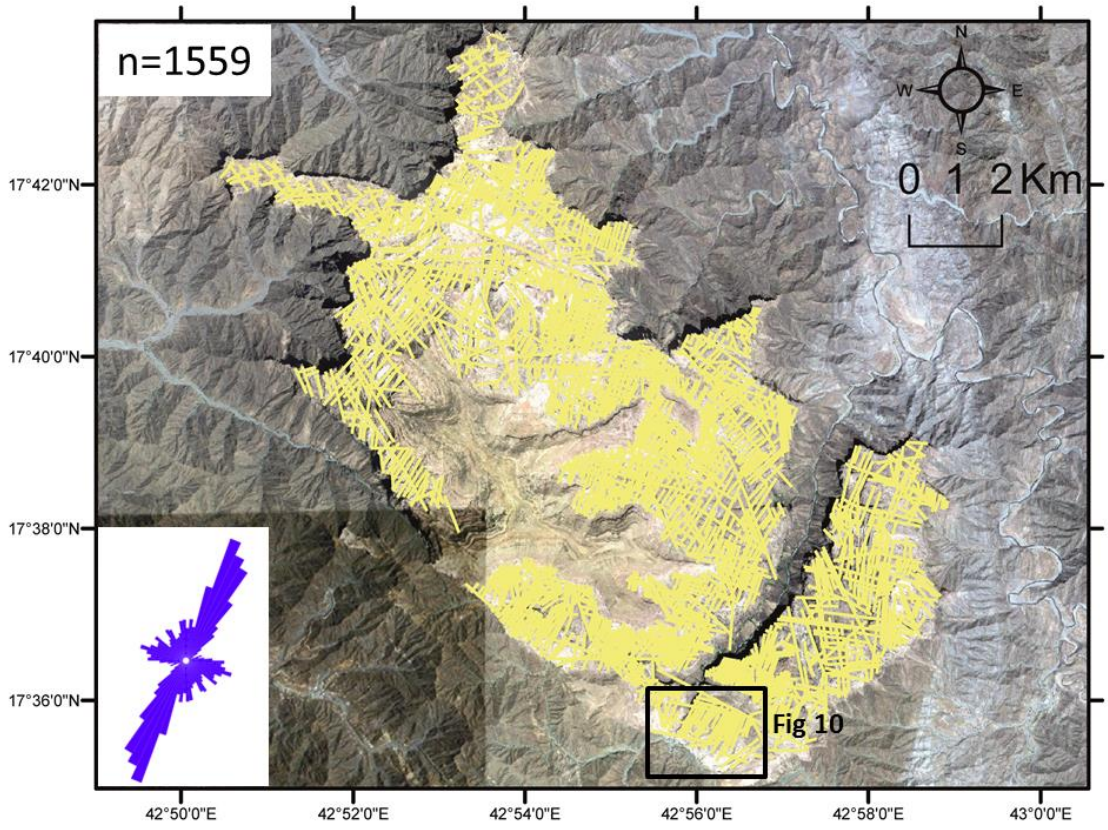

Figure 3.9: Satellite-derived Lineament trace map of Wajid Group outcrop in Jabal Al-Gahar (black box is an outline of Figure 3.10), and the rose diagram shows NE-SW and ESE-WNW lineament trends.

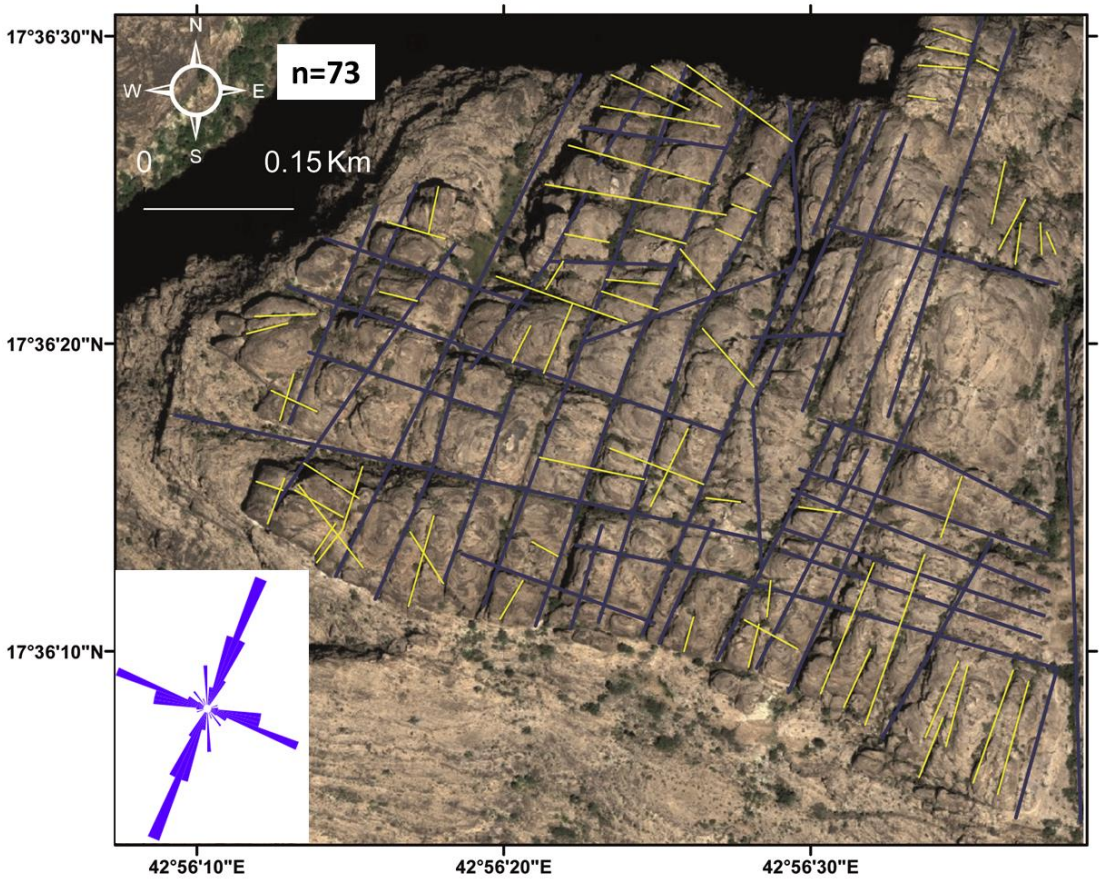

Figure 3.10: Satellite-derived Lineament trace map with a scale of 1:6000 of Wajid Group outcrop in Jabal Al-Gahar and the rose diagram shows NE-SW and ESE-WNW lineament trends.

The satellite images and DEM-shaded derived lineament trace maps supplemented by the aeromagnetic lineament map with a scale of 1:1500000, and 77 major lineaments of the eastern parts of Wajid Group outcrops. The aeromagnetic lineament traces within Wajid Group outcrop classified into three trends included NW-SE (135^0), E-W(090^0), and N-S (000^0) (Figure 3.11). The NW-SE (135^0) trending lineament traces are predominant in the studied outcrops. The trends of lineaments derived from aeromagnetic anomalies are almost consistent with trends of lineament traces derived from satellite images and DEM-shaded.

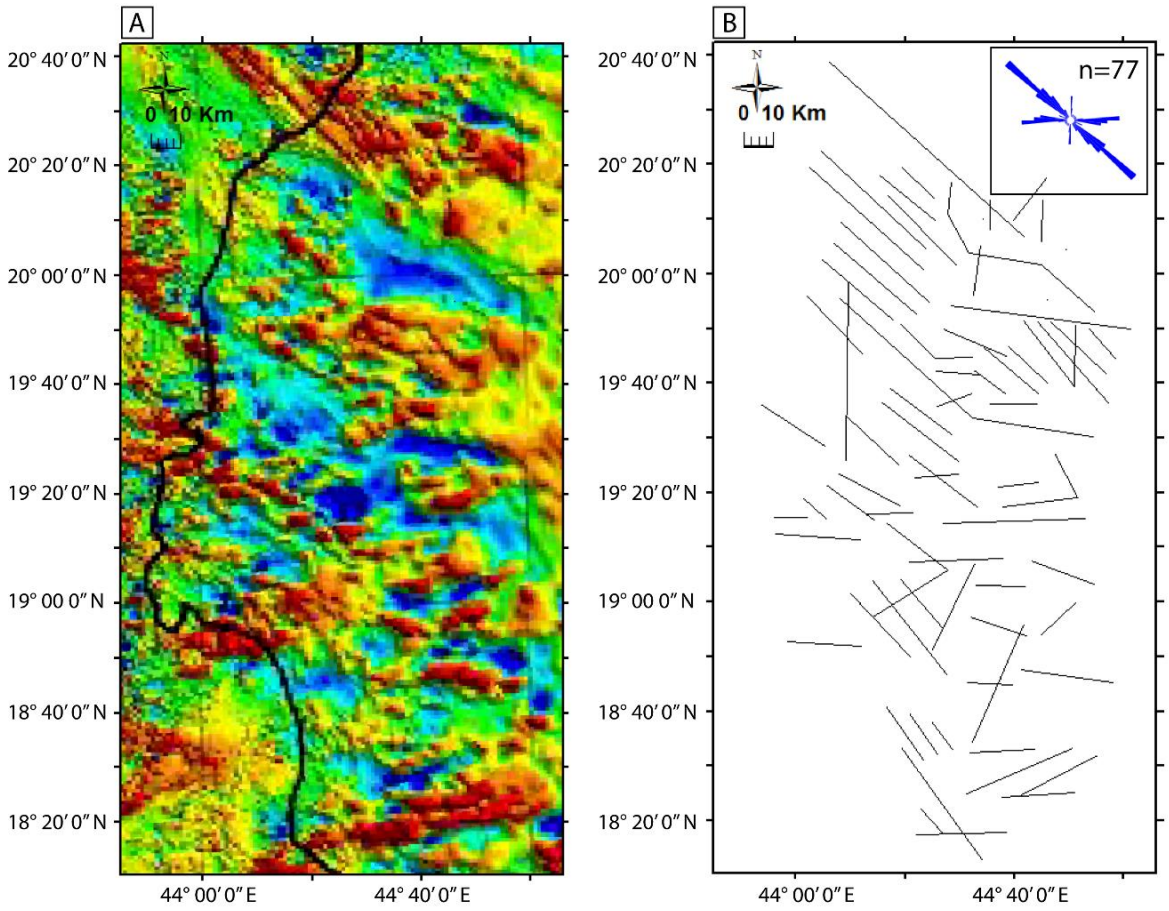

Figure 3.11: A) Reduced-to-the pole magnetic anomaly map of Wajid Group outcrop (provided by Saudi Geological Survey), B) Interpreted lineament trace map from the magnetic anomalies, and the rose diagram shows NW-SE and E-W lineament trends.

3.3 Lineament Orientation Analysis

Histograms of lineaments orientation dataset were established for northern, central, southern and western parts and for the whole outcrop of Wajid Group as well, to classify lineaments into sets and delineate the frequency of each set (Table 3.1). The frequency of large-scale lineament trace orientations for the whole outcrop is analyzed using the histogram. The orientations are classified into five sets that include NW-SE (145^0), NW-SE (135^0), NNE-SSW (015^0), NE-SW (035^0), and ENE-WSW (070^0). The most dominant sets of lineament are NW-SE (145^0) and NNE-SSW (015^0) (Figure 3.12).

Lineament traces in the northern part of studied outcrop in Wadi Al-Dawasir area occurred in four sets that include NW-SE(135^0), NW-SE(150^0), NNW-SSE(165^0), and ENE-WSW(075^0) (Figure 3.13). In Tathalith area, the lineament traces occurred in four sets that include NW-SE (135^0), NW-SE (155^0), N-S (005^0), and E-W (090^0) (Figure 3.13). The NW-SE trending lineament set is predominant.

Table 3.1: Table summarizes the lineament trends of Wajid Group at a different scale.

Wajid Outcrops	Lineament Maps	Number of Lineaments	Lineament Sets	Dominant Trends
Eastern Outcrops	1:1500000	38	NW-SE NNE-SSW ENE-WSW ESE-WNW N-S	NW-SE NNE-SSW
	1:500000	382	NW-SE NNE-SSW NE-SW E-W	NW-SE NNE-SSW
	1:200000	96	NW-SE NNW-SSE ENE-WSW	NW-SE NNW-SSE ENE-WSW
	1:200000	102	NW-SE NNE-SSW E-W	NW-SE NNE-SSW
	1:200000	197	NW-SE NNW-SSE N-S NNE-SSW NE-SW WNW-ESE	NW-SE N-S
	1:200000	676	NW-SE N-S NNE-SSW NE-SW WNW-ESE	NW-SE N-S NE-SW
Western Outcrops	1:12000	342	NE-SW NW-SE N-S E-W	NE-SW
	1:125000	1559	NE-SW WNW-ESE	NE-SW
	1:6000	73	NE-SW WNW-ESE	NE-SW

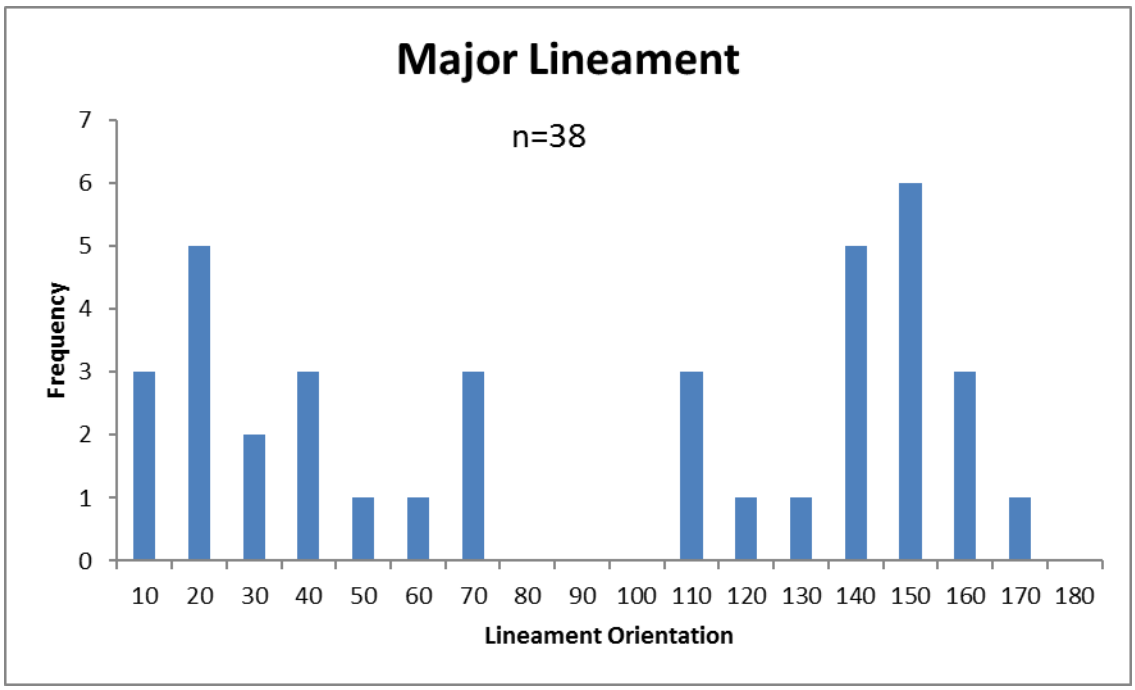

Figure 3.12: Histogram shows the frequency of large-scale lineament traces within the whole outcrop of Wajid Group in the eastern area. The NW-SE and NNE-SSW are the dominant lineament trends.

In the central part of Wajid Group outcrop, lineament traces are classified into five sets that include NW-SE (135^0), NW-SE (145^0), NNW-SSE (165^0), N-S (005^0), and NE-SW (035^0) (Figure 3.13). The NW-SE trending lineament set is predominant (Figure 3.13).

In the southern part of studied outcrop (Najran area), the lineament traces orientation classified into five sets that include NW-SE (145^0), N-S (000^0), NNE-SSW (015^0), NE-SW (030^0), and NE-SW (055^0) (Figure 3.13). The most dominant lineament sets in this area are N-S (000^0), NE-SW (055^0) and NW-SE (145^0). However, the NNE-SSW (010^0) and NE-SW (030^0) are also frequent. The dominant lineament trends in the western part of Wajid Group outcrop is the NE-SW (035^0); however, the WNW-ESE(110^0) is also observed as a frequent trend in Jabal Al-Gahar (Figure 3.14).

The NW-SE and northerly (include N-S, NNW-SSE, and NNE-SSW) trending lineament sets were observed as dominant sets in the multi-scale trace maps of the eastern outcrops of Wajid Group which are exposed in area extend from Wadi Al-Dawasir till Najran city. Western outcrops of Wajid Group in Abha area dominated by NE-SW trending lineament set.

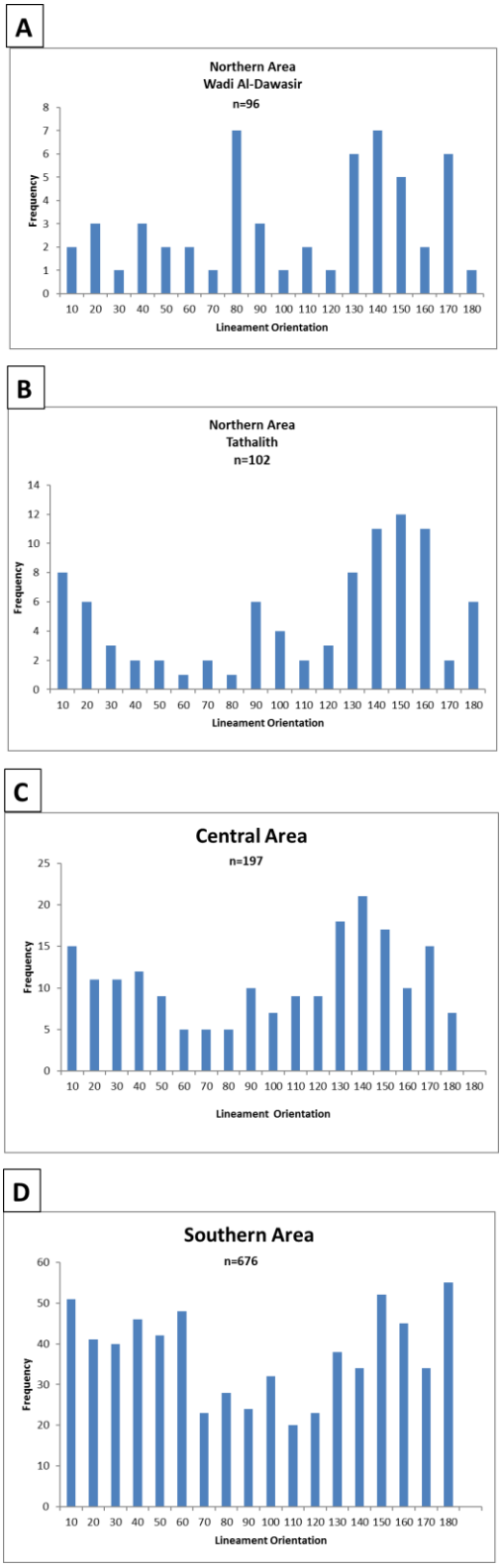

Figure 3.13: Histograms showing the frequency of lineament traces in, A) northern area (Wadi Al-Dawasir), B) northern area (Tathlith), C) central area and D) southern area.

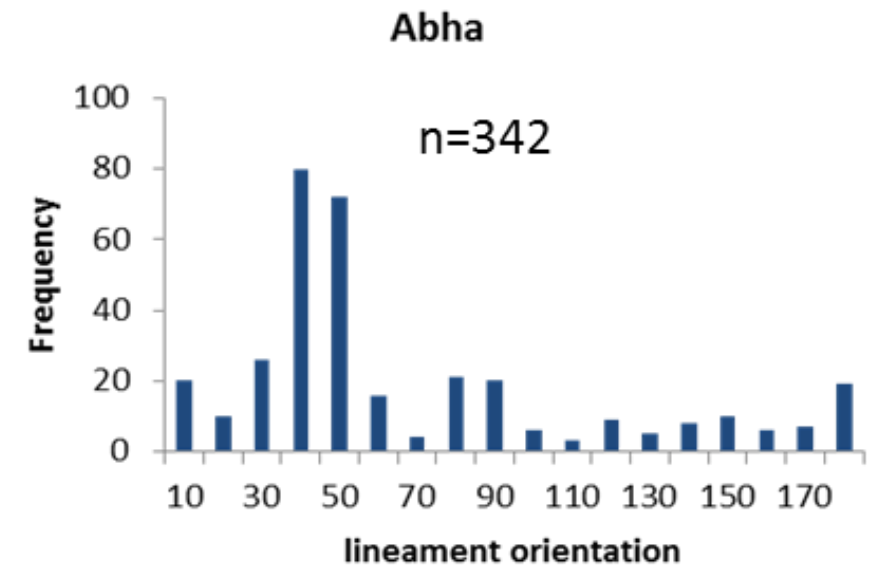

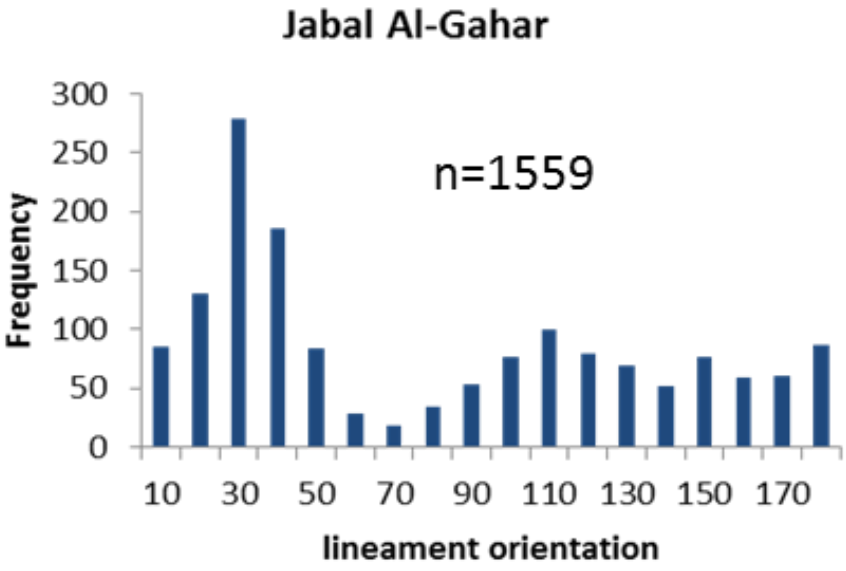

Figure 3.14: Histograms of lineaments orientation for the western part of Wajid Group outcrop(Abh and Jabal Al-Gahar).

3.4 Lineament Length Analysis

The lineaments trace length distribution of Wajid Group outcrop was obtained by plotting the cumulative length frequency versus the length using a log-log diagram (Figure 3.15). The lineament trace-length of the whole Wajid Group outcrop was distributed according to the power-law distribution (straight line on the log-log diagram) with R^2= 0.956.

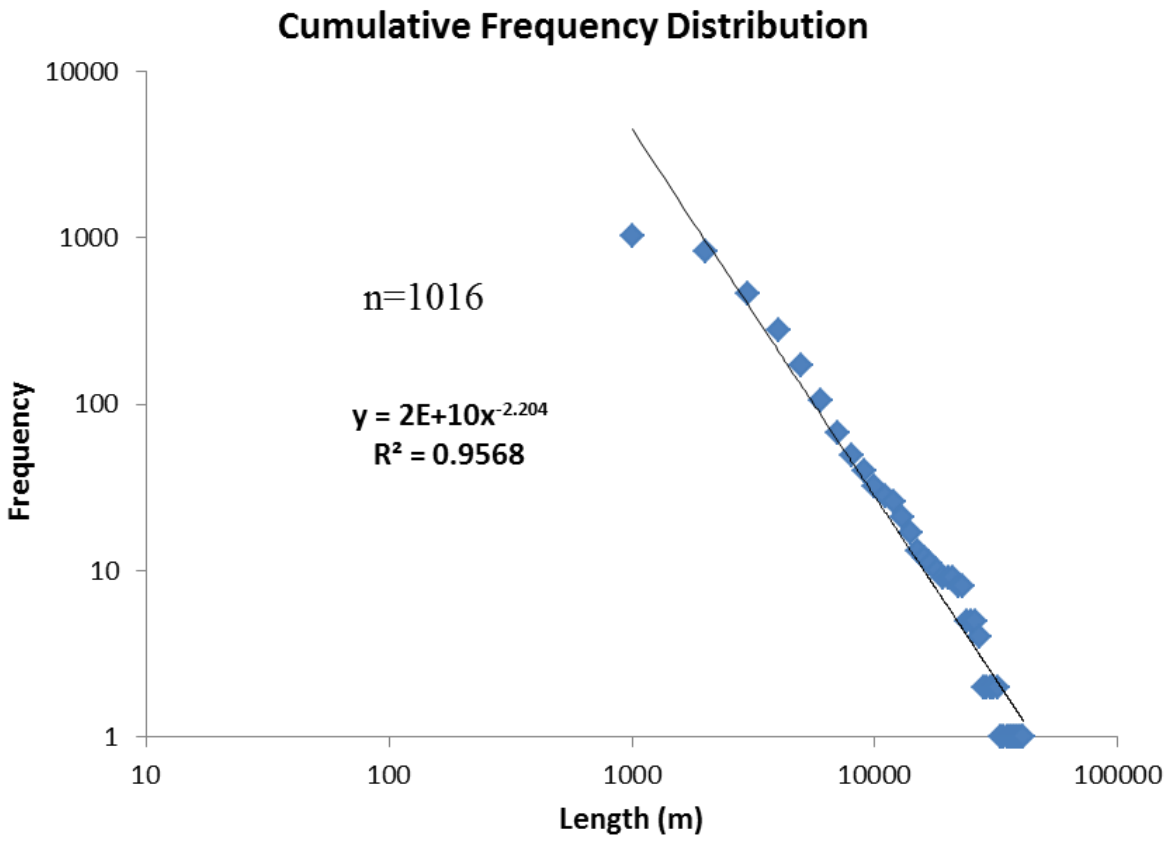

Figure 3.15: Cumulative frequency distribution of lineament trace lengths (power law distribution).

The joint frequency of lineament sets and their trace-lengths was established to define the length range for each lineament set Figure 3.16). The result showed that the northerly (including N-S, NNE-SSW, and NNW-SSE), NE-SW and NW-SE trending lineament sets are the most frequent within Wajid Group outcrop with a wide range of length. The NW-SE trending set of lineament (yellow color in Figure 3.16) is observed as a frequent lineament set with length range extending to 20 km. The northerly (including N-S, NNE-SSW, and NNW-SSE) lineament sets are frequent with length range extending to 15 km. The NE-SW trending lineament set is frequent with length range extending to 10 km.

On the contrary, the easterly (including E-W, ENE-WSW, and WNW-ESE) trending sets of lineament are frequent within a short range of length extending to 5 km. Based on the joint frequency analysis of lineament sets and their lengths (Figure 3.16), lineament traces within length less than 5 km occurred in a variety of trends and high frequency. However, the large-scale lineament traces with a length greater than 5 km are mostly associated with three major trends including the northerly (including N-S, NNE-SSW, and NNW-SSE), NE-SW, and NW-SE trends.

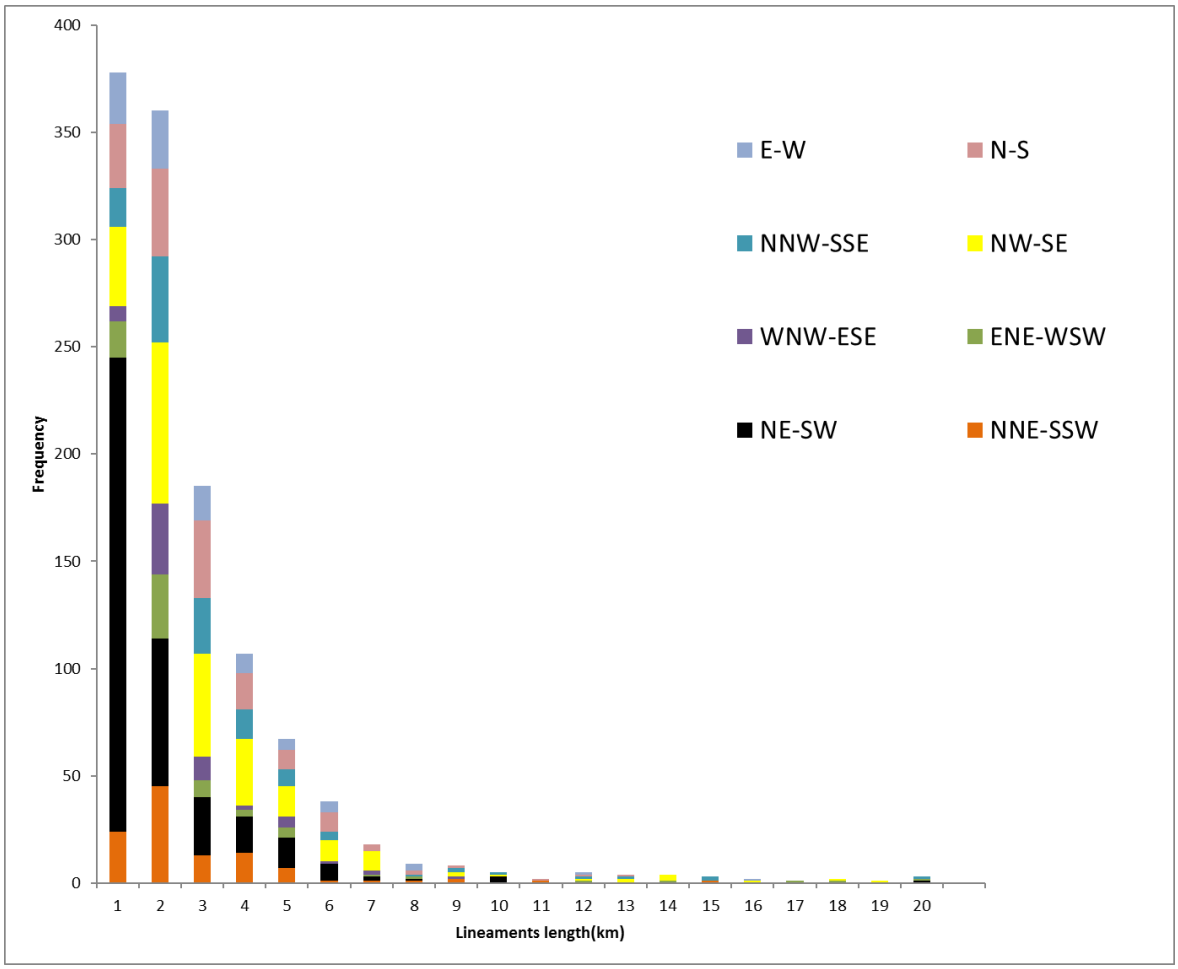

Figure 3.16: Joint frequency histogram shows the occurrence of lineament sets at different length classes.

3.5 Tectonic Implication of Lineament Analysis

Each lineament trend determined in this study may indicate a specific tectonic and structural setting. The northerly trending lineament traces found in the north, central and southern parts of the studied outcrop (including N-S, NNE-SSW, and NNW-SSE) are consistent with the N-S trending basement faults (Arabian trend) in the Ghawar oil field (Edgell, 1992; Hariri, 2008)(Figure 2.4). This trend of lineaments also corresponded to the N-S trending Nabitah suture zone in the southern part of the Arabian shield (Nehlig et al., 2002; Johnson & Stewart, 1995). This trend is most probably due to the E-W extensional tectonics (Edgell, 1992). The presence of the northerly trending lineaments within the Wajid Group outcrop (Cambrian to Permian) reflects the influence of the Precambrian basement structures on the sedimentary succession in the southwestern part of Saudi Arabia. Therefore, the repeated rejuvenation of the basement faults during the Phanerozoic Era is most probably exerted such lineament trends within the Wajid Group outcrop.

The E-W trending lineament traces most probably related to the E-W trending Precambrian basement structures reported by Edgell (1992). This trend might be generated by an N-S extension stress regime due to the initial updoming of the Arabian-Nubian Shield (Edgell, 1992).

The NW-SE trending lineament traces (predominant in the study area) are most probably inherited from the Precambrian basement structure, and related to the NW-SE trending left-lateral Najd Fault system which is exposed over 1100 km over the Arabian shield (Brown & Jackson, 1960), with 300 km left-lateral dislocation (Brown, 1972; Moore & Al-Shanti, 1979; Davies, 1984). It extends under the Phanerozoic age section across the

western part of Rub' Al-Khali Basin (the area of this study) (Brown, 1972; Husseini, 2000; Nehlig et al., 2002, Johnson & Stewart, 1995) (Figure 2.4). Moreover, this trend is also concordant with the NW-SE trending Infracambrian Graben system in the western part of the Rub' Al-Khali Basin reported by Dyer & Husseini, (1991) and Lange, (2006). This basement structure could have been reactivated during the Phanerozoic and hence produced such a lineament trend within the Wajid Group outcrop (Edgell, 1992; Lange, 2006; Dyer & Al-Husseini, 1991). The domination of such trend of lineament within Wajid Group outcrop reveals that the study area was significantly affected by the southern segment of Najd fault zones (Ruwah fault zone)(Figure 2.4)(Figure 2.5)(Figure 2.6).

The NE-SW trend of lineament traces within Wajid Group outcrop is consistent with the NE-SW trending basement suture zones within the Precambrian basement in Yemen which were formed during the Pan-African orogeny(Quick 1991; Windley et al., 1996; Whitehouse et al., 2001). Thus, the NE-SW trending lineament traces are most likely inherited from the NE-SW trending Precambrian basement structures.

Three major trends of aeromagnetic lineament traces including NW-SE(135^{o}), E-W(090^{o}), and N-S(000^{o}) observed in the Wajid Group outcrop (Figure 3.11), and they are consistent with the trends of aeromagnetic lineament traces in the southern part of the Arabian shield reported by Nehlig et al. (2002). The similarity between aeromagnetic lineament trace of Arabian Shield and Wajid Group outcrops reveals that the Wajid Group lineaments most probably inherited from Precambrian basement structures and reflect their influence on the sedimentary cover in the study area.

The occurrence of the NE-SW lineaments and fracture trend as a dominant trend in the western part of the studied area(Abha area) is most probably due to the dominance of the NE-SW fracture zones in the western part of the Arabia Shield((Nehlig et al., 2002; Stewart, 2016).

Chapter 4

Outcrop Fracture characterization

4.1 Introduction

The fracture system can provide a significant increase in reservoir permeability when the fractures are open and connected. It can have a major impact on the fluid flow behavior in the fractured reservoir(Nelson, 2001). Therefore, characterization of fracture system parameters(included orientation, aperture size, type, infilling materials, height and termination, spacing, cross-cutting relationship, and spatial distribution) of reservoir rock is important for understanding the fluid flow in fractured reservoir (Nelson, 2001;Odling et al., 1999; Bertotti et al., 2007). The natural fractures in sandstones as a role of mechanical stratigraphy was studied by many researchers(Fall et al., 2015; Guiton et al., 2003; Hooker et al., 2009; Hooker et al., 2014; Hooker et al., 2015; Odling, 1997; Olson et al., 2009; Ortega et al., 2006; Zahm & Hennings, 2009).Outcrop analogues are widely used to study the fracture systems of the fractured sandstone reservoirs(Olson et al., 2009; Nelson, 2001; Odling et al., 1999; Strijker et al., 2012; Bertotti et al., 2007; Sonntag et al., 2012; Hennings et al., 2000; Laubach & Ward 2006).

This chapter intended to investigate the outcrop-scale fracture systems within Wajid Group in the Wadi Al-Dawasir area, southwestern part of Saudi Arabia, where the four formations of Wajid Group are exposed. The fracture characteristics include the orientation, type, infilling materials, cross-cutting relationship were described in 15 outcrop stations (Figure 1.2). Other characteristics include the average fracture spacing, height, and fracture terminations were quantified in five outcrops stations (sub-vertical outcrops) (included S01, S03, S04, S10, and S13 in Figure 1.2) using the scanline

method. At the outcrop scale, three main fracture sets were identified as predominant; N165º, N015º, and N075º. However, the N135º and N035º are also present. The extensional fractures (mode 1) are the dominant type of fracture which formed the fracture system in Wajid Group outcrops. These fractures are mainly open and observed cutting across the whole outcrop in the vertical dimension. In some places, those fractures are filled or coated with calcite or iron oxides as the dominant filling material. Fracture swarms were also observed in the studied outcrops, and they oriented N015º.

4.2 Fracture Data Analysis

4.2.1 Fracture Orientation

Five sets of the outcrop-scale fractures were delineated include N015º, N165º, N075º, N135º, and N035º (Figure 4.1). However, the N015º, N165º, and N075º were observed as predominant fracture sets in the studied outcrops. The N165º and N075º were observed as dominant fracture sets in the northern part of the studied outcrops; however, in the southern part, the N015º is more dominant (Figure 4.1).

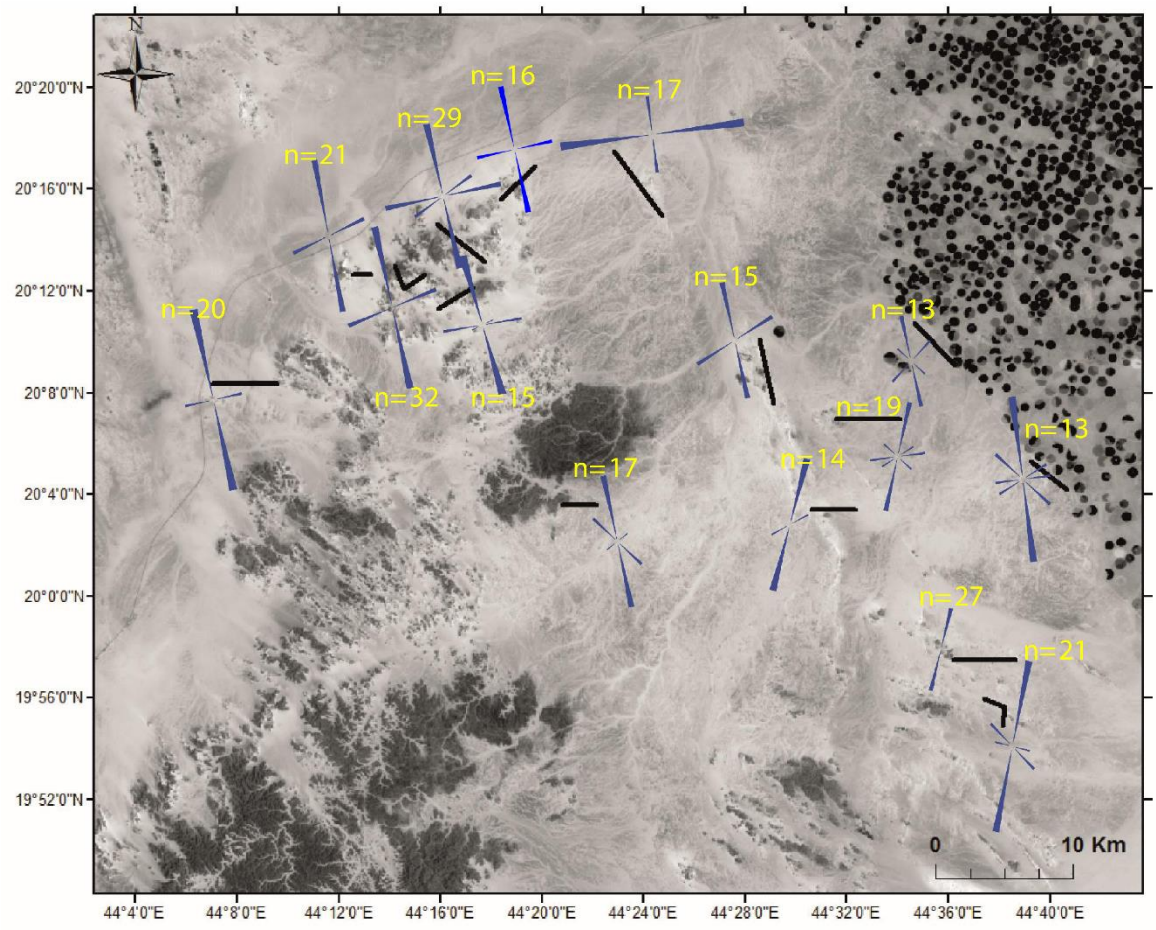

Figure 4.1: Fracture trends in 15 fracture stations (the dark line is the outcrop face direction)

4.2.2 Fracture Height and Termination

The heights of the N015º, N165º, and N075º oriented fracture sets were measured in five outcrop stations (included S01, S03, S04, S10, and S13 in Figure 1.2). The reported heights of non-strata-bounded fractures oriented N015º, N165º, and N075º were larger than the bed thickness and generally as large as the outcrop height (Figure 4.2); However, between those fractures, there were strata-bounded fractures observed with heights equal or less than bed thickness. The fracture terminations were observed at the bedding planes and inside the sandstone layers. The terminations at bedding planes were dominant,

particularly at the bedding plane between the fine and coarse-grained sandstone layers. The degree of fracture termination at bedding plane varied from one formation to another. The degree of fracture terminations at bedding plane in the well-stratified fluvial and shallow marine sandstone formations (Khusayyayn and Dibsiyah Formations) are higher than the poorly stratified glacial origin sandstone formations (Sanamah and Juwayl)(Figure 4.3).

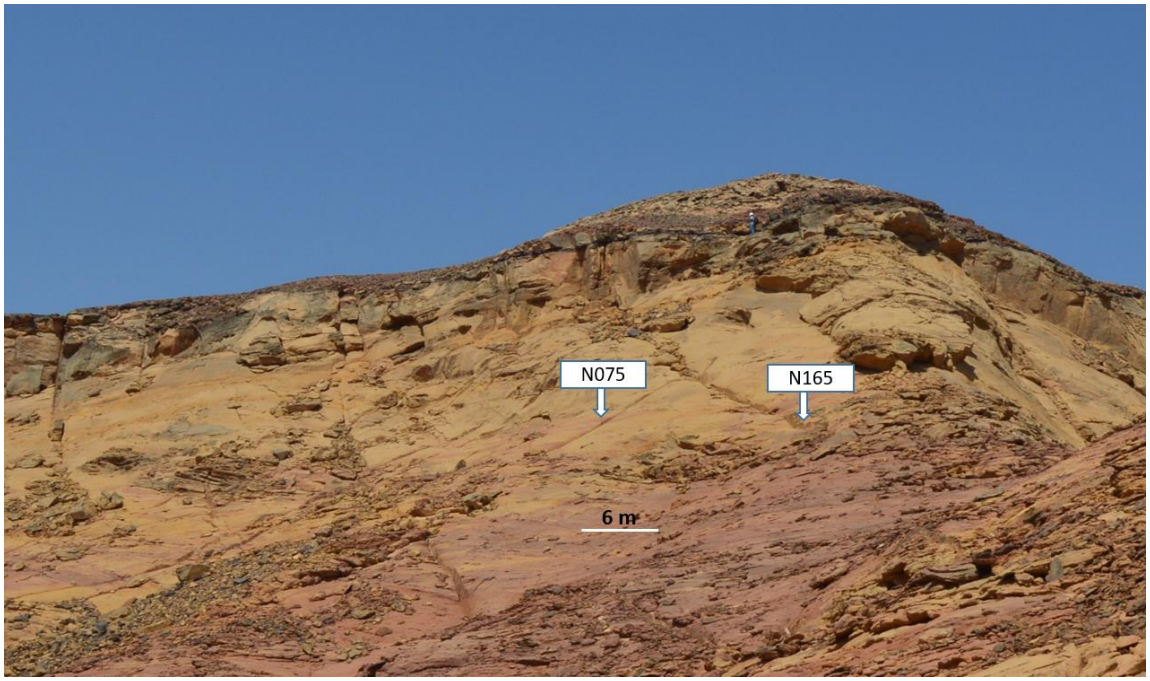

Figure 4.2: Two fracture sets (N165º and N075º) persisting along the vertical outcrop of Sanamah Formation (station S03).

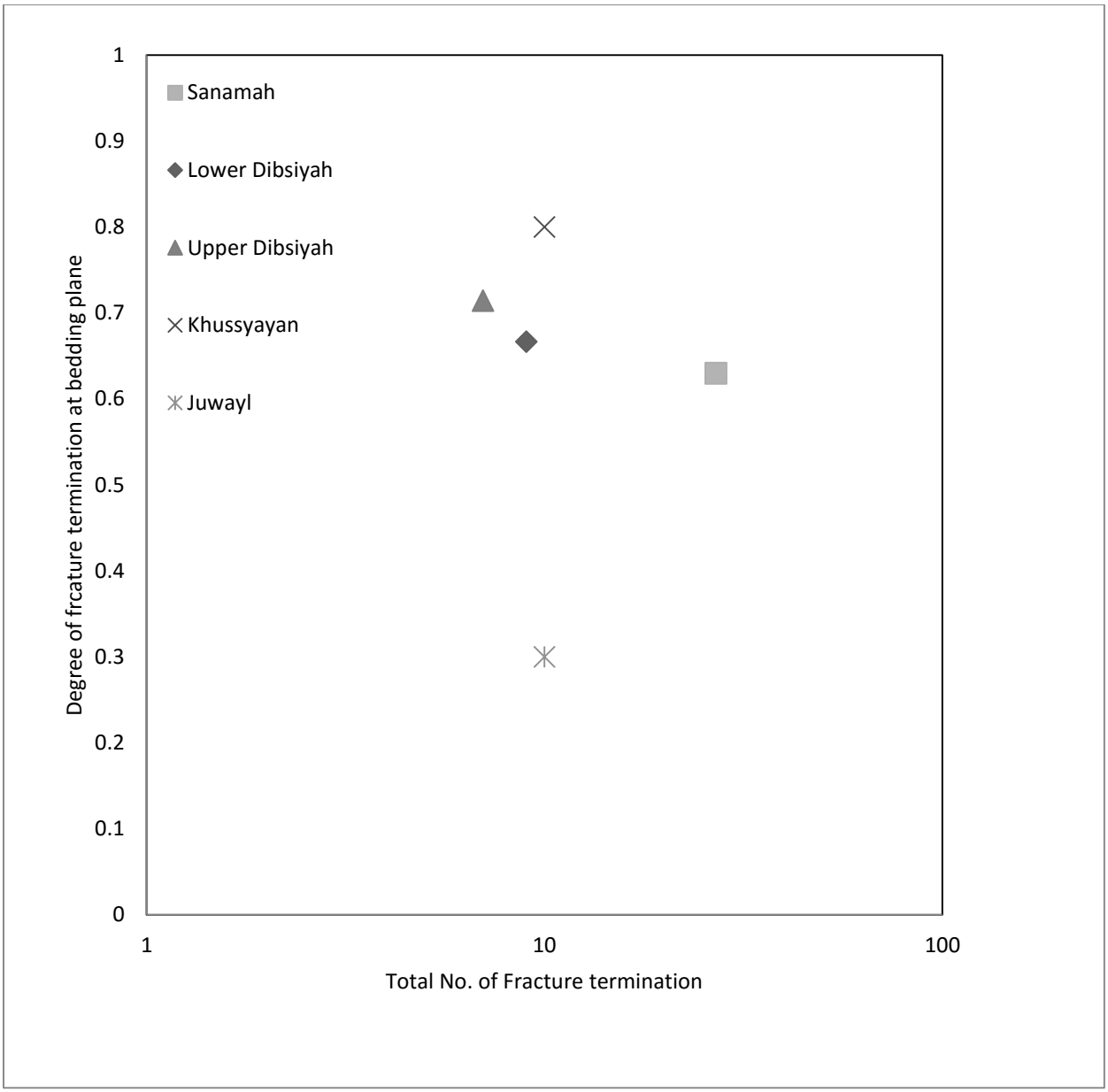

Figure 4.3: The degree of fracture termination at bedding plane versus a total number of fracture terminations within the outcrop for N165^{o} fracture set.

4.2.3 Fracture Spacing Analysis

Fracture spacing is an important quantitative fractures parameter that considered as a key parameter to predict fracture porosity and permeability in the fractured reservoirs (Nelson, 2001). The average fracture spacing was directly quantified from the outcrop in five outcrop stations (included S01, S03, S04, S10, and S13 in Figure 1.2) (Table 4.1) (Figure 4.4) using scanline oriented normal to the fractures strike. The average fracture spacing was quantified for N165^{o} oriented fracture set in the outcrop stations S01, S03, S04, and S10, and for N015^{o} oriented fracture set in outcrop station S13.

In the lower Dibsiyah Formation (station S01), the average fracture spacing was quantified for the N165o fracture set in 13 scanlines (Table 4.1). The reported results showed that the average fracture spacing ranges from 1.3-m to 2.8-m with an average spacing equal to 1.9-m (Figure 4 4). In the upper Dibsiyah Formation (station S04), the average fracture spacing of the N165o oriented fracture set ranges from 1.23-m and 15.2-m with an average value equal to 9.3-m (Figure 4 4). In the Sanamah Formation (station S03), the average fracture spacing of N165o ranges from 0.4-m and 16.4-m with an average value equal to 7.9 m (Figure 4 4). In the Khusayyayn Formation (station S10), The average spacing of N165o fracture set ranges from 0.35-m to 9-m with an average value equal to 5.8-m (Figure 4 4). In Juwayl Formation (station S13), the average fracture spacing of N015o fracture set ranges from 1.3-m to 11.6-m with an average value equal to 5.3-m (Figure 4 4).

Table 4.1: Table shows the number of scanlines and fractures in five outcrop stations.

Station Name	Scanline #	Length(m)	Fractures Intersected by Scanline
S01	SL1	22.5	11
	SL2	22.5	18
	SL3	22.5	10
	SL4	22.5	10
	SL5	22.5	10
	SL6	22.5	10
	SL7	22.5	16
	SL8	22.5	10
	SL9	22.5	16
	SL10	22.5	12
	SL11	22.5	9
	SL12	22.5	18
	SL13	22.5	4
S04	SL2	45.5	5
	SL3	45.5	7
	SL4	45.5	6
	SL5	3.8	3
	SL6	3.8	3
	SL8	7.6	7
S03	SL1	11	10
	SL2	6.5	2
	SL3	9.9	5
	SL4	9.5	6
	SL5	9.2	7
	SL6	8.1	3
	SL7	25	8
	SL8	24.6	15
	SL9	3	6
	SL10	2	5
S10	SL1	19	3
	SL2	19	3
	SL3	2.5	5
	SL4	9	3
	SL5	9	2
	SL6	12	4
	SL7	4.5	2
S13	SL1	35	4
	SL2	35	4
	SL3	5	5
	SL4	3.5	3
	SL5	2	1
	SL6	7	6

Generally, the increasing of the average fracture spacing is mainly associated with increasing in the sandstone bed thickness or increasing in sandstone grains size, or both. The braided river sandstone of lower Dibsiyah Formation displayed thin layers than the upper Dibsiyah Formation, and this associated with small values of average fracture spacing than the upper Dibsiyah Formation. The effect of sandstone grain size on the average fracture spacing was documented in the Sanamah Formation, where fine-grained sandstone in the uppermost part displayed small values of average fracture spacing than the coarse to conglomeratic sandstone in the lower part.

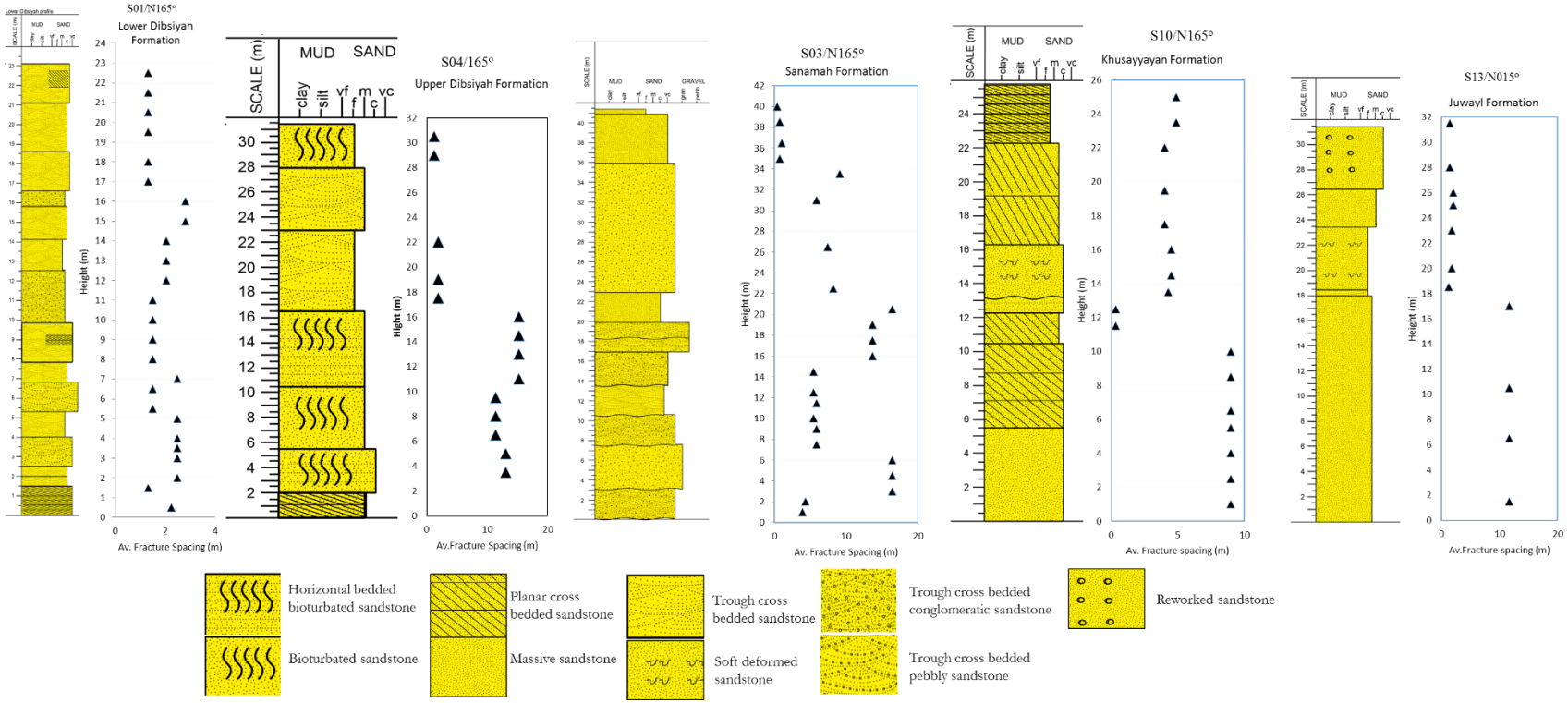

Figure 4.4: Vertical sedimentological logs and vertical profiles of average fracture spacing of lower Dibsiyah, upper Dibsiyah, Sanamah, Khusayyayn, and Juwayl Formations.

4.2.4 Fracture Type and Infilling Materials

The fracture type and infilling and coating material (44 readings) were characterized in Wajid Group outcrop. Most of the studied fractures are vertical to sub-vertical and open (mode I) (joints) (Figure 4.5). Some fractures are sealed either by iron oxides or calcite minerals or coated by iron oxides, or calcite minerals or both (the calcite coated the iron oxide)(Figure 4.5)(Figure 4.6). Moreover, reworked sandstone was observed as infilling material of the N035^{o} oriented fracture set in Khusayyayn Formation outcrop in station S11, and siltstone/clay was observed as the infilling material of the N135^{o} oriented fracture set in Khusayyayn Formation (station S11)(Figure 4.6). The distribution of fracture infilling materials in the studied outcrop with respect to fracture orientation was studied by establishing the joint histogram of fracture infilling materials and fracture orientation (Figure 4.7). The iron oxide minerals were observed in all sets of fractures, while the calcite infilling and coating material characterized the N015^{o}, N075^{o}, and N165^{o} oriented fracture sets(Figure 4.7).

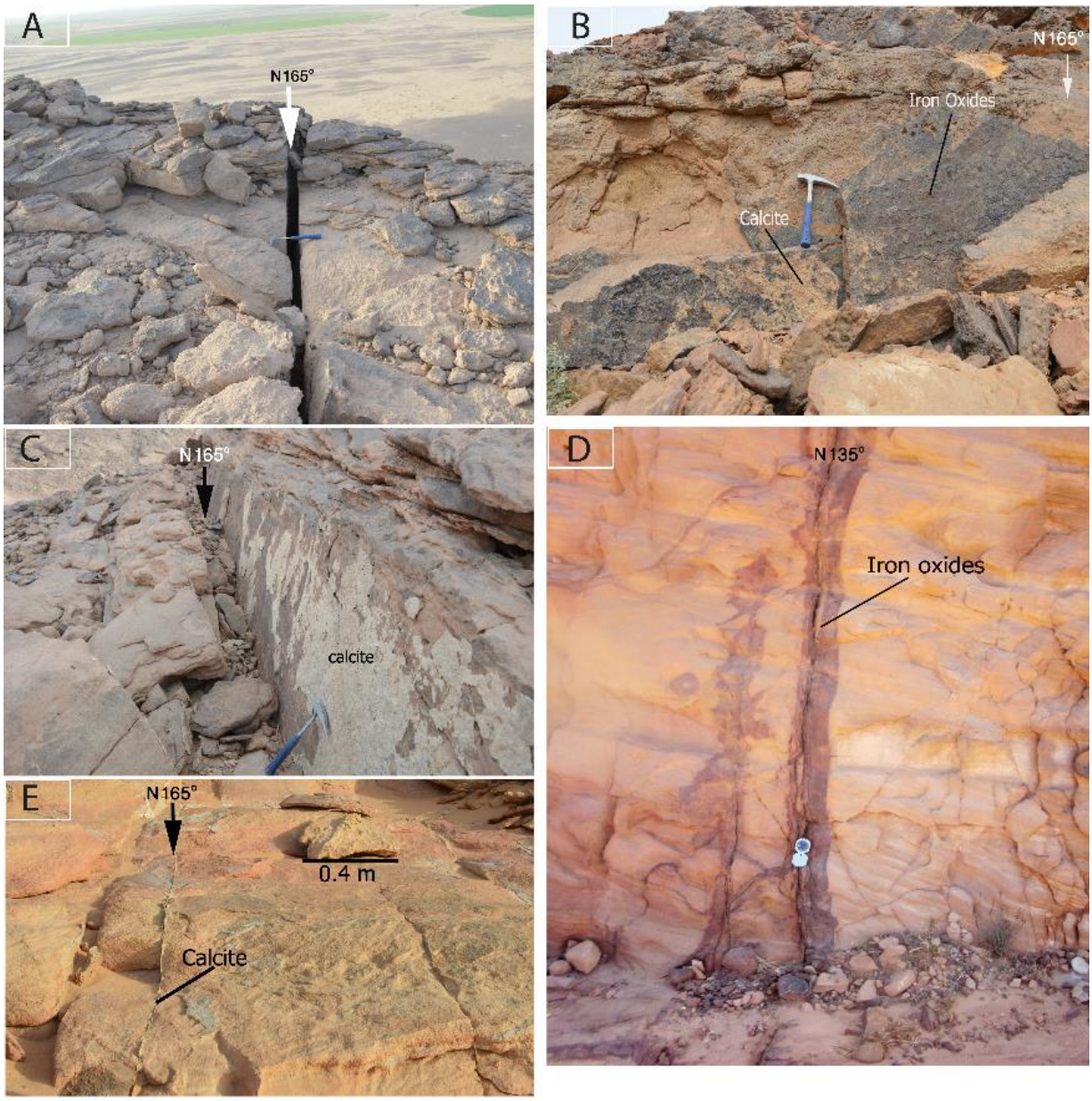

Figure 4.5: Outcrop photographs showing; A) Open fracture (joint). B) Iron oxides and calcite minerals coated the fracture surface. C) Calcite mineral coated the fracture surface. D) Iron oxide mineral infilled the fracture. E) Calcite mineral infilled fracture.

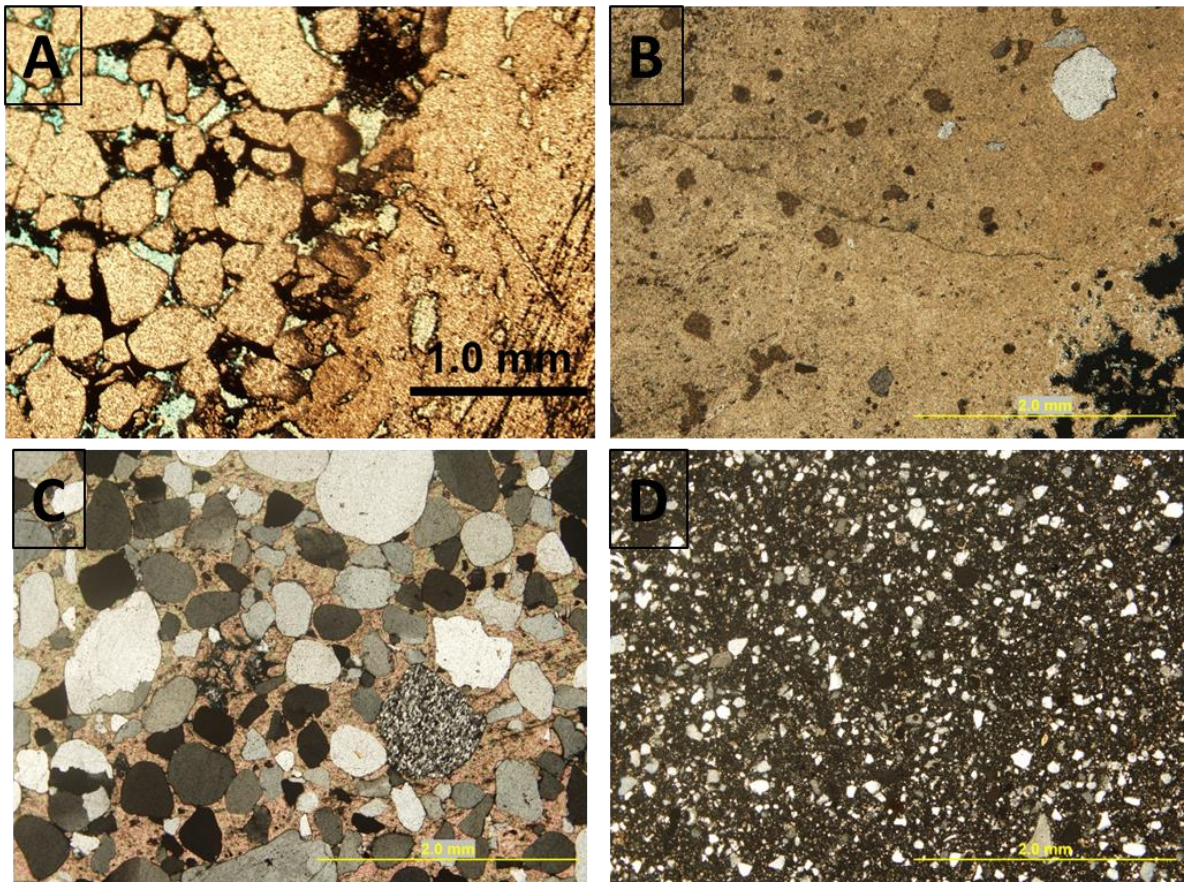

Figure 4.6: Microphotographs of fracture infilling material. A) Iron oxides, B) calcite, C) reworked sandstone, D) siltstone.

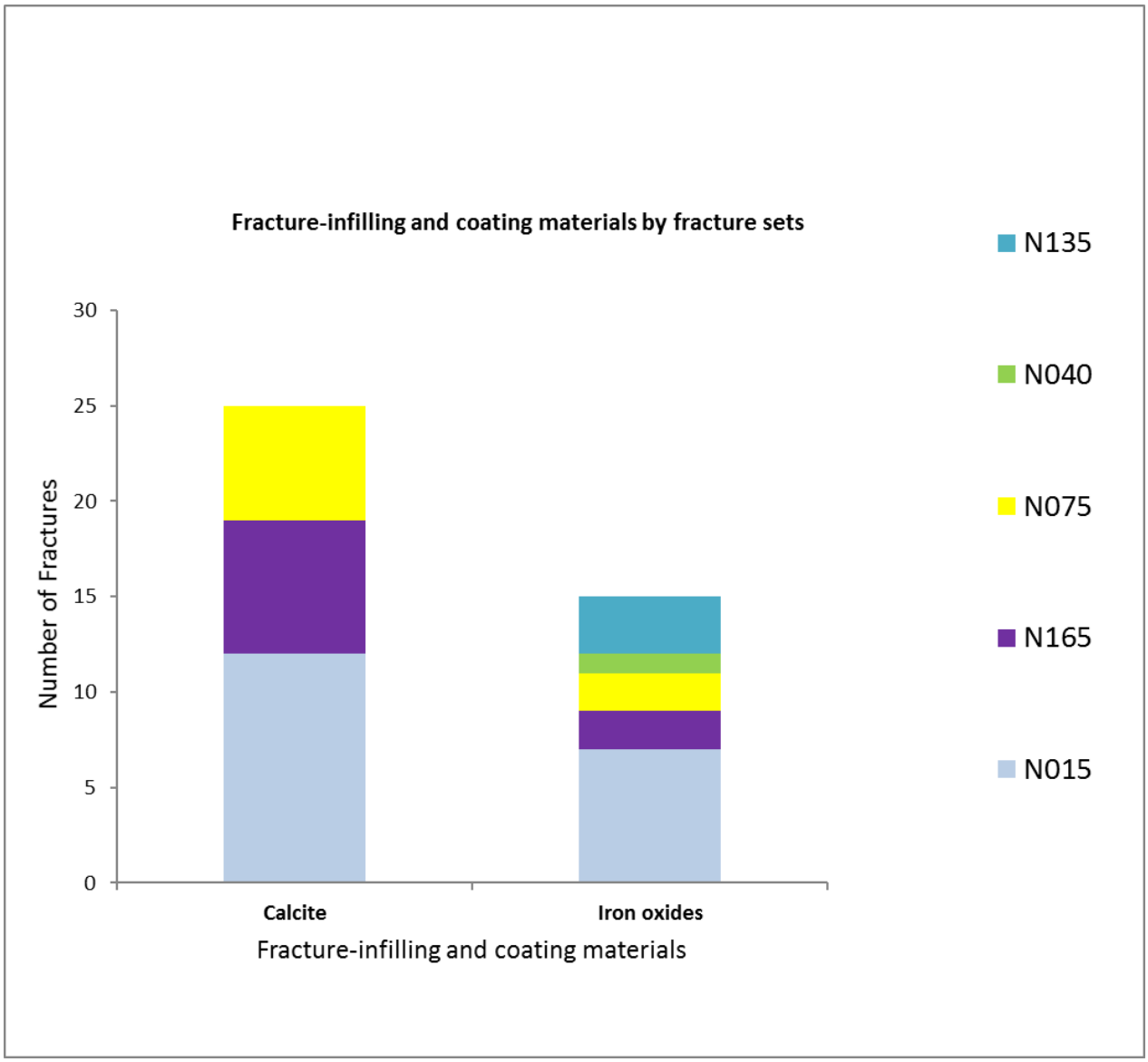

Figure 4.7: Column chart shows the frequency distribution of the fracture-infilling and coating materials for the entire Wajid Group outcrops (44 readings).

4.2.5 Fracture Swarms

Fracture swarms defined as a narrow (few meters), long, and continuous zone of intensive fractures which usually well developed and exposed where the sedimentary rock is massive and dense (Nelson, 2001; Peacock, 2001; Mandl, 2005). N015^{o} oriented fracture swarms were observed within Khusayyayn Formation outcrop in the eastern part of the study area (station S14), and they vertically extend and cutting across the entire succession of Wajid Group (Figure 4.8). Fracture swarms in the studied outcrops are mainly open fractures, and in some places, they are coated by iron oxide minerals. The density of fracture swarms is ten times higher than the density of the normal fracture pattern, and it is around 10 m^{-1} in the average in the studied outcrops (Figure 4.8).

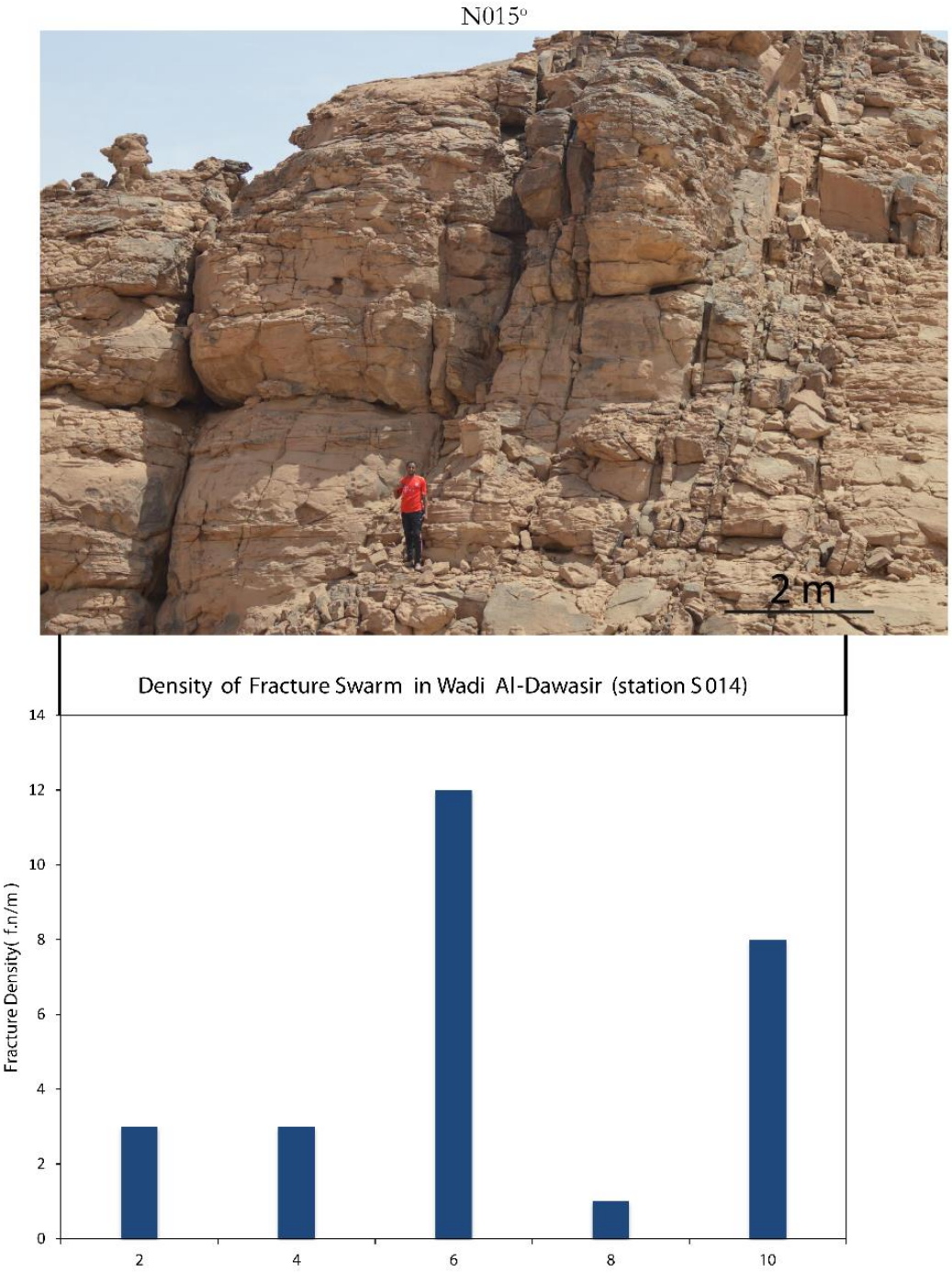

Figure 4.8: Fracture density profile across fracture swarms in the outcrop station S014, Khusayyayn Formation, Wadi Al-Dawasir area.

Chapter 5

Geomechanical Characterization

5.1 Introduction

Understanding the geomechanical behavior of Wajid Group sandstones is important for groundwater and hydrocarbon (unconventional resources) exploration and production from Wajid and Rub' Al-Khali Basins, respectively. In this chapter, the geomechanical characteristics of Wajid Group sandstones included rock strength (Schmidt reading number (RN) and the uniaxial compressive strength (UCS)) and static Young's Modulus (E) were characterized. The Schmidt reading number (RN) and the uniaxial compressive strength (UCS) are strength index of rock where high values indicate that the rock is strong and vice versa. The static Young's Modulus (E) is the stiffness index of the rocks, where, the rock with high values of static Young's Modulus (E) is more brittle than the rock with low values(Rickman, 2008). A further target of this chapter is to investigate the relationships between the geomechanical properties and the petrographic and petrophysical properties of the studied sandstones. These relationships will help to understand the distribution and intensity of the fractures in different lithological units and will help to establish predictive models of the geomechanical properties. Schmidt hammer rebound device was used to measure the strength of Wajid Group sandstones in the outcrop. In addition, the uniaxial compressive strength (UCS) of studied sandstones was measured in the laboratories using the uniaxial compression test equipment. The static Young's Modulus as rock brittleness and stiffness index was derived from the measured stress and strain values from a uniaxial compression test. The relationships between geomechanical properties and the petrographic and petrophysical properties of

the studied sandstones were established for Wajid Group sandstones as one succession and for each formation as well.

Strong relationships were observed between the geomechanical properties and the petrographic and petrophysical properties in the glacial origin sandstones of Sanamah and Juwayl Formations. On the contrary, the non-glacial origin sandstones from lower Dibsiyah (braided river), upper Dibsiyah (shallow marine), and Khusayyayn formations (fluvial) characterized by weak correlation between geomechanical, petrographic and petrophysical properties. Predictive models were established to account for the Schmidt readings number (RN), uniaxial compressive strength (UCS), and the static Young's Modulus (E). The whole succession of Wajid Group sandstone in the study area subdivided into 27 discrete mechanical units based on its geomechanical properties.

5.2 Geomechanical Properties Data Analysis

5.2.1 Schmidt Hammer Rebound Readings Number (RN)

The strength values of Wajid Group sandstones measured in the field using the Schmidt hammer rebound device and the results of Schmidt reading number (RN) are shown in Table 5.1. The highest values of the RN were observed in sandstone samples from Juwayl Formation with average values equal to 31.40. The values of the RN of sandstone samples from Dibsiyah Formation (lower and upper) and Khusayyayn Formation displayed similarity with an average value equal to 28.45 for Dibsiyah Formation and 29.85 for Khusayyayn Formation(Table 5.2). The smallest average value of RN (25.76) was observed in sandstone samples from Sanamah Formation, which indicate that the Sanamah Formation sandstone is weak.

The variability of RN values in the vertical dimension investigated by calculating the coefficient of variation (CV) as shown in Table 5.2. The variability of the RN values of sandstone samples from Juwayl and Sanamah Formation (CV equal to 0.28 and 0.23, respectively) is higher than the variability of RN values of lower Dibsiyah, upper Dibsiyah and Khusayyayn Formations (CV equal to 0.13, 0.14 and 0.15, respectively). Accordingly, the variation of RN values within the Sanamah and Juwayl Formations is higher than the variation within the other formations, which indicates that the lithological and diagenetic variation is high in Sanamah and Juwayl Formations than the other formations.

The RN values vertically fluctuated within Dibsiyah Formation outcrop and formed increasing upward cycles (small cycles in lower Dibsiyah Formation and large in upper Dibsiyah Formation)(Figure 5.1). The RN values increased upward in Sanamah Formation, with highest values in the uppermost of Sanamah Formation succession (Figure 5.1). In Khusayyayn Formation, the (RN) values are high in the lower and upper part of the section, and low in the middle part (Figure 5.1). In Juwayl Formation, the RN values are fluctuated from low in the lower part, high in the middle part, low in upper middle part, and high again in the uppermost part of the Juwayl succession(Figure 5.1).

5.2.2 Uniaxial Compressive Strength (UCS)

The uniaxial compressive strength (UCS) values for 82 sandstone samples from Wajid Group were obtained and the results shown in Table 5.1. The highest values of UCS were observed in sandstone samples from Juwayl Formation with an average value equal to 7.97 Mpa; however, sandstone samples from Sanamah Formation also showed high

average values of UCS (4.34 Mpa) (Table 5.1). On the contrary, the average values of UCS (3.42 Mpa for Dibsiyah Formation and 3.6 Mpa for Khusayyayn Formation) of sandstone samples from Dibsiyah Formation (lower and upper) and Khusayyayn Formations showed similarity and smaller than other formations(Table 5.2).

High variability of the UCS values observed in all sandstone samples; however, the highest variability characterized sandstone samples from Juwayl and Sanamah Formations (CV equal to 0.92, and 1.96, respectively) (Table 5.2). On the other side, the moderate variability of UCS values observed in the lower Dibsiyah, upper Dibsiyah and Khusayyayn Formations with CV equal 0.70, 0.86, and 0.65, respectively Table 5.2).

The UCS values within Dibsiyah Formation vertically oscillated due to the variation of sandstones texture and mineral composition with large cycles within upper Dibsiyah Formation(Figure 5.1). In Sanamah Formation, the UCS values formed a large increasing upward cycle with highest values in the uppermost of Sanamah formation succession (Figure 5.1). In Khusayyayn Formation, the UCS values are high in the lower and upper part of the section, and low in the middle part (Figure 5.1). In Juwayl Formation, the UCS values are fluctuated from low in the lower, high in the middle, low again in upper middle part, and high in the uppermost part of the studied section where the sandstones are highly cemented with calcite (Figure 5.1).

5.2.3 Static Young's Modulus (E)

The static Young's Modulus(E) values were determined for 82 sandstone samples from Wajid Group (Table 5.1). The highest values of static Young's Modulus were observed in sandstone samples from Juwayl Formation with an average value equal to 48.28 Gpa;

however, sandstone samples from Sanamah Formation also showed high average values of static Young's Modulus (38.10 Gpa). The values of the static Young's modulus of the Dibsiyah (lower and upper) and Khusayyayn Formations sandstones are almost similar with average equal to 31.92 Gpa for Dibsiyah and 32.81 for Khusayyayn Formations Table 5.2). The sandstone samples from glacial origin sandstone formations (Sanamah and Juwayl) displayed high average values of E than the non-glacial origin sandstone (Dibsiyah and Khusayyayn Formations) which indicate that the glacial origin sandstone is more brittle than the non-glacial origin sandstone.

In the vertical dimension, the values of static Young's Modulus (E) of lower Dibsiyah sandstones are fluctuated and formed small increasing upward cycles (Figure 5.1). In the upper Dibsiyah formation, the values of static Young's Modulus (E) of sandstone distributed in two increasing upward cycles as shown in Figure 5.1. The values of static Young's Modulus (E) of Sanamah Formation succession are low in lower and middle part and high at the uppermost units. In Khusayyayn Formation, the values of static Young's Modulus (E) of sandstones are high in lower and uppermost parts of the sandstone succession and low in the middle part. Within Juwayl formation, the values of static Young's Modulus (E) are low in the lower and upper middle parts of the succession and high at middle and uppermost parts (Figure 5.1). The reported variations in static Young's Modulus (E) value within Wajid Group sandstones are mainly due to variations in lithology, texture and diagenesis features of studied sandstones.

Table 5.1: Table shows the geomechanical properties of 82 sandstone samples fromWajid Group.

Formations	Samples	Schmidt Reading Number(RN)	UCS(Mpa)	Static Young's Modulus(Gpa)	Formations	Samples	Schmidt Reading Number(RN)	UCS(Mpa)	Static Young's Modulus(Gpa)
Juwayl	J3.5	41	19.93	120	Upper Dibsiyah	2UD18	27	1.76	9
	J3.4	21	1.94	20.3		2UD17	27	3.02	42.7
	J3.3	26	4.63	31.9		2UD16	22	0.24	8.8
	J3.2	40	10	47.2		2UD15	30	0.55	10.4
	J3.1	29	3.42	22		2UD14	32	2.11	14.8
Khussyayan	K1.7	29	6.43	59.7		2UD13	28	0.87	7.5
	K1.6	24	6.7	36		2UD12	28	1.13	10.1
	K1.5	24	2.36	16.3		2UD11	28	2.7	32.5
	K1.4	32	1.037	16		2UD10	28	5.3	82.9
	K1.3	32	1.39	8		2UD9	24	1.23	17.9
	K1.2	36	2.47	30.7		2UD8	36	2.75	15.2
	K1.1	32	4.98	63		2UD7	24	2.06	43.7
Sanamah	SUD22	45	33.69	130		2UD6	24	1.85	24.6
	SUD21	33	16.98	127.7		2UD5	27	0.41	29.7
	SUD20	26	0.4	20.7		2UD4	27	1.15	17.3
	SUD19	25	3.59	29.4		2UD3	25	0.12	3
	SUD18	22	3	34.27		2UD2	25	0.57	11.7
	SUD17	21	0.34	17		2UD1	17	0.63	13.1
	SUD16	23	1.5	12	Lower Dibsiyah	LD22	30	3.53	108.4
	SUD15	24	1.09	22.5		LD21	30	7.07	62.4
	SUD14	25	0.73	15.7		LD20	35	1.83	8.4
	SUD13	24	1.37	24.4		LD19	28	3.9	27.9
	SUD12	25	0.9	11		LD18	27	3.42	34.7
	SUD11	26	0.73	12.6		LD17	26	4.86	46.7
	SUD10	29	0.58	15.4		LD16	21	3.01	27
	SUD9	30	0.7	8		LD15	34	1.21	8.8
	SUD8	20	2.5	61.9		LD14	34	1.36	21.5
	SUD7	20	2.6	36.5		LD13	31	2.67	18
	SUD6	20	2.97	68.57		LD12	31	1.5	26.9
Upper Dibsiyah	D3.7	32	8.84	129.9		LD11	30	3.8	21.1
	D3.6	26	3.85	40.3		LD10	29	0.42	8
	D3.5W	33	2.3	15.2		LD9	30	9.33	18.2
	D3.5R	34	5.6	47.2		LD8A	30	8.1	37.3
	D3.4	30	1.38	23.3		LD7	29	3.8	26.6
	D3.3	30	3.11	40.6		LD6	30	1.96	24.5
	D3.2	30	3.11	39.5		LD5	34	1.24	8.2
	D3.1	31	8.31	98.4		LD4	20	0.81	11
	2UD23	34	6.81	27		LD3	24	6.22	41.4
	2UD22	32	6.4	56.5		LD2	26	5.24	74.4
	2UD20	25	3.76	28.5		LD1B	27	4.33	42.8
	2UD19	26	0.99	7.2		LD1	30	0.6	13.5

Table 5.2: Statistical parameters of geomechanical properties for all data and for each formation.

Formations	Parameters	Schmidt Reading Number(RN)	UCS(Mpa)	Static Young's Modulus(Gpa)
All Data	Nbr. of observations	82	82	82
	Minimum	17.00	0.12	3.00
	Maximum	45.00	33.69	130.00
	Range	28.00	33.57	127.00
	1st Quartile	25.00	1.14	14.90
	Median	28.00	2.49	24.55
	3rd Quartile	31.00	4.22	41.20
	Mean	28.20	3.68	33.96
	Standard deviation (n)	4.96	4.72	29.54
	Variation coefficient	0.18	1.28	0.87
Juwayl	Nbr. of observations	5	5	5
	Minimum	21.00	1.94	20.30
	Maximum	41.00	19.93	120.00
	Range	20.00	17.99	99.70
	1st Quartile	26.00	3.42	22.00
	Median	29.00	4.63	31.90
	3rd Quartile	40.00	10.00	47.20
	Mean	31.40	7.98	48.28
	Standard deviation (n)	7.86	6.56	37.11
	Variation coefficient	0.25	0.82	0.77
Khussyayan	Nbr. of observations	7	7	7
	Minimum	24.00	1.04	8.00
	Maximum	36.00	6.70	63.00
	Range	12.00	5.66	55.00
	1st Quartile	26.50	1.88	16.15
	Median	32.00	2.47	30.70
	3rd Quartile	32.00	5.71	47.85
	Mean	29.86	3.62	32.81
	Standard deviation (n)	4.16	2.20	20.07
	Variation coefficient	0.14	0.61	0.61
Sanamah	Nbr. of observations	17	17	17
	Minimum	20.00	0.34	8.00
	Maximum	45.00	33.69	130.00
	Range	25.00	33.35	122.00
	1st Quartile	22.00	0.73	15.40
	Median	25.00	1.37	22.50
	3rd Quartile	26.00	2.97	36.50
	Mean	25.76	4.33	38.10
	Standard deviation (n)	5.96	8.25	36.97
	Variation coefficient	0.23	1.90	0.97
Upper Dibsiyah	Nbr. of observations	32	32	32
	Minimum	17.00	0.12	3.00
	Maximum	36.00	8.84	129.90
	Range	19.00	8.72	126.90
	1st Quartile	25.75	1.10	12.75
	Median	28.00	2.21	25.80
	3rd Quartile	30.25	3.78	42.95
	Mean	28.19	2.92	34.98
	Standard deviation (n)	3.89	2.40	30.94
	Variation coefficient	0.14	0.82	0.88
Lower Dibsiyah	Nbr. of observations	23	23	23
	Minimum	20.00	0.42	8.00
	Maximum	35.00	9.33	108.40
	Range	15.00	8.91	100.40
	1st Quartile	27.00	1.43	15.75
	Median	30.00	3.42	26.60
	3rd Quartile	30.50	4.60	39.35
	Mean	28.96	3.49	31.20
	Standard deviation (n)	3.75	2.39	23.58
	Variation coefficient	0.13	0.69	0.76

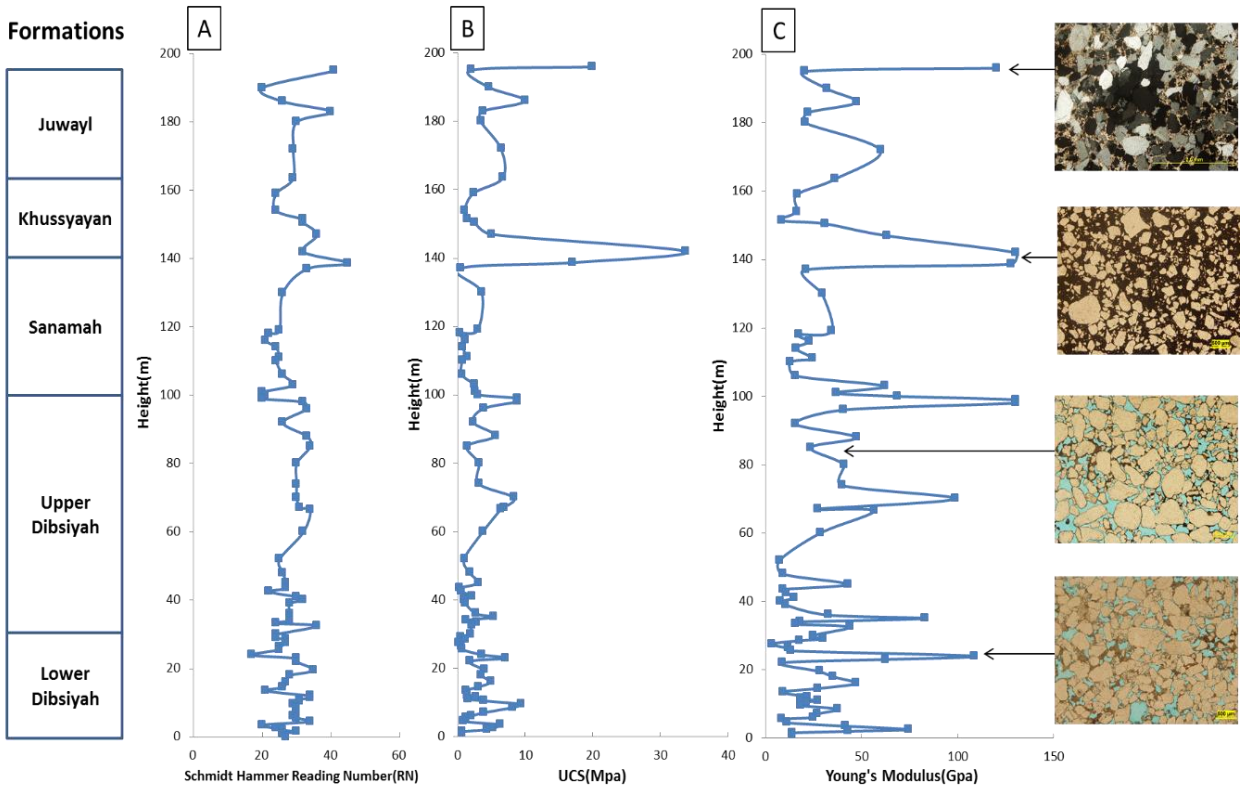

Figure 5.1: Vertical profiles of the geomechanical properties of Wajid Group sandstones associated with thin section microphotographs of the highest peaks, A)Schmidt hammer reading numbers(RN), B) uniaxial compressive strength(UCS(Mpa)), C) static Young's Modulus(Gpa).

5.3 Geomechanical Relationships with Petrographic and Petrophysical Properties

The Wajid Group sandstones showed variation in the petrographic and petrophysical properties (included mean grain size (mm), cement content (%), mineral composition, matrix porosity (%), and the matrix permeability (mD) (Table 5.3). This variation is associated with variation in the geomechanical properties (Schmidt reading number(RN), uniaxial compressive strength(UCS) and static Young's Modulus(E)) of the studied sandstone. Consequently, the relationships between geomechanical properties and the petrographic and petrophysical properties of the Wajid Group sandstone were obtained through correlation and linear regression analysis for the entire Wajid Group as one succession and for each formation (included lower Dibsiyah, upper Dibsiyah, Sanamah, Khusayyayn, and Juwayl Formations) as well.

5.3.1 Grain Size and Geomechanical Properties Relationship

Generally, a weak and negative correlation was observed between the mean grain size and geomechanical properties (included Schmidt reading number (RN), uniaxial compressive strength (UCS) and static Young's Modulus (E)) for the entire Wajid group as one succession. Strong and negative correlation was observed between the mean grain size and the Schmidt reading number (RN), uniaxial compressive strength (UCS) and static Young's Modulus (E) of sandstone samples from Juwayl Formation with The correlation coefficients equal to -0.79, -0.82 and -0.83, respectively (Table 5.4)(Figure 5.2). Weak correlation observed between mean grain size and the Schmidt reading number (RN), uniaxial compressive strength (UCS) and static Young's Modulus (E) of sandstone samples from Dibsiyah, Sanamah and Khusayyayan Formations (Table 5.4).

Predictive models for the Juwayl Formation have been established using linear regression, to account for the Schmidt reading number (RN), uniaxial compressive strength (UCS) and static Young's Modulus (E) with correlation coefficients equal to -0.79, -0.82 and -0.83, respectively (Figure 5.2). Thus, 79% of the variation in Schmidt reading number (RN), 82% in uniaxial compressive strength (UCS), and 83% in static Young's Modulus (E) can be described by the mean grain size (mm) (Figure 5.2).

Table 5.3: Table shows the petrographic and petrophysical properties of Wajid Group sandstones.

Formation	Sample	Mean Grain size (mm)	cement %	Porosity(%)	Permeability(mD)
Juwayl	J3.5	0.51	40	8.19	1.3168
	J3.4	0.49	5	31.69	389.803
	J3.3	0.22	4	32.85	422.649
	J3.2	0.18	10	27.67	112.751
	J3.1	0.32	7	28.29	302.7959
Khussyayan	K1.7	0.36	3	31.43	381.3234
	K1.6	0.55	2	33.50	430.1231
	K1.5	0.43	10	31.43	353.3627
	K1.4	0.52	4	34.33	407.1154
	K1.3	0.79	4	33.26	359.0759
	K1.2	0.44	5	34.55	352.216
	K1.1	0.48	5	29.11	319.3601
Sanamah	SUD22	0.41	40	2.34	0.2683
	SUD21	0.37	40	17.34	0.6476
	SUD20	0.51	8	38.44	204.0315
	SUD19	0.49	8		
	SUD18	0.51	9	33.38	186.5458
	SUD17	0.42	10	33.56	426.4009
	SUD16	0.58	4		
	SUD15	0.52	6	33.87	173.2567
	SUD14	0.56	25	34.27	171.6409
	SUD13	0.70	7		
	SUD12	0.48	8		
	SUD11	0.70	12		
	SUD10	0.49	5		
	SUD9	0.63	8		
	SUD8	0.71	11	30.55	254.0856
	SUD7	0.38	10	30.55	336.2455
	SUD6	0.29	7	33.13	476.4141
Upper Dibsiyah	D3.7	0.33	2	28.39	329.5125
	D3.6	0.45	3	32.65	413.2899
	D3.5W	0.21	10	32.48	334.5102
	D3.5R	0.22	10	34.02	352.859
	D3.4	0.24	15	28.37	453.7758
	D3.3	0.37	3	28.71	433.6607
	D3.2	0.52	4		
	D3.1	0.30	4	31.26	388.4805
	2UD23	0.44	25	26.08	405.9306
	2UD22	0.40	35	29.25	144.3517
	2UD20	0.47	38	43.05	53.7263
	2UD19	0.51	20	27.46	229.5549
	2UD18	0.25	31	28.07	87.14
	2UD17	0.61	20		
	2UD16	0.55	2		
	2UD15	0.44	20	34.94	219.4567
	2UD14	0.29	30	29.97	44.974
	2UD13	0.42	4		
	2UD12	0.35	4	41.64	548.313
	2UD11	0.27	20	29.84	128.835
	2UD10	0.47	3	28.88	379.3727
	2UD9	0.35	17	30.83	150.8318
	2UD8	0.37	7	25.99	140.922
	2UD7	0.58	18	33.66	157.1772
	2UD6	0.50	5		
	2UD5	0.62	5		
	2UD4	0.31	9	37.27	233.9164
	2UD3	0.57	5		
	2UD2	0.55	4		
	2UD1	0.45	6	39.75	144.6953
lower Dibsiyah	LD22	0.54	25		
	LD21	0.46	28	29.95	327.5907
	LD20	0.47	19	10.41	169.6312
	LD19	0.53	15	32.85	394.6075
	LD18	0.60	15	32.72	369.537
	LD17	0.35	20	29.33	107.97
	LD16	0.46	25	31.95	232.3229
	LD15	0.61	20		
	LD14	0.44	35	30.95	269.0447
	LD13	0.60	30		
	LD12	0.42	5	34.38	372.0399
	LD11	0.58	20	29.32	324.5624
	LD10	0.64	10	32.24	432.6143
	LD9	0.49	15	29.31	75.7313
	LD8A	0.48	30	31.11	13.5647
	LD7	0.65	29	31.55	342.6229
	LD6	0.72	30	29.94	400.4455
	LD5	0.31	11	29.15	339.9415
	LD4	0.56	12		
	LD3	0.31		26.24	313.1347
	LD2	0.35	25	26.01	2.0766
	LD1B	0.49		33.32	374.2505
	LD1	0.58	40	29.73	413.4977

Table 5.4: Correlation coefficients between geomechanical properties with petrographic and petrophysical properties of sandstone samples from Wajid Group.

Formations	All Data			Lower Dibsyah			Upper Dibsyah			Sanamah			Khussyayan			Juwayl		
Rock Properties	**Schmidt Reading Number(RN)**	**Uniaxial Compressive Strength(UCS)**	**Young's Modulus**	**Schmidt Reading Number(RN)**	**Uniaxial Compressive Strength(UCS)**	**Young's Modulus**	**Schmidt Reading Number(RN)**	**Uniaxial Compressive Strength(UCS)**	**Young's Modulus**	**Schmidt Reading Number(RN)**	**Uniaxial Compressive Strength(UCS)**	**Young's Modulus**	**Schmidt Reading Number(RN)**	**Uniaxial Compressive Strength(UCS)**	**Young's Modulus**	**Schmidt Reading Number(RN)**	**Uniaxial Compressive Strength(UCS)**	**Young's Modulus**
Cement(%)	0.33	**0.37**	0.22	0.08	0.01	0.12	0.10	0.05	-0.24	**0.82**	**0.82**	**0.78**	-0.21	-0.45	-0.31	**0.90**	**0.79**	**0.67**
Mean Grain Size(r	-0.20	-0.22	-0.21	0.10	**-0.33**	-0.26	**-0.51**	**-0.29**	-0.12	-0.15	-0.38	-0.47	-0.12	-0.41	-0.58	**-0.79**	**-0.82**	**-0.83**
Porosity(%)	**-0.58**	**-0.83**	**-0.63**	**-0.34**	0.03	0.12	**-0.52**	**-0.31**	**-0.22**	**-0.59**	**-0.94**	**-0.89**	0.23	-0.43	-0.65	**-0.78**	**-0.56**	**-0.40**
Permeability(mD)	-0.20	**-0.40**	-0.23	0.08	**-0.61**	**-0.39**	0.26	0.27	0.28	**-0.79**	**-0.67**	-0.55	**-0.42**	0.22	-0.22	**-0.94**	**-0.86**	**-0.81**

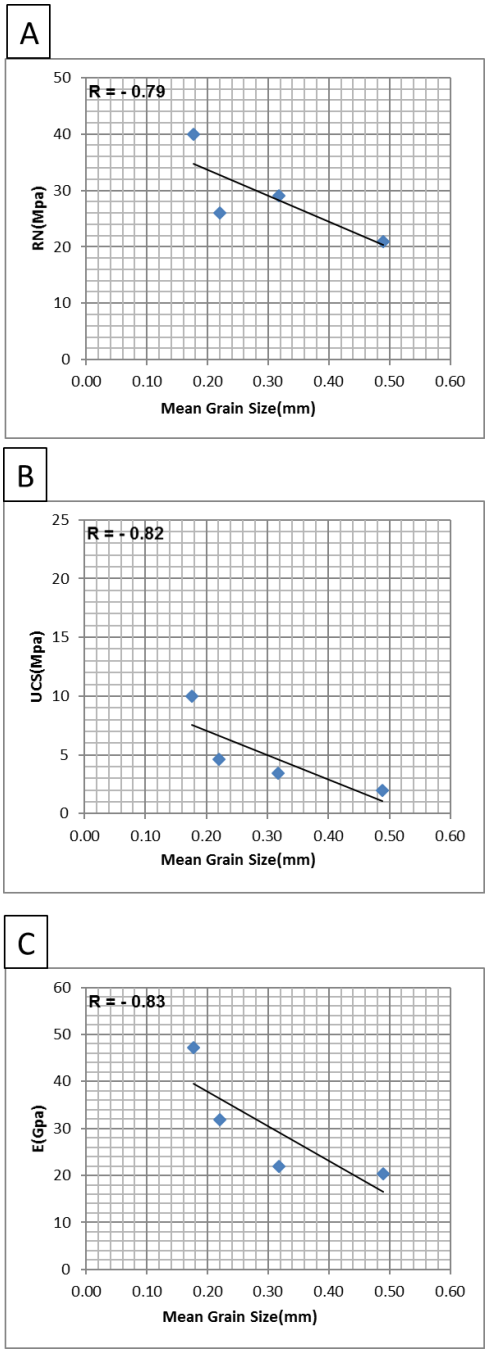

Figure 5.2: Scatterplot shows the linear relationship between mean grain size and A) Schmidt reading number (RN), B)uniaxial compressive strength (UCS), C)static Young's Modulus (E) of Juwayl Formation sandstones.

5.3.2 Cement Content and Geomechanical Properties Relationship

The Wajid Group sandstones contain cement materials including calcite, iron oxides, silica, and clay(Figure 5.3). The cement materials quantity ranges from traces to 40% of the sandstone framework. The relationships between the cement content and the geomechanical properties (included Schmidt reading number(RN), uniaxial compressive strength(UCS) and static Young's Modulus(E)) were established for the whole outcrop as one succession, and for each Formation as well (Table 5.4). The reported relationships between cement content and geomechanical properties (Schmidt reading number (RN), uniaxial compressive strength (UCS) and static Young's Modulus (E)) of Wajid Group outcrop as one succession is weak with correlation coefficients equal to 0.33, 0.37, and 0.22, respectively. Significant correlation was observed between cement content and the geomechanical properties of the sandstone sample from Sanamah and Juwayl Formations. As shown in (Table 5.4), the correlation coefficients between cement content and the Schmidt reading number (RN), uniaxial compressive strength (UCS) and static Young's Modulus (E) are 0.82, 0.82, and 0.78 for Sanamah Formation and 0.90, 0.79, and 0.67 for the Juwayl Formation, respectively. On the contrary, a weak correlation was observed between the cement content and the geomechanical properties of the sandstone samples from the other formations (included Dibsiyah and Khusayyayn Formations) (Table 5.4).

As shown in Figure 5.4, predictive models for Juwayl Formation have been established to account for the Schmidt reading number (RN), uniaxial compressive strength (UCS) and static Young's Modulus (E) with coefficients of correlation (R) equal to 0.90, 0.79, and 0.67, respectively. Thus, 90% of the variation in Schmidt reading number (RN), 79% in

uniaxial compressive strength (UCS), and 67% in static Young's Modulus (E) can be described by the cement content (%)(Figure 5.4). For Sanamah Formation, predictive models have been established to account for the Schmidt reading number (RN), uniaxial compressive strength (UCS) and static Young's Modulus (E) with coefficients of correlation (R) equal to 0.82, 0.82, and 0.78, respectively. Thus, 82% of the variation in Schmidt reading number (RN), 82% in UCS, and 78% in static Young's Modulus (Gpa) of sandstone samples from Sanamah Formation can be explained by the cement content (%) (Figure 5.4).

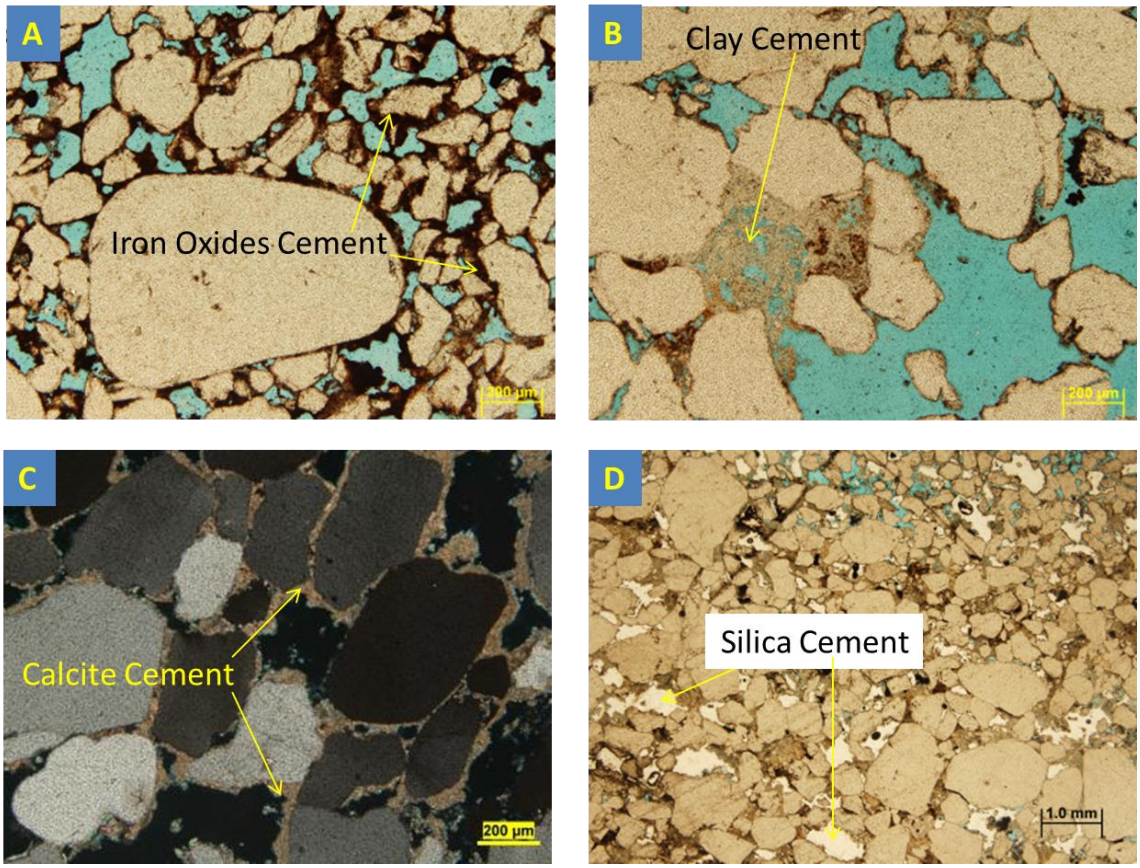

Figure 5.3: Microphotographs showing the cement type of sandstone samples from Wajid Group. A) iron oxides minerals, B) clay minerals, C) calcite mineral, and D) silica cement.

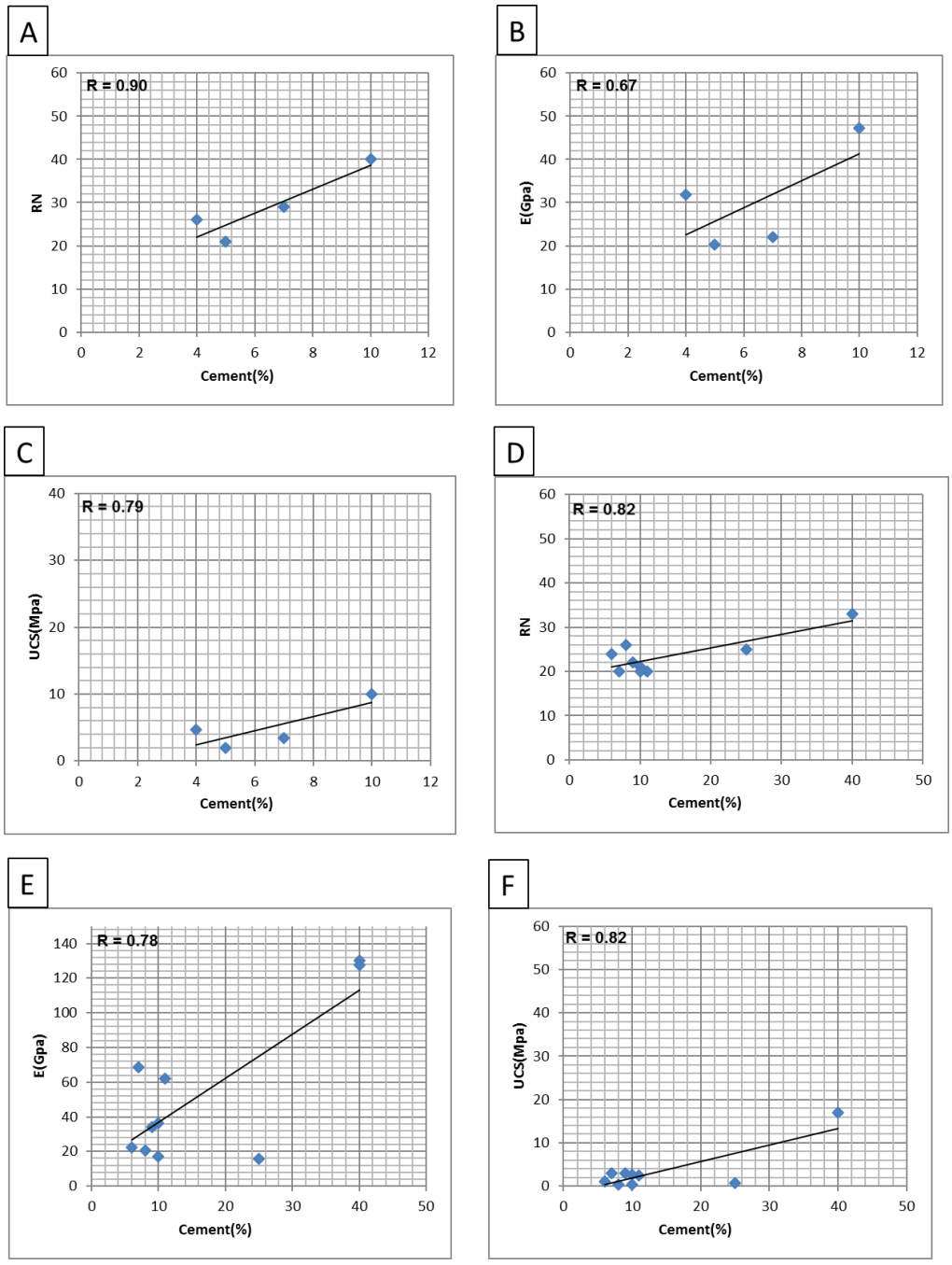

Figure 5.4: Scatterplots showing the linear relationship between cement content and geomechanical properties of Juwayl Formation(A, B, and C), and Sanamah Formation (D, E, and f)(Schmidt reading number(RN), uniaxial compressive strength(UCS), static Young's Modulus (E)).

5.3.3 Porosity and Geomechanical Properties Relationship

The relationships between matrix porosity and the geomechanical properties (Schmidt reading number (RN), uniaxial compressive strength (UCS) and the static Young's Modulus (E)) were constructed for each formation of Wajid Group. Significant correlation observed between the matrix porosity and geomechanical properties (Schmidt reading number (RN), uniaxial compressive strength(UCS)and the static Young's Modulus(E)) of sandstone samples from Sanamah and Juwayl formations, with correlation coefficient equal to -0.59, -0.94, -0.89 for Sanamah Formation and -0.78, -0.56, -0.40 for Juwayl Formation, respectively. However, weak correlation observed between the matrix porosity and geomechanical properties ((RN), (UCS) and (E)) of the upper Dibsiyah and Khusayyayn Formations with correlation coefficients equal to -0.52, -0.31, -.22 for upper Dibsiyah Formation, and -0.23, -0.43, -0.65 for Khusayyayn Formation, respectively. Moreover, weak relationships were observed between porosity and the geomechanical properties of lower Dibsiyah Formation sandstones (Table 5.4).

As shown in Figure 5.5, predictive models for Juwayl Formation have been established to account for the Schmidt reading number (RN), uniaxial compressive strength (UCS) and static Young's Modulus (E) with coefficients of correlation (R) equal to -0.78, -0.56, and -0.40, respectively. Thus, 78% of the variation in Schmidt reading number (RN), 56% in uniaxial compressive strength (UCS), and 40% in static Young's Modulus (E) can be described by the porosity (%).

For Sanamah Formation, predictive models have been established to account for the Schmidt reading number (RN), uniaxial compressive strength (UCS) and static Young's Modulus (E) with coefficients of correlation (R) equal to -0.59, -0.94, and -0.89,

respectively (Figure 5.6). Thus, 59% of the variation in Schmidt reading number(RN), 94% in uniaxial compressive strength(UCS), and 89% in static Young's Modulus (E) of sandstone samples from Sanamah Formation can be explained by the porosity.

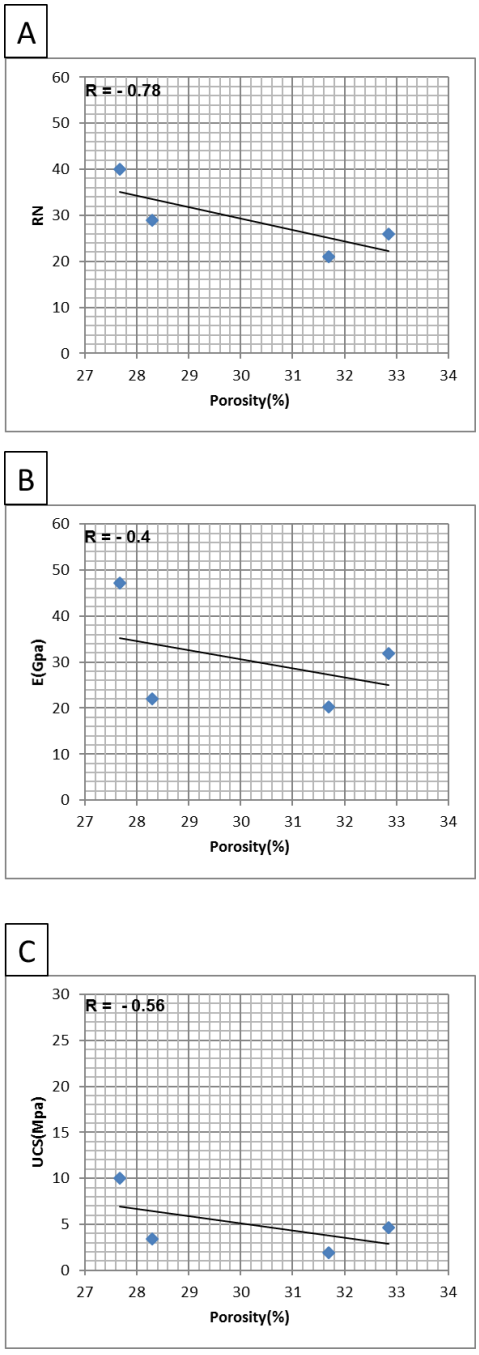

Figure 5.5: Scatterplots showing the linear relationship between porosity and geomechanical properties of Juwayl Formation (Schmidt reading number(RN), uniaxial compressive strength(UCS), static Young's Modulus (E)).

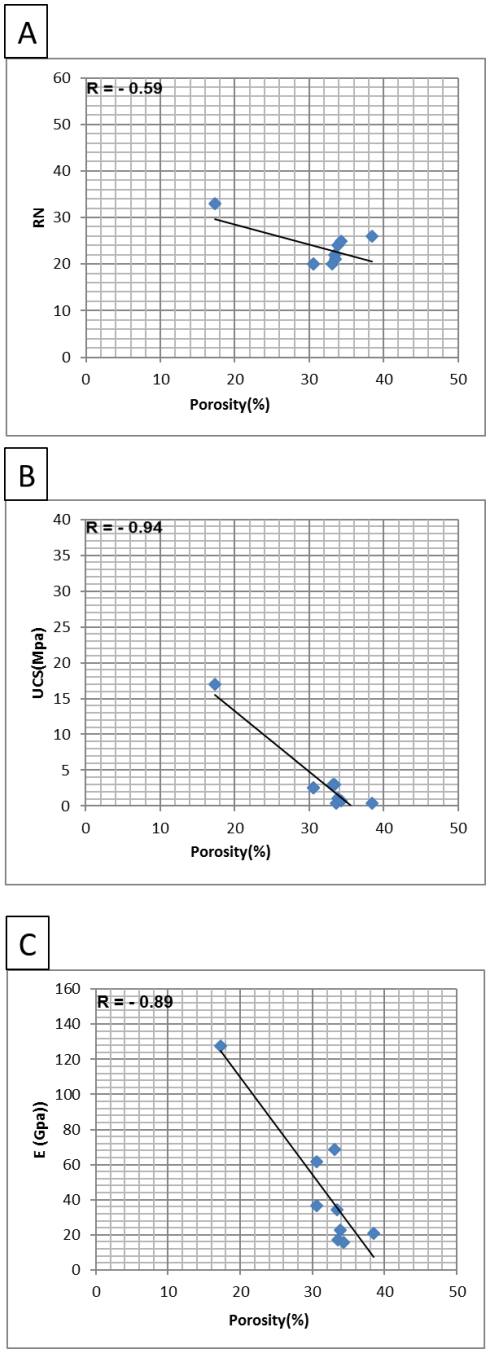

Figure 5.6: Scatterplots showing the linear relationship between porosity and geomechanical properties of Sanamah Formation (Schmidt reading number(RN), uniaxial compressive strength(UCS), static Young's Modulus (E)).

5.3.4 Permeability and Geomechanical Properties

The relationships between the matrix permeability and the geomechanical properties were investigated for the entire Wajid Group sandstones and for each formation as well (Table 5.4). Weak and negative correlation observed between the matrix permeability and the Schmidt reading number(RN), and the static Young's Modulus(E), and moderate with uniaxial compressive strength(UCS) of sandstone samples from the entire Wajid Group with correlation coefficients equal to -0.20, -0.23, and -0.4 respectively (Table 5.4). Significant correlation observed between the permeability and the Schmidt reading number(RN), uniaxial compressive strength(UCS) and the static Young's Modulus(E) properties of sandstone samples from Juwayl Formations with correlation coefficients equal to -0.94, -0.86, and -0.81 (Table 5.4)(Figure 5.7). Moreover, a moderate correlation observed between the permeability and the Schmidt reading number(RN), uniaxial compressive strength(UCS) and the static Young's Modulus(E) properties of Sanamah Formation with correlation coefficients equal to -0.79, -0.67, -0.55.

Weak relationships were observed between the permeability and the Schmidt reading number (RN), uniaxial compressive strength (UCS) and the static Young's Modulus (E) of sandstones sample from Dibsiyah and Khusayyayn Formations. However, there is a moderate correlation was observed between the uniaxial compressive strength(UCS) and the permeability of the lower Dibsiyah sandstone samples with correlation coefficient equal to -0.61.

Since the strongest relationship between permeability and geomechanical properties were observed in Juwayl Formation, then predictive models have been established to account for the Schmidt reading number (RN), uniaxial compressive strength (UCS) and static Young's Modulus (E) with coefficients of correlation (R) equal to -0.94, -0.86, and -0.81, respectively (Figure 5.7). Thus, 94% of the variability of the Schmidt reading number (RN), 86% of uniaxial compressive strength (UCS), and 81% of static Young's Modulus (E) can be explained by the permeability (mD).

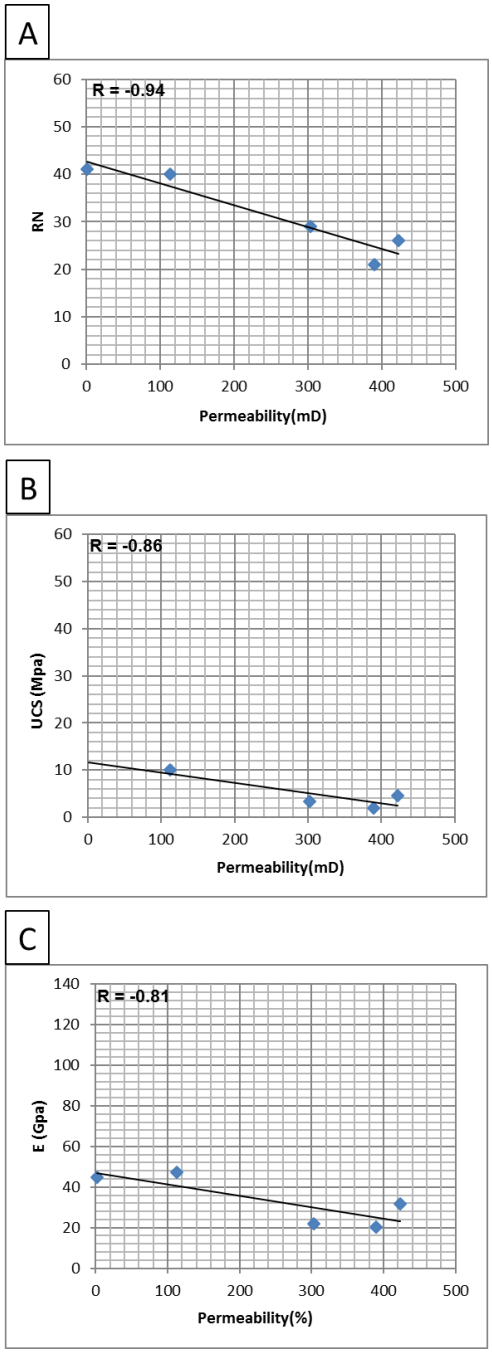

Figure 5.7: Scatterplots showing the linear relationship between permeability and geomechanical properties of Juwayl Formation, A)Schmidt reading number(RN), B)uniaxial compressive strength(UCS), c)static Young's Modulus (E).

5.4 Mechanical versus Lithological Units

Stratified rock can be divided into discrete mechanical units based on its geomechanical properties such as strength, elastic stiffness, brittleness (Laubach et al., 2009). Based on this concept, the whole succession of Wajid group in the study area subdivided into 27 discrete mechanical units defined by the rock strength (UCS) and elastic stiffness (static Young's Modulus(E)). The correlation between lithological and mechanical units has been conducted for each formation of Wajid Group.

The lower Dibsiyah Formation (23-m thick) which consists of 15 lithological units has been subdivided into seven mechanical units (Figure 5.8). The result showed that most of the mechanical units correlated with more than one lithological units, except mechanical unit1 (MU1 in Figure 5.8) associated with only one lithological unit (LU1 in Figure 5.8) (Figure 5.8).

The upper Dibsiyah Formation (44-m thick) consists of 14 lithological units have been divided into eight mechanical units (Figure 5.8). The mechanical units of upper Dibsiyah Formation associated with one or more than one lithological units, such as mechanical unit 4 (MU4 in Figure 5.9) corresponded with three lithological units (unit 7, 8 and 9) (Figure 5.9).

The Sanamah Formation (41.5-m thick) consists of ten lithological units has been subdivided into five mechanical units (Figure 5.10). The mechanical units correlated with the lithological units and the results showed that some of the mechanical units correlated with more than one lithological unit. The mechanical unit 2(MU2 in Figure 5.10) associated with four lithological units, namely unit 2-6 in Figure 5.10). Thus, the

correlation indicated that this mechanical unit associated with pebbly to conglomeratic sandstone layers. The mechanical unit 5(MU5 in Figure 5.10) characterized by high values of uniaxial compressive strength(UCS), and static Young's Modulus (E) and associated with highly cemented fine to medium grained sandstone layers (lithological units (LU9 and LU10)). Generally, the uppermost part of Sanamah Formation mechanically displayed high values of uniaxial compressive strength (UCS), and static Young's Modulus (E) comparing to the lower and middle parts due to the high concentration of cemented materials. The Khusayyayn Formation sandstones (26-m thick) which consist of seven lithological units has been subdivided into three mechanical units (Figure 5.11). The mechanical unit 1(MU1 in Figure 5.11) associated with the coarse-grained massive sandstone layers (lithological units (LU1 and LU2) in Figure 5.11). The mechanical unit 2(MU2 in Figure 5.11) correlated with coarse-grained planar cross-bedded, coarse-grained horizontal bedded, and coarse-grained deformed sandstone Lithofacies (lithological units (LU3, LU4, and LU5) in Figure 5.11) in the middle part of the lithological log (Figure 5.11). The mechanical unit 3(MU3 in Figure 5.11) associated with medium to coarse-grained planar cross-bedded sandstone and fine to medium-grained small scale planar cross-bedded sandstone (lithological units LU6 and LU7 in Figure 5.11) (Figure 5.11). The Juwayl Formation sandstone succession (32.5-m thick) consist of five lithological units and has been divided into four mechanical units (Figure 5.12). The mechanical unit 1(MU1 in Figure 5.12) associated with the medium-grained massive sandstone layer (lithological unit (LU1 in Figure 5.12). The mechanical unit 2(MU2 in Figure 5.12) correlated with fine-grained small scale trough cross-bedded sandstone Lithofacies (lithological unit (LU2 in Figure 5.12). The mechanical unit

3(MU3 in Figure 5.12) correlated to fine to medium-grained soft deformed sandstone, and medium-grained massive sandstone Lithofacies (lithological units (LU3 and LU4 in Figure 5.12) (Figure 5.12). The coarse-grained, highly cemented reworked sandstone Lithofacies (lithological unit (LU5 in Figure 5.12) in the upper part of Juwayl succession correlated with the mechanical unit 4(MU4 in Figure 5.12).

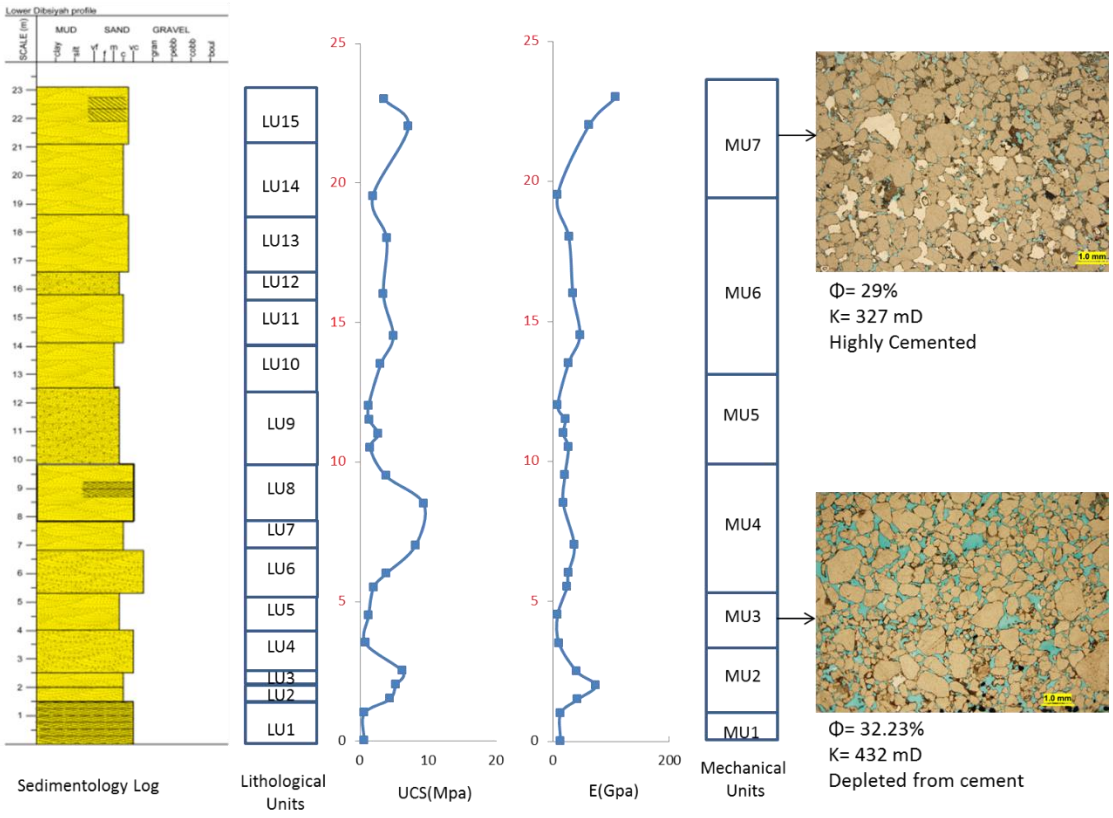

Figure 5.8: Lithological and Mechanical units of the lower Dibsiyah Formation succession associated with thin section microphotographs showing cement, porosity (Φ), and permeability (k) of different type of sandstones(UCS= uniaxial compressive strength, E = static Young's modulus).

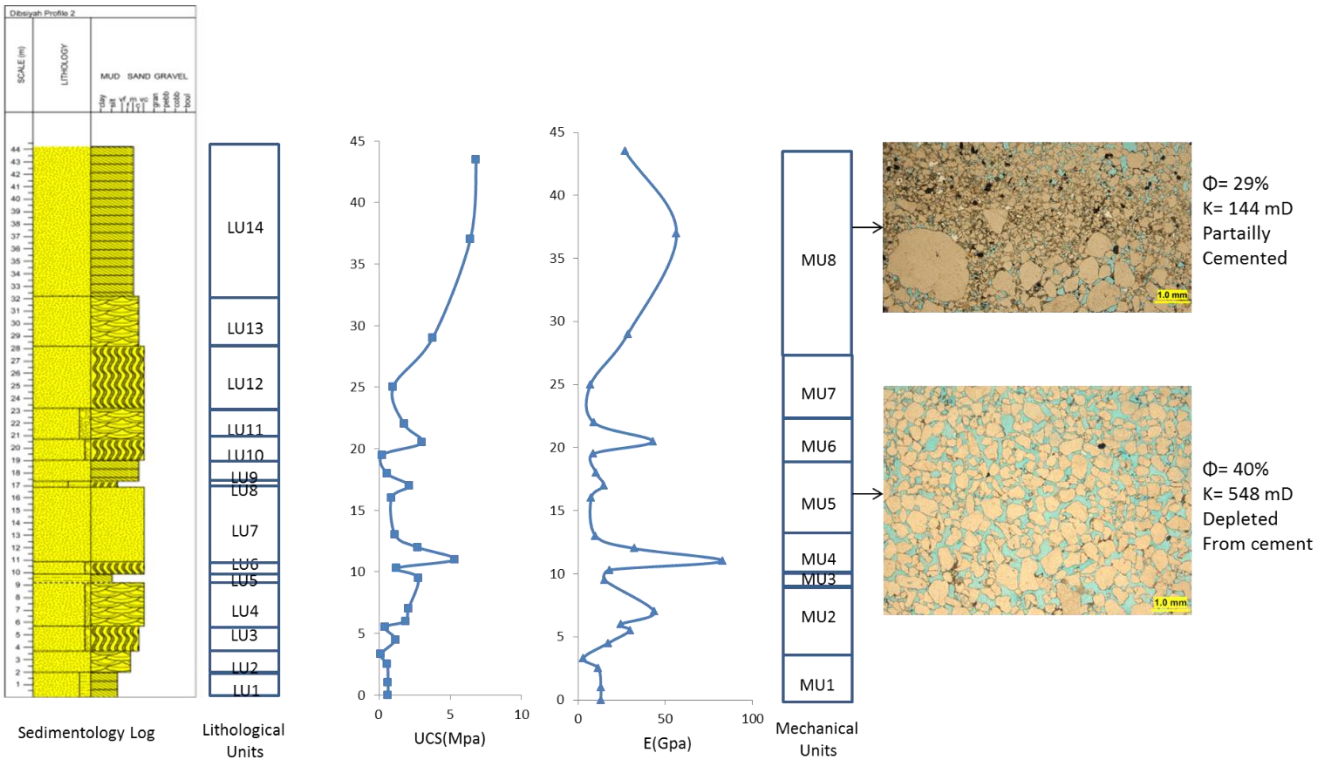

Figure 5.9: Lithological and Mechanical units of the upper Dibsiyah Formation succession associated with thin section microphotographs showing mean grain size, cement, porosity (Φ), and permeability (k) of different type of sandstones(UCS= uniaxial compressive strength, E = static Young's modulus).

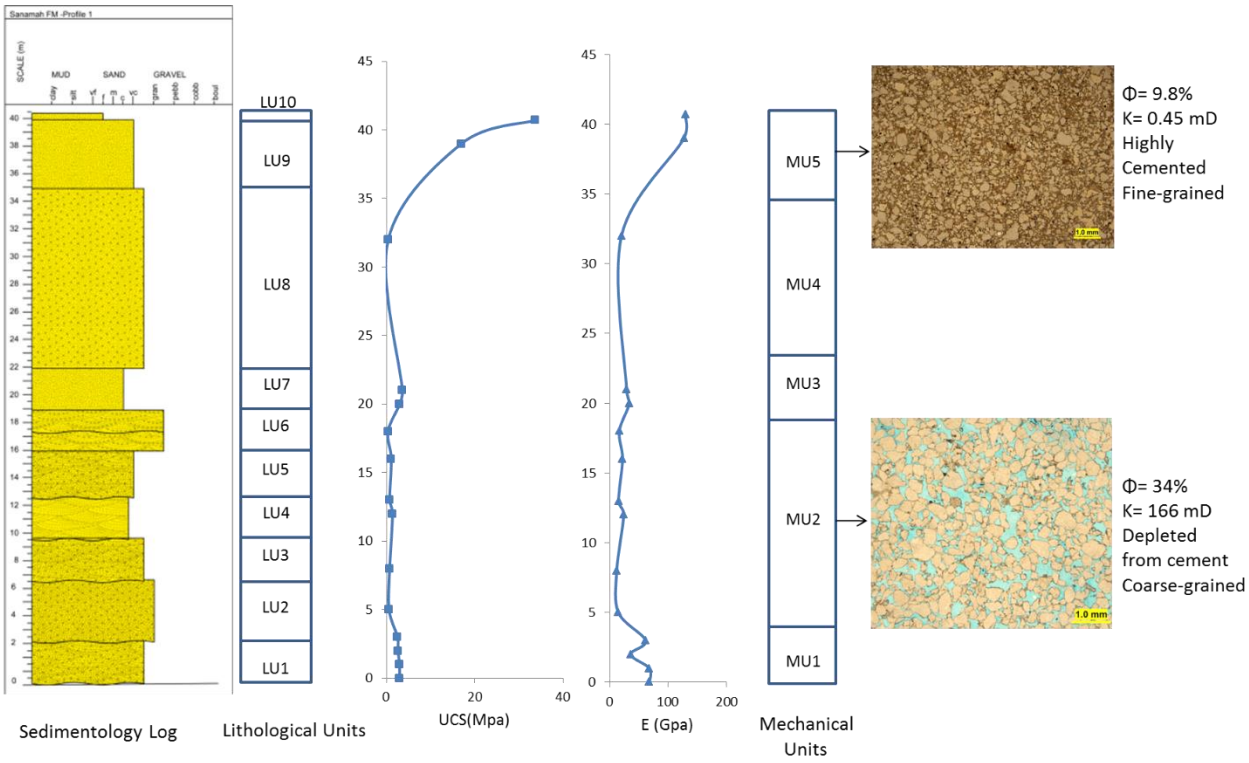

Figure 5.10: Lithological and Mechanical units of the Sanamah Formation succession associated with thin section microphotographs showing mean grain size, cement, porosity (Φ), and permeability (k) of different type of sandstones.(UCS= uniaxial compressive strength, E = static Young's modulus).

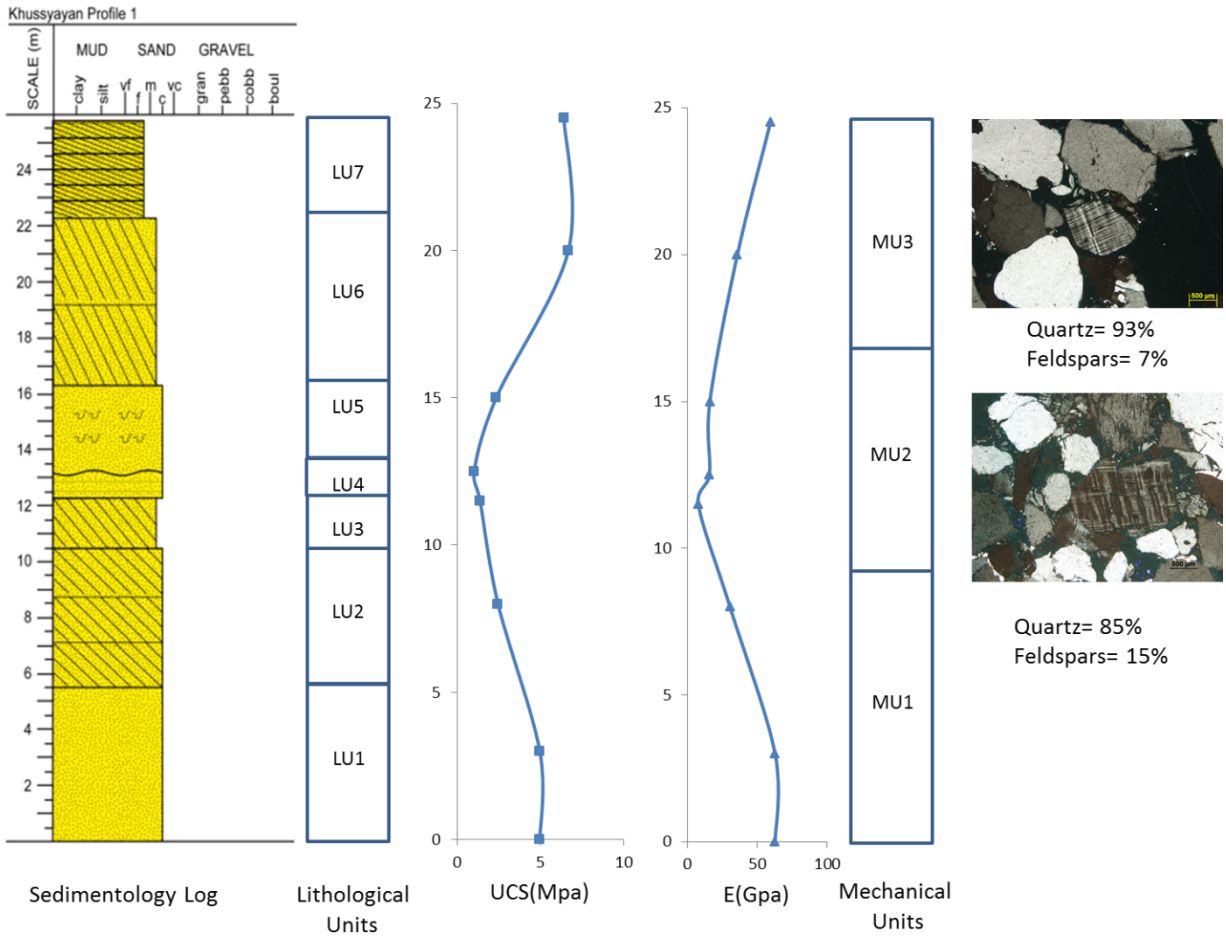

Figure 5.11: Lithological and Mechanical units of the Khusayyayn Formation succession associated with thin section microphotographs showing different mineral composition. (UCS= uniaxial compressive strength, E = static Young's modulus).

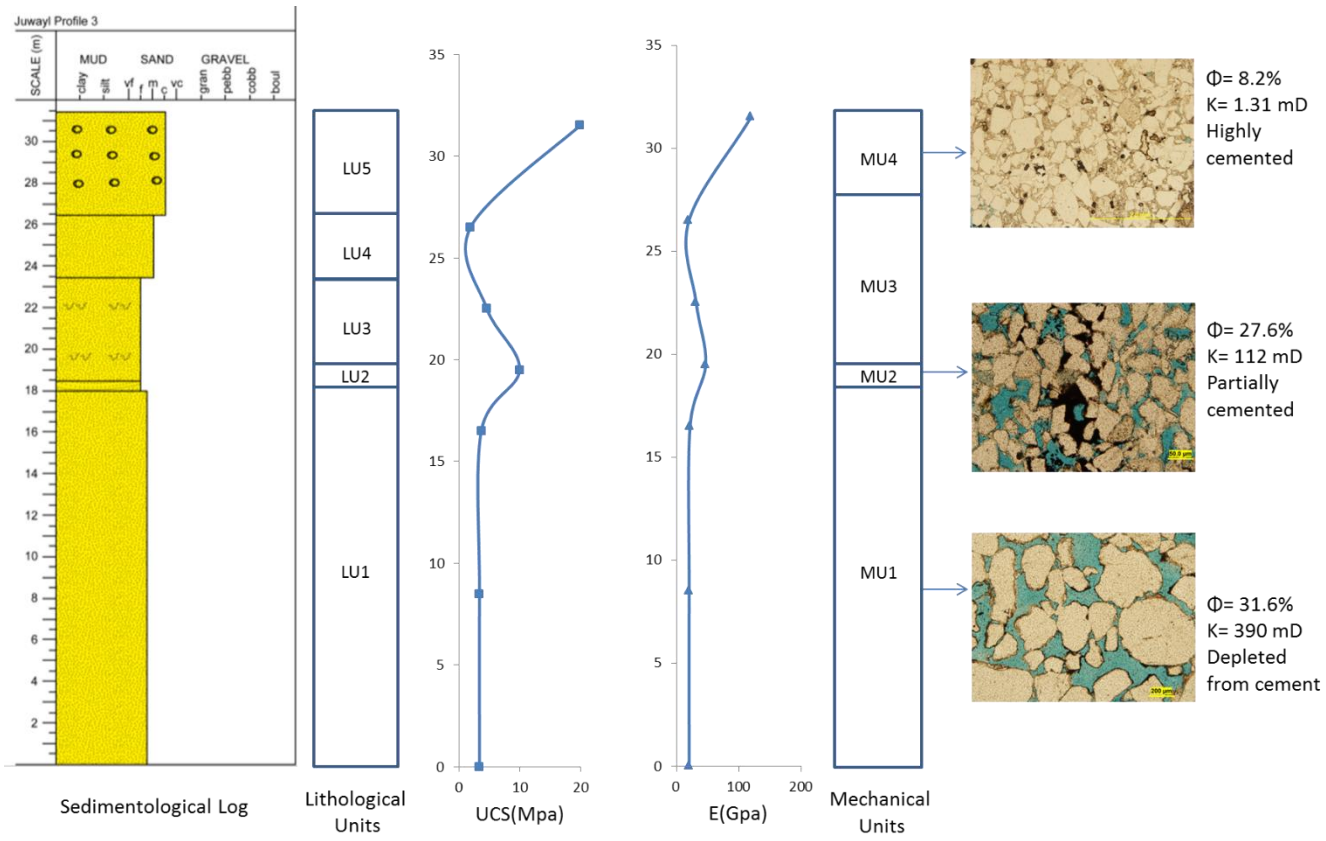

Figure 5.12: Lithological and Mechanical units of the Juwayl Formation succession associated with thin section microphotographs showing cement, porosity (Φ), and permeability (k) of different type of sandstones. (UCS= uniaxial compressive strength, E = static Young's modulus).

Chapter 6

Controls on Fracture System

6.1Introduction

Distribution of the natural fractures within the reservoir rocks is mainly controlled by the rock physical properties(included sedimentological, stratigraphic, and petrophysical) (Nelson, 2001). Understanding of these properties can help to predict natural fracture distribution. In this chapter, the average fracture spacing within Wajid Group sandstone has been correlated to the sedimentological, stratigraphic, and petrophysical properties of such sandstones in the 1-D model, to define the controls on the average fracture spacing. The sedimentological and stratigraphic characteristics included lithofacies type, texture, mineral composition, diagenetic features (degree of cementation and cement type), and bed thickness were defined and correlated to the average fracture spacing to evaluate their influence on the fracture distribution within the studied sandstones. The petrophysical properties included matrix porosity, grain density, and matrix permeability of Wajid Group sandstones were measured and correlated with the average fracture spacing. The reported results showed that the main rock properties controlling the average fracture spacing are the bed thickness, porosity, degree of cementation, and lithology (lithofacies type). Thus, these controlling factors can be used to predict the

relative average fracture spacing within the subsurface equivalent sandstone hosts groundwater and hydrocarbons in Wajid and Rub' Al-Khali Basins, respectively.

6.2 Results

6.2.1 Sedimentology and Stratigraphy

6.2.1.1 Facies

One section was measured from each formation of Wajid Group, and detailed description of lithology, texture, and stratigraphy carried out. 82 representative sandstone samples were collected from the measured sections for further laboratory analyses.

6.2.1.1.1 Lower Dibsiyah Formation Section

The lower Dibsiyah formation section (S01 in Figure 1.2) has a total thickness of 23 m (Figure 6.1). Four major lithofacies were identified from the lower Dibsiyah Formation included fine to medium-grained trough cross-bedded sandstone, medium to coarse-grained trough cross-bedded sandstone, coarse-grained trough cross-bedded pebbly sandstone, and coarse-grained trough cross-bedded conglomeratic sandstone(Figure 6.2)(Figure 6.3). The average thickness of sandstone beds equals to 1.53 m. Fining-upward cycles of sandstone observed in the lower Dibsiyah Formation with conglomerate at the base. The interpreted depositional environment is fluvial (braided river). Alternative thin layers of fine and coarse-grained sandstone distinguished the lower Dibsiyah Formation.

6.2.1.1.2 Upper Dibsiyah Formation Section

The upper Dibsiyah Formation section (S02 in Figure 1.2) has a total thickness 44 m (Figure 6.1). Six lithofacies were identified included fine-grained planar cross-bedded

sandstone, medium to coarse-grained planar cross-bedded sandstone, fine to medium trough cross-bedded sandstone, coarse-grained trough cross-bedded pebbly sandstone, coarse-grained bioturbated pebbly sandstone, and coarse-grained massive pebbly sandstone (Figure 6.2)(Figure 6.3). The average thickness of sandstone layers within upper Dibsiyah Formation equal to 3.06 m.

6.2.1.1.3 Sanamah Formation Section

The Sanamah Formation section (S03 in Figure 1.2) has a total thickness 41.5 m (Figure 6.1). Seven lithofacies were identified included iron rich, black colored fine-grained massive sandstone, fine to medium-grained massive sandstone, medium to coarse-grained massive sandstone, coarse-grained massive pebbly sandstone, coarse-grained massive conglomeratic sandstone, coarse-grained trough cross-bedded pebbly sandstone, and coarse-grained trough cross-bedded conglomeratic sandstone (Figure 6.2)(Figure 6.2).The studied section is fining upward succession ended by a thin layer(0.5) of fine-grained iron-rich sandstone. The average thickness of sandstone layers equal to 3.76 m.

6.2.1.1.4 Khusayyayn Formation Section

The Khusayyayn Formation section (S10 in Figure 1.2) has a total thickness 26 m (Figure 6.1). Five lithofacies were observed included medium-grained planar cross-bedded sandstone, coarse-grained planar cross-bedded sandstone, medium to coarse-grained soft deformed sandstone, medium to coarse-grained horizontal bedded sandstone, and coarse-grained massive sandstone (Figure 6.2)(Figure 6.3). The average thickness of sandstone layers within Khusayyayn Formation equal to 3.7 m.

6.2.1.1.5 Juwayl Formation Section

The Juwayl Formation section (S13 in Figure 1.2) has a total thickness of 31.5 m (Figure 6.1). Four lithofacies were observed included fine-grained trough cross-bedded sandstone, fine-grained soft deformed sandstone, medium to coarse-grained massive sandstone, and coarse-grained reworked sandstone (Figure 6.2)(Figure 6.3). The average thickness of sandstone layers within Juwayl Formation equal to 6.33 m.

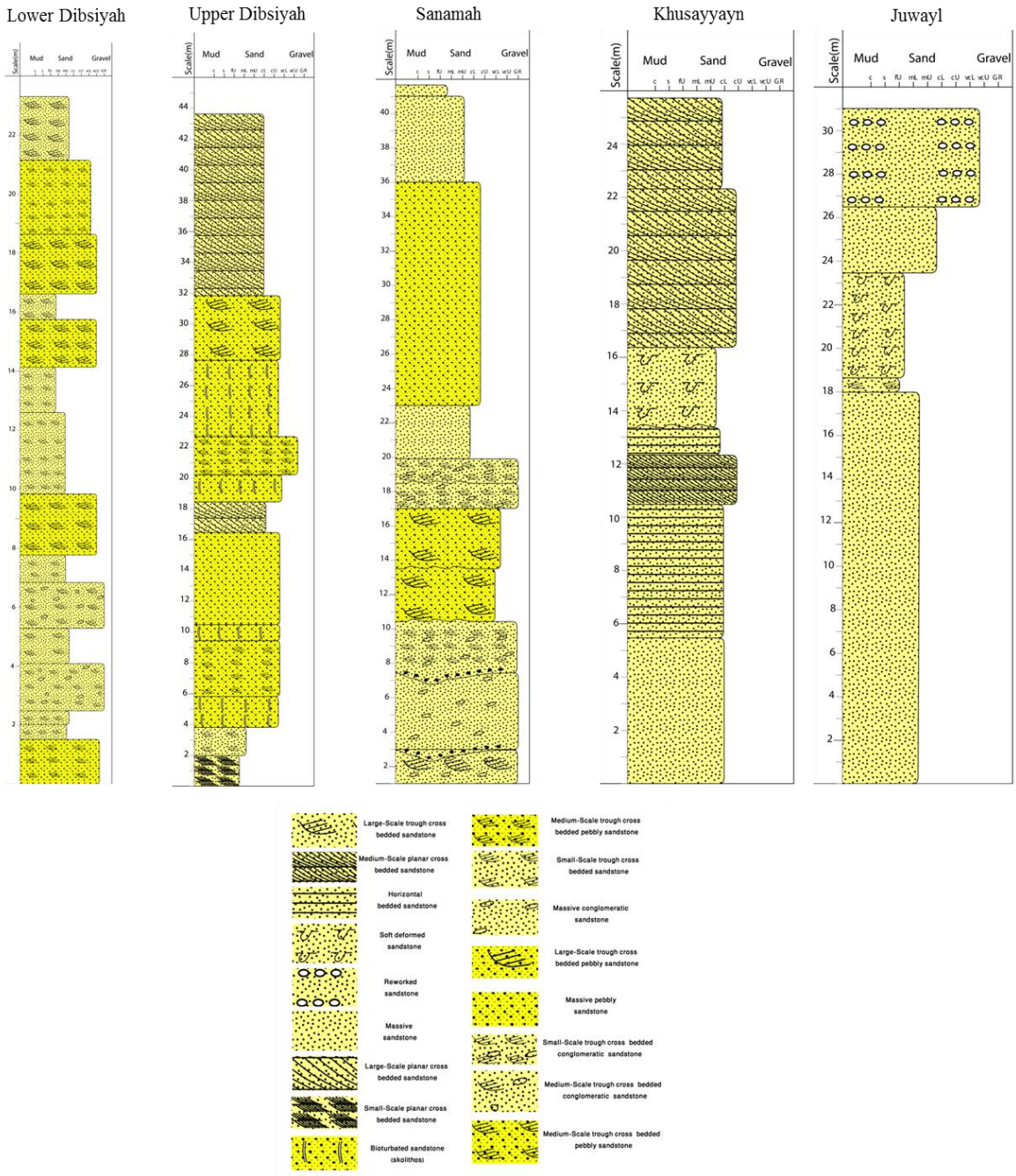

Figure 6.1: Sedimentological logs of Wajid Group formations (included lower Dibsiyah, upper Dibsiyah, Sanamah, Khusayyayn, and Juwayl Formations).

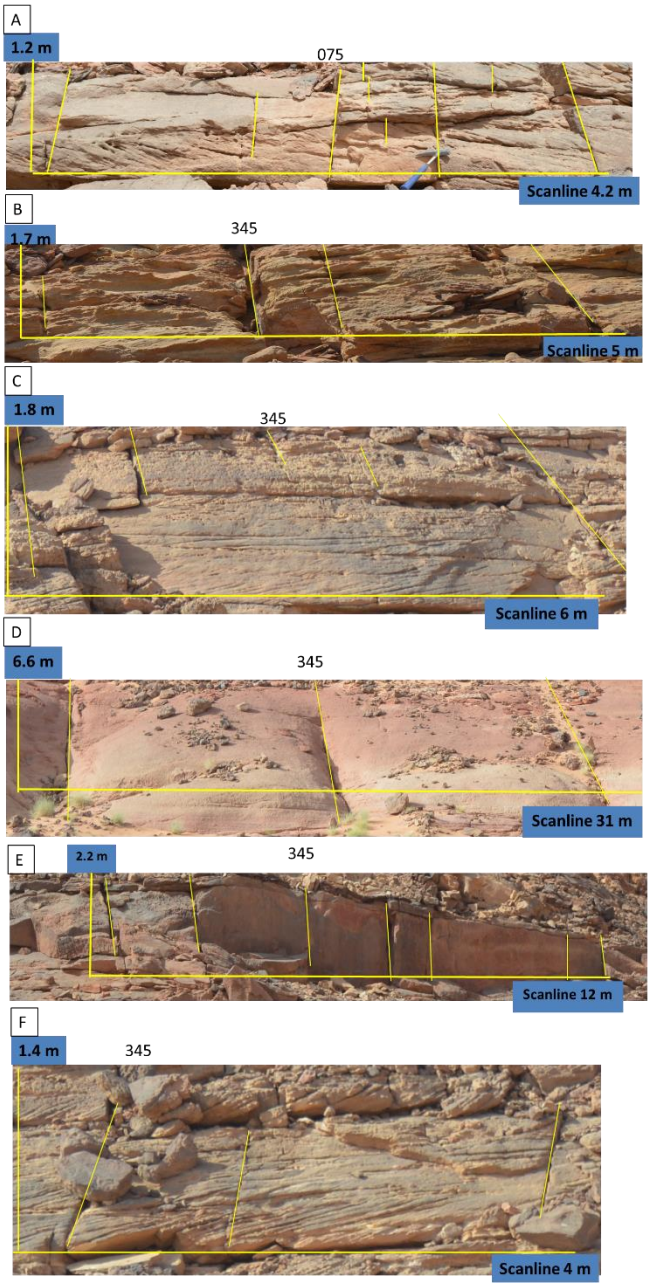

Figure 6.2: Sandstone lithofacies types observed in Wajid Group, A) medium to coarse-grained medium-scaled planar cross-bedded sandstone with N075 oriented Fractures, B)coarse-grained small scale trough cross-bedded pebbly sandstone, C) coarse-grained skolithos sandstone, D) medium to coarse-grained horizontally bedded skolithos sandstone, E) fine to medium-grained skolithos sandstone, F) medium to coarse-grained medium-scaled planar cross-bedded sandstone with N165 oriented Fractures.

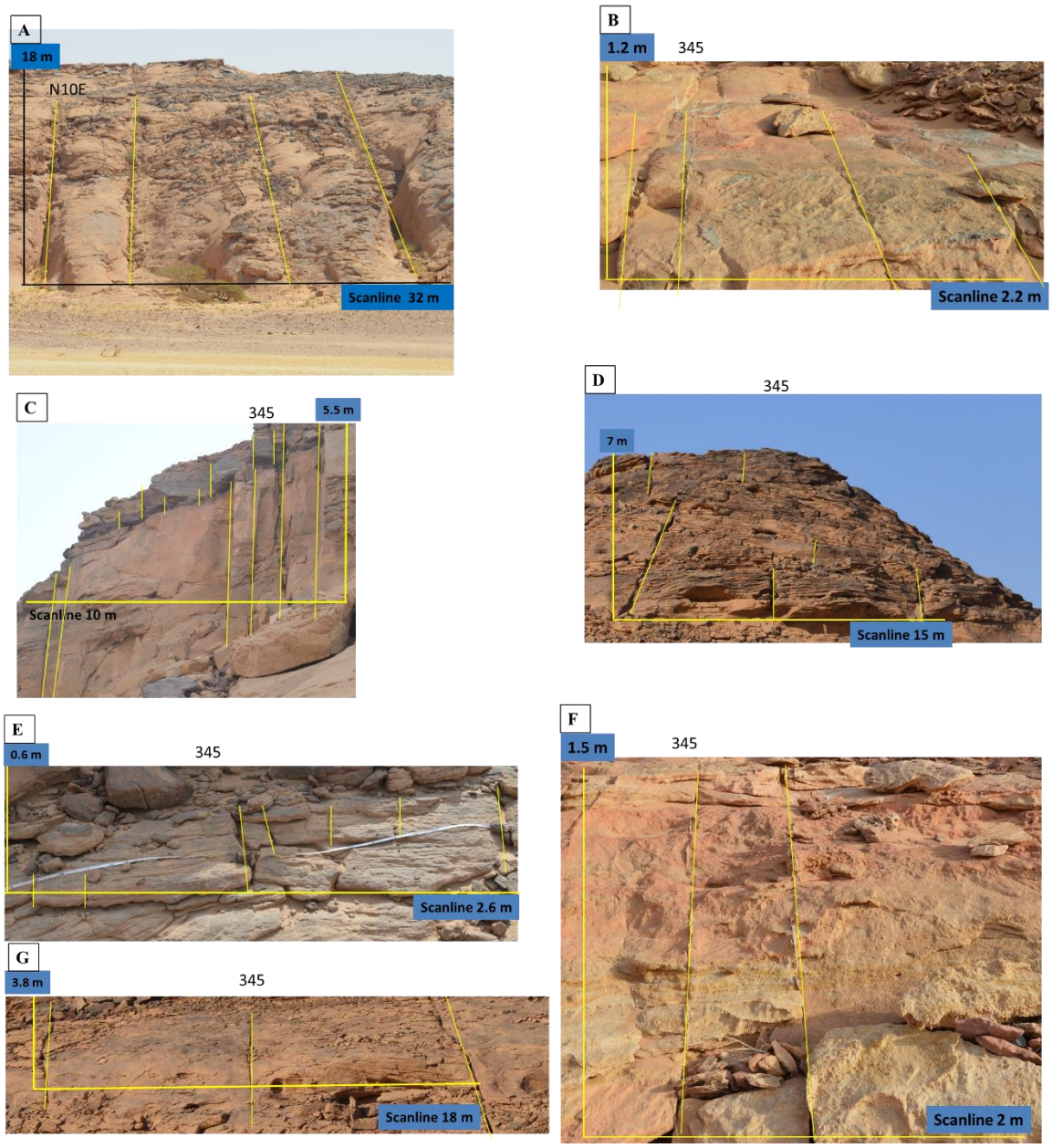

Figure 6.3: Sandstone lithofacies types observed in Wajid Group, A) thick layer, medium-grained massive sandstone, B) thin layer, medium-grained small scale trough cross-bedded sandstone, C)thick layer, fine to medium-grained massive sandstone, D) thick layer, medium to coarse-grained large scale planar cross-bedded sandstone, E) coarse-grained medium scale planar cross-bedded sandstone, F)coarse-grained small scale trough cross-bedded conglomeratic sandstone, G)coarse-grained, partially horizontal bedded massive sandstone.

6.2.2 Texture and Mineral Composition of Wajid Group Sandstone

On the basis of thin section analysis, the texture of Wajid Group sandstone samples generally showed fine to coarse, poorly to well sorted, sub-rounded to sub-angular grains (Table 6.1). Based on the thin section, X-Ray diffraction and SEM-EDX analyses, the framework-grain mineralogy of the studied sandstone is quartz, feldspars and rock fragments, where the quartz is predominant (96.63%), and the feldspars (1.98%) and rock fragments (1.39%) (Table 6.2) formed low percentage of the composition framework of the studied sandstone. However, the sandstone samples from Khusayyayn Formation showed a significant amount of the feldspars grains (including the microcline and plagioclase) (14.55%) (Figure 6.4)(Figure 6.6).

The quartz grains occurred as monocrystalline grain; however, a significant amount of the polycrystalline quartz grains observed (Figure 6.4). Strained quartz grains observed (undulose extinction) in the studied sandstone samples with a significant amount (average 15%) from the sample framework (Figure 6.4). The authigenic cement (observed in the thin section, SEM-EDX microphotographs, and XRD analysis) of the studied sandstone samples range from traces to 40% (average 14.52%) of the samples composition framework. Iron oxides, calcite, silica and clay minerals were observed as cemented material of the studied sandstones (Figure 6.4). The iron oxide (hematite), calcite minerals, and the Kaolinite type of clay minerals are dominant cement type(Figure 6.4)(Figure 6.5)(Figure 6.7)(Figure 6.8)(Figure 6.9)(Table 6.2)(Table 6.3).

Table 6.1: Texture of Wajid Group sandstone, included the mean grain size, sorting, roundness, and sphericity.

Texture									
Sample ID	**Mean Grain Size(Phi)**	**Grain Sorting (Phi)**	**Roundness**	**Sphericity**	**Sample ID**	**Mean Grain Size(P**	**Grain Sorting (Phi)**	**Roundness**	**Sphericity**
J3.5	0.97	1.10	sub-angular to sub-rounded	high	**2UD18**	2.02	0.82	angular	low
J3.4	1.03	1.01	sub-rounded to rounded	high	**2UD17**	0.71	1.01	sub-angular to sub-rounded	medium
J3.3	2.18	0.86	sub-angular to sub-rounded	high	**2UD16**	0.87	1.05	sub-rounded	medium
J3.2	2.50	0.74	sub-angular to sub-rounded	high	**2UD15**	1.19	0.71	sun-angular	medium
J3.1	1.66	0.93	sub-angular to sub-rounded	high	**2UD14**	1.78	0.87	angular	low
K1.7	1.49	0.89	sub-angular	low	**2UD13**	1.25	0.79	sub-angular to sub-rounded	medium
K1.6	0.86	0.77	sub-angular to sub-rounded	medium	**2UD12**	1.53	0.91	sub-angular to sub-rounded	high
K1.5	1.23	0.85	sub-angular to sub-rounded	medium	**2UD11**	1.90	0.78	sub-angular to sub-rounded	high
K1.4	0.95	0.96	sub-angular to sub-rounded	low	**2UD10**	1.10	0.97	sub-angular to sub-rounded	medium
K1.3	0.34	0.93	sub-rounded	medium	**2UD9**	1.51	0.96	sub-angular to sub-rounded	medium
K1.2	1.18	0.78	sub-rounded	medium	**2UD8**	1.45	1.06	sub-rouned	medium
K1.1	1.07	0.83	sub-angular to sub-rounded	low	**2UD7**	0.80	0.77	sub-angular to sub-rounded	low
SUD22	1.30	1.1	sub-angular to sub-rounded	low	**2UD6**	1.01	0.99	sub-angular to sub-rounded	low
SUD21	1.45	1.1	sub-angular to sub-rounded	low	**2UD5**	0.70	1.06	sub-angular to sub-rounded	low
SUD20	0.96	0.83	sub-angular to sub-rounded	high	**2UD4**	1.68	0.85	sub-angular to sub-rounded	low
SUD19	1.02	0.86	sub-angular to sub-rounded	medium	**2UD3**	0.80	1.10	sub-angular to sub-rounded	low
SUD18	0.96	0.86	sub-angular to sub-rounded	medium	**2UD2**	0.85	1.00	sub-angular to sub-rounded	low
SUD17	1.26	0.71	sub-angular to sub-rounded	medium	**2UD1**	1.14	0.90	sub-angular to sub-rounded	low
SUD16	0.80	0.82	sub-rounded to rounded	high	**LD22**	0.88	0.80	sub-angular to sub-rounded	low
SUD15	0.94	0.78	sub-angular to sub-rounded	medium	**LD21**	1.12	0.76	sub-angular to sub-rounded	low
SUD14	0.84	0.92	sub-angular to sub-rounded	high	**LD20**	1.08	1.08	sub-angular to sub-rounded	low
SUD13	0.52	0.87	sub-rounded to rounded	low	**LD19**	0.92	0.83	sub-angular to sub-rounded	high
SUD12	1.07	0.74	sub-rounded to rounded	high	**LD18**	0.73	0.70	sub-rounded	medium
SUD11	0.51	1.04	sub-rounded	low	**LD17**	1.50	0.82	sub-rounded	low
SUD10	1.03	0.96	sub-angular to sub-rounded	medium	**LD16**	1.11	0.88	sub-angular	high
SUD9	0.66	0.78	sub-rounded to rounded	high	**LD15**	0.70	0.81	sub-rounded	low
SUD8	0.49	0.86	sub-angular	low	**LD14**	1.17	0.90	sub-angular to sub-rounded	low
SUD7	1.38	0.78	sub-rounded to rounded	high	**LD13**	0.74	1.07	sub-angular to sub-rounded	low
SUD6	1.77	0.42	sub-angular to sub-rounded	low	**LD12**	1.24	0.82	sub-rounded	high
D3.7	1.61	0.83	sub-angular to sub-rounded	low	**LD11**	0.78	0.99	sub-rounded	medium
D3.6	1.15	0.66	sub-angular to sub-rounded	low	**LD10**	0.65	1.10	sub-rounded	medium
D3.5W	2.24	0.60	sub-angular to sub-rounded	medium	**LD9**	1.01	0.83	sub-rounded	medium
D3.5R	2.20	0.67	sub-angular to sub-rounded	medium	**LD8A**	1.06	1.16	sub-rounded	medium
D3.4	2.03	0.72	Rounded	medium	**LD7**	0.63	1.06	sub-angular to sub-rounded	medium
D3.3	1.45	0.90	sub-rounded to rounded	high	**LD6**	0.47	1.06	sub-angular to sub-rounded	medium
D3.2	0.94	0.89	sub-rounded to rounded	high	**LD5**	1.67	0.79	sub-rounded	low
D3.1	1.74	0.75	sub-angular	low	**LD4**	0.82	0.91	sub-angular to sub-rounded	high
2UD23	1.20	1.00	sub-angular to sub-rounde	medium	**LD3**	1.67	0.95	sub-rounded	low
2UD22	1.31	0.95	sub-angular to sub-rounde	medium	**LD2**	1.50	1.18	sub-rounded to rounded	high
2UD20	1.08	1.08	sub-angular to sub-rounde	low	**LD1B**	1.04	0.88	sub-rounded	low
2UD19	0.98	1.01	sub-angular to sub-rounde	low	**LD1**	0.78	0.89	sub-rounded to rounded	high

Table 6.2: Overall mineral composition of Wajid Group sandstone.

Mineral Composition											
Sample ID	Quartz	Feldspars	Lith Fragments	Mica	Opaque Minerals	Matrix	Cement				
							Iron oxides	Calcite	Silica	Clay minerals	Total
J3.5	49.5	4	0.5	1.5	0	0	5	20	15	0	40
J3.4	59	0	0	0	1	0	4	1	0	0	5
J3.3	66	0	0	0	0	0	3.5	0	0	0.5	4
J3.2	57	0	0	1	1	1	2	8	0	0	10
J3.1	55	0	0	0	1	2	2	5	0	0	7
K1.7	60	10	0	0.5	0	0	2	1	0	0	3
K1.6	68	4	0	0.5	0	0	2	0	0	0	2
K1.5B	52	2	0	5	4	1	0	10	0	0	10
K1.4	51	5	0	0	0	0	2	0	0	2	4
K1.3	59	2	0	0.5	0	0	4	0	0	0	4
K1.2	60.5	3.5	0	1	0	0	3	2	0	0	5
K1.1	58	2	0	0	3	2	3	2	0	0	5
SUD22	62	0	0	0	0	0	40	0	0	0	40
SUD21	45	0	0	0	5	0	5	0	5	30	40
SUD20	70	0	1	0	2	0	6	0	0	2	8
SUD19	71	0	0	0	1	0	0.5	6	0	1.5	8
SUD18	61	0	0	0	2	0	7	2	0	0	9
SUD17c	69	0	0	0	1	0	7	2	0.5	0.5	10
SUD16	68	0	0	0	3	0	2	2	0	0	4
SUD15	76	0	0	0	1	0	1	3	2	0	6
SUD14	62	0	0	0	1	0	1	23	2	0	26
SUD13	79	0	1	0	1	0	2	5	0	0	7
SUD12	78	0	0	0	1	0	3	5	0	0	8
SUD11	51.5	1	2	0.5	1	0	2	10	0	0	12
SUD10	73	0	0	0	2	0	0	5	0	0	5
SUD9	45	0	0	1	3	0	3	5	0	0	8
SUD8	72	0	0	0	2	0	3	8	0	1	12
SUD7	65	0	0	0	2	0	3	5	0	2	10
SUD6	68	0	0	0	1	0	2	5	0	0	7
D3.7	71	0	0	0	0	0	2	0	0	0	2
D3.6	66	0	0	0	0	0	1	0	0	2	3
D3.5W	56	0	0	1	3	0	10	0	0	0	10
D3.5R	59	0	0	1	1	0	2	8	0	0	10
D3.4	59	0	0	1	0	0	15	0	0	0	15
D3.3	63	0	0	1	0	0	3	0	0	0	3
D3.2	61	0	0	2	1	0	1	0	0	3	4
D3.1	70	0	0	0.5	0	0	4	0	0	0	4
2UD23	51	0	0	1	2	0	5	15	0	5	25
2UD22	51	0.5	0.5	0	1	0	15	0	0	20	35
2UD20	43	0	0	1	2	3	20	5	0	12	37
2UD19	51	0	1	1	2	0	2	16	0	2	20
2UD18	65	0	0	2	2	0	5	2	0	24	31
2UD17	53.5	0	0	1.5	2	0	3	17	0	0	20
2UD16	65	0	0	0	1	0	0	0	0	2	2
2UD15	43	0	0.5	1	0.5	10	0	0	0	20	20
2UD14	55	0	0.5	0.5	1	0	5	1	0	24	30
2UD13	78	0	0	0	1	0	0	2	0	2	4
2UD12	71.5	0	0.5	0	1	0	0	3	0	1	4
2UD11	65	0	0		2	0	0	19	1	0	20
2UD10	73	0	0	0	2	0	0	3	0	0	3
2UD9	59	0	0.5	0	2	0	0	8	8	1	17
2UD8	56	0.5	0.5	0	2	0	0	7	0	0	7
2UD7	60	0	0	0	1	0	2	15	0	1	18
2UD6	83	0	1	0	1	0	0	1	0	4	5
2UD5	84	0	0	0	1	0	0	4	0	1	5
2UD4	78	0	0	1	1	0	1	6	1	1	9
2UD3	57		0.5	0.5	5	0	0	0	0	5	5
2UD2	82	0	1	1	2	0	1	1	0	2	4
2UD1	75.5	0	0.5	0	3	0	0	1	0	5	6
LD22	40	0	0	0	0	2	10	10	5	0	25
LD21	40	0	0	0	0	2	8	8	12	0	28
LD20	41.5	0	0	0	2	2	0	2	1	16	19
LD19	44	0	0.5	0.5	0	15	0	5	10	0	15
LD18	54	0	1	1	0	0	10	0	5	0	15
LD17	53	0	0	0	0	2	15	3	2	0	20
LD16	54	0	0	0	0	1	25	0	0	0	25
LD15	48	0	0	0	1	1	0	20	0	0	20
LD14	45	0	0	0	0	5	0	5	20	10	35
LD13	45	0	0	0	0	5	0	12	13	5	30
LD12	57	0	0	0	0	3	1	4	0	0	5
LD11	62	0	0	0	0	0	0	0	10	10	20
LD10	44	0	0	0	5	10	0	5	5	0	10
LD9	52	0	0	0	0	3	15	0	0	0	15
LD8	35	0	0	0	0	10	15	3	12	0	30
LD7	40	0	0	0	1	0	0	29	0	0	29
LD6	51.5	0	0	0	0	0	5	15	10	0	30
LD5	67	0	0	0	2	5	1	3	7	0	11
LD4	65	0	0	0	0	0	7	5	0	0	12
LD2	62	0	0	0	0	0	10	15	0	0	25
LD1	29	0	0	0	1	0	50	10	0	0	60

Table 6.3: XRD results for representative samples from Wajid Group sandstones.

Formation	Sample ID	Minerals	Phase	Weight%
Juwayl	J3.5	Quartz	Major	84.4
		Calcite	Minor	15.6
Khussyayan	K1.7	Quartz	Major	82.6
		Microcline	Minor	17.4
	K1.3	Quartz	Major	100
Sanamah	S22	Quartz	Major	87.7
		Hematite	Minor	12.3
	S21	Quartz	Major	83.5
		Kaolinite	Minor	16.5
	S13	Quartz	Major	100
	S7	Quartz	Major	97.9
		Kaolinite	Minor	2.09
Upper Dibsiyah	D3.7	Quartz	Major	98.8
		Kaolinite	Minor	1.2
	D3.5R	Quartz	Major	93.9
		Kaolinite	Minor	6.1
	2UD18	Quartz	Major	91.5
		Kaolinite	Minor	6.5
		Calcite	Minor	2.1
	2UD14	Quartz	Major	94.4
		Kaolinite	Minor	5.6
	2UD11	Quartz	Major	96.1
		Kaolinite	Minor	3.8
	2UD9	Quartz	Major	100
	2UD7	Quartz	Major	100
Lower Dibsiyah	LD21	Quartz	Major	100
	LD20	Quartz	Major	100
	LD13	Quartz	Major	100
	LD7	Quartz	Major	100
	LD6	Quartz	Major	100
	LD2	Quartz	Major	95.9
		Kaolinite	Minor	1.1
		Anatase	Minor	3

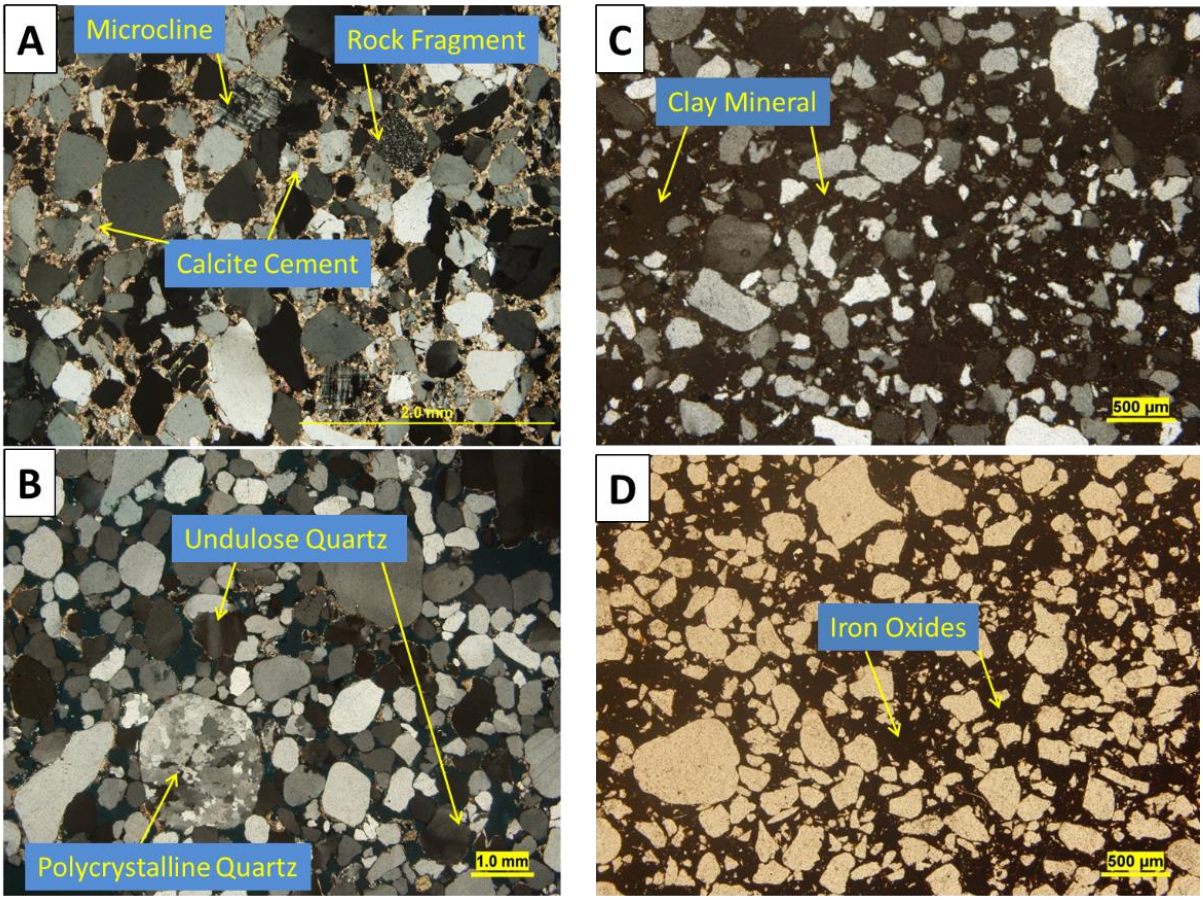

Figure 6.4: Microphotographs showing: A) quartz, feldspar(microcline), rock fragments and calcite cement, B) polycrystalline quartz grain, and the undulating quartz, C) clay minerals cement. D) iron oxides minerals cement.

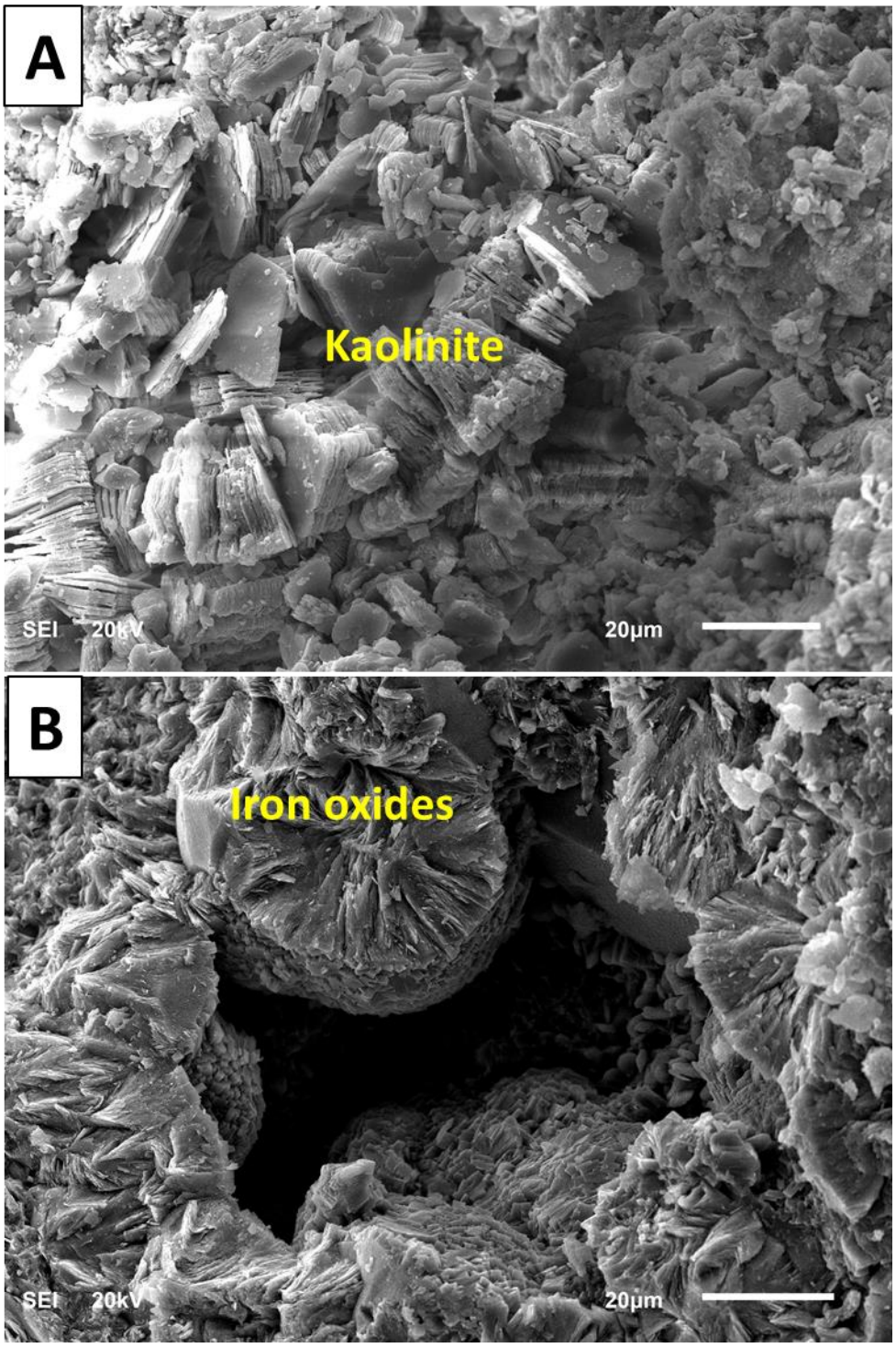

Figure 6.5: SEM microphotographs showing: A) kaolinite booklets. B) iron oxides cement.

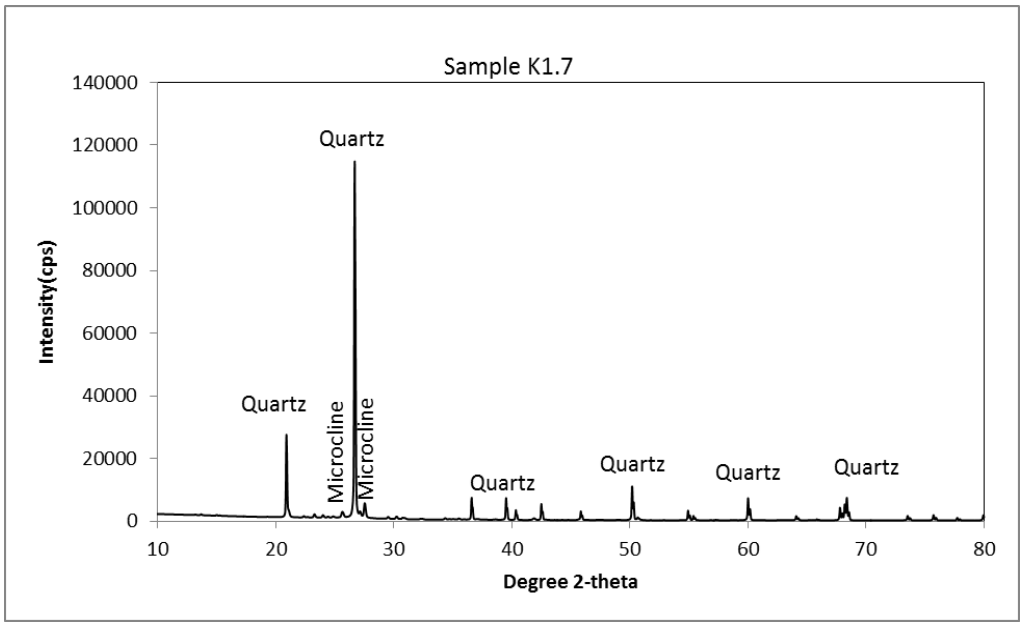

Figure 6.6: XRD chart of sandstone sample from Khusayyayn formation shows quartz and microcline minerals.

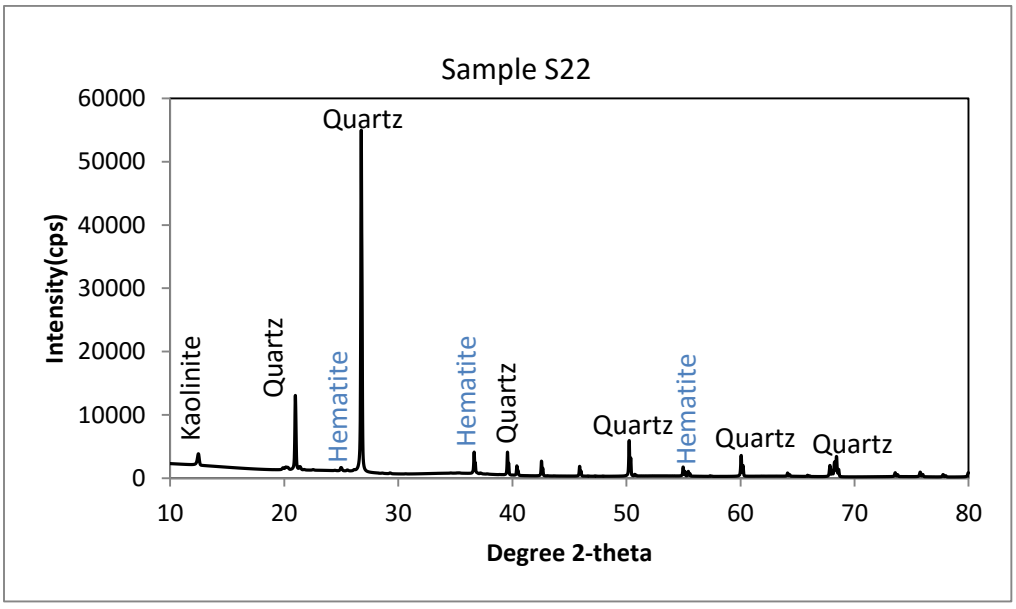

Figure 6.7: XRD chart of sandstone sample from Sanamah formation shows quartz, hematite and kaolinite minerals.

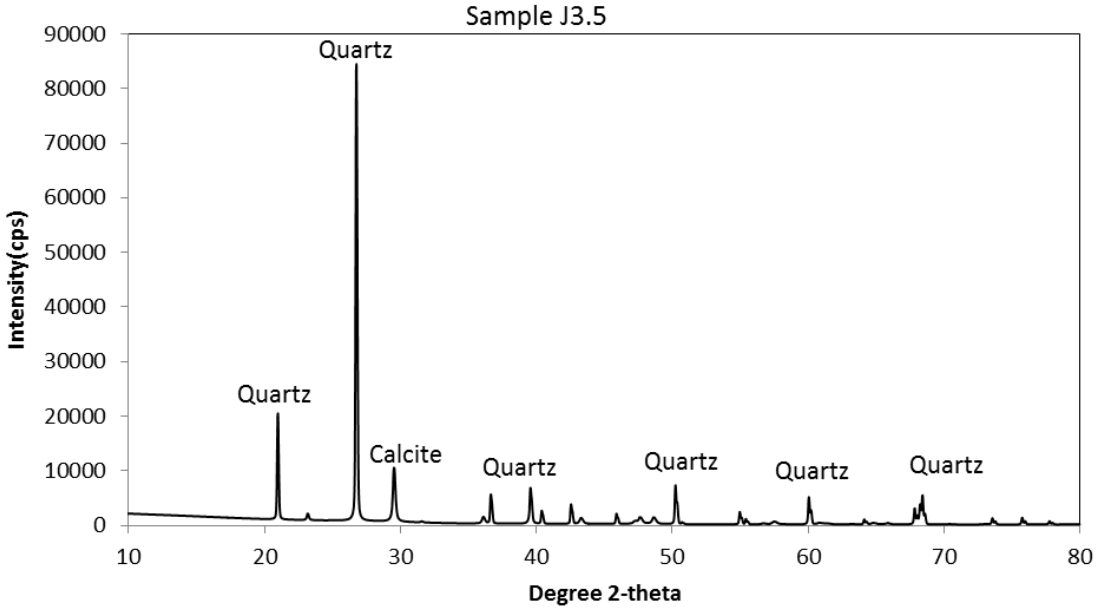

Figure 6.8: XRD chart of J3.5 sandstone sample from Juwayl formation shows quartz and calcite minerals.

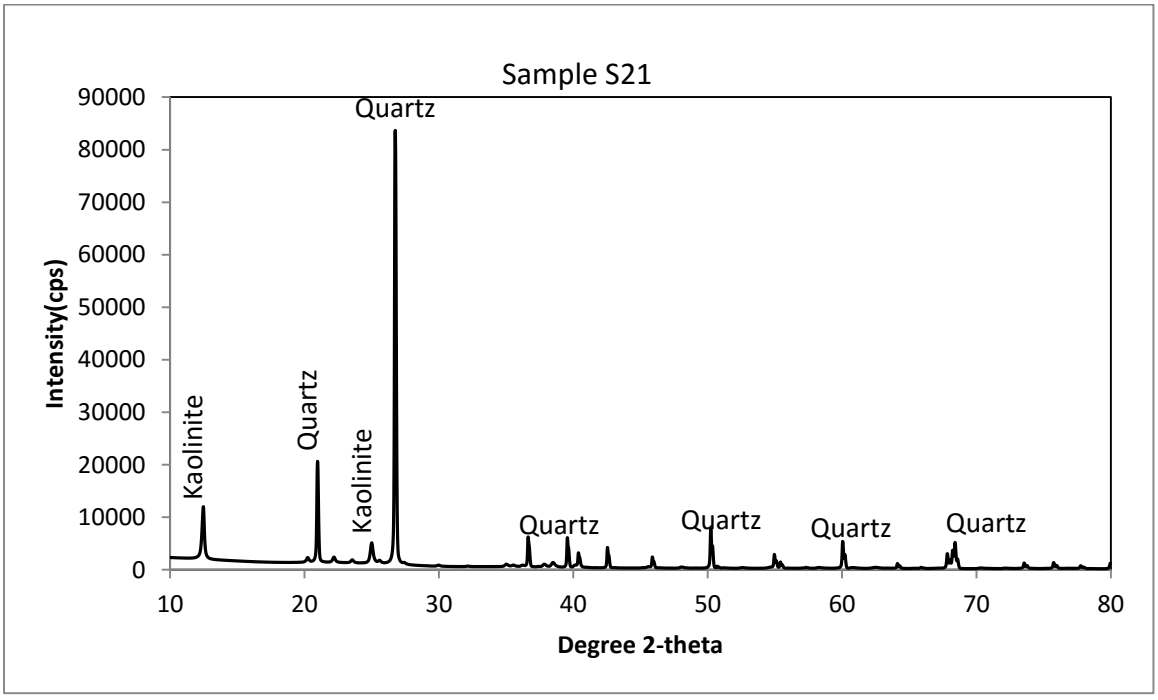

Figure 6.9: XRD chart of S21 sandstone sample from Sanamah formation shows quartz and Kaolinite minerals.

6.2.3 Petrophysical Analysis

6.2.3.1 Porosity

The porosity of 63 sandstone samples from Wajid Group was measured in a quantitative way using the porosimeter equipment. The porosity values ranging from 2.34 % to 43 %, with an average value of 30.27% as shown in Table 6.4 and Table 6.5. The porosity values of Wajid Group sandstone displayed low variability in the vertical dimension with a coefficient of variation (CV) equal to 0.22 (Table 6.5).

The distribution of porosity values in the glaciofluvial sandstone lithofacies of Sanamah and Juwayl Formations is less homogeneous than the braided fluvial and shallow marine sandstone lithofacies of lower Dibsiyah, upper Dibsiyah, and Khussyayan Formations (Table 6.5). The Sanamah and Juwayl Formations have a coefficient of variation (CV) values equal to 0.38 and 0.39, respectively (Table 6.5); however, the lower Dibsiyah, upper Dibsiyah, and Khusayyayn Formations have a coefficient of variation (CV) values equal to 0.17, 0.15, and 0.06, respectively (Table 6.5).

Inter-granular and Intra-granular types of porosity were observed in the thin section of the studied sandstone samples. High porosity values were observed in poorly cemented sandstone samples, whereas, the highly cemented sandstones samples displayed low values of porosity(Figure 6.10).

6.2.3.2 Permeability

The permeability of 63 sandstone samples from the Wajid Group was measured and the result showed a wide range of permeability values ranging from 0.27 mD to 548.31 mD , with an average of 271.26 (Table 6.4)(Table 6.5).

The distribution of permeability values displays more heterogeneous distribution in the glaciofluvial sandstone lithofacies of Sanamah and Juwayl Formations than the braided fluvial and shallow marine sandstone lithofacies of lower Dibsiyah, upper Dibsiyah, and Khussyayan Formations (Table 6.5). The Sanamah and Juwayl Formations have a coefficient of variation (CV) values equal to 0.71 and 0.74, respectively; however, the lower Dibsiyah, upper Dibsiyah, and Khussyayan Formations have a coefficient of variation (CV) values equal to 0.50, 0.56, and 0.10, respectively (Table 6.5).

The permeability values of the studied sandstone varied in the vertical dimension, and this variation associated with lithological, textural, and diagenetic variation of the studied sandstone. In thin section microphotographs, the cemented materials (included the iron oxides minerals, calcite, silica, and clay) were observed blocking the pore throats and reduce the permeability of studied sandstone (Figure 6.10).

6.2.3.3Grain Density

The grain density of the Wajid Group sandstone samples was measured for 63 samples and the values ranging from 2.62 g/cc to 2.89 g/cc, with an average of 2.67 g/cc (Table 6.4)(Table 6.5). The grain density has a coefficient of variation (CV) value equal to 0.02 which indicated the homogenous distribution of grain density values in the Wajid Group sandstones.

Table 6.4: Grain density, porosity, and permeability data of Wajid Group sandstone.

Sample ID	Density (g/cc)	Porosity (%)	Permeability (mD)	Sample ID	Density (g/cc)	Porosity (%)	Permeability (mD)
Juwayl Formation				**Upper Dibsiyah Formation**			
J3.5	2.692	8.193	1.3168				
J3.4	2.6864	31.689	389.803	2UD20	2.758	43.045	53.7263
J3.3	2.7252	32.849	422.649	2UD19	2.6478	27.46	229.5549
J3.2	2.6798	27.669	112.751	2UD18	2.6439	28.068	87.14
J3.1	2.6892	28.291	302.7959	2UD15	2.7217	34.937	219.4567
Khussyayan Formation				2UD14	2.7316	29.968	44.974
K1.7	2.6385	31.428	381.3234	2UD12	2.6563	41.64	548.313
K1.6	2.6604	33.503	430.1231	2UD11	2.6416	29.84	128.835
K1.5	2.6382	31.43	353.3627	2UD10	2.6603	28.875	379.3727
K1.4	2.6355	34.33	407.1154	2UD9	2.6724	30.831	150.8318
K1.3	2.6369	33.262	359.0759	2UD8	2.6952	25.985	140.922
K1.2	2.6349	34.549	352.216	2UD7	2.886	33.658	157.1772
K1.1	2.6316	29.11	319.3601	2UD4	2.7381	37.27	233.9164
Sanamah Formation				2UD1	2.8054	39.753	144.6953
SUD22	2.8361	2.343	0.2683	**Lower Dibsiyah Formation**			
SUD21	2.6839	17.335	0.6476	LD21	2.6509	29.95	327.5907
SUD20	2.663	38.444	204.0315	LD20	2.7724	10.41	169.6312
SUD18	2.6593	33.382	186.5458	LD19	2.6458	32.847	394.6075
SUD17	2.6621	33.558	426.4009	LD18	2.627	32.724	369.537
SUD15	2.667	33.872	173.2567	LD17	2.6553	29.326	107.97
SUD14	2.6702	34.268	171.6409	LD16	2.6313	31.948	232.3229
SUD8	2.6514	30.551	254.0856	LD14	2.645	30.945	269.0447
SUD7	2.6308	30.554	336.2455	LD12	2.6498	34.377	372.0399
SUD6	2.6305	33.125	476.4141	LD11	2.6503	29.322	324.5624
Upper Dibsiyah Formation				LD10	2.6384	32.235	432.6143
D3.7	2.6375	28.393	329.5125	LD9	2.6489	29.31	75.7313
D3.6	2.6528	32.651	413.2899	LD8A	2.6669	31.107	13.5647
D3.5W	2.6197	32.48	334.5102	LD7	2.6231	31.554	342.6229
D3.5R	2.6563	34.016	352.859	LD6	2.6452	29.944	400.4455
D3.4	2.6531	28.372	453.7758	LD5	2.6506	29.146	339.9415
D3.3	2.6684	28.712	433.6607	LD3	2.6386	26.236	313.1347
D3.1	2.6483	31.255	388.4805	LD2	2.6666	26.013	2.0766
2UD23	2.6525	26.076	405.9306	LD1B	2.638	33.315	374.2505
2UD22	2.6642	29.251	144.3517	LD1	2.6357	29.731	413.4977

Table 6.5: Statistical parameters of grain density, porosity, and permeability measurements

Parameters	Density (g/cc)	Porosity (%)	Permeability (mD)	Parameters	Density (g/cc)	Porosity (%)	Permeability (mD)
All Data				**Sanamah Formation**			
N	63	63	63	N	10	10	10
Mean	2.67	30.27	271.62	Mean	2.68	28.74	222.95
Median	2.65	31.11	324.56	Median	2.66	33.25	195.29
Minimum	2.62	2.34	0.27	Minimum	2.63	2.34	0.27
Maximum	2.89	43.05	548.31	Maximum	2.84	38.44	476.41
Range	0.27	40.70	548.04	Range	0.21	36.10	476.15
Lower Quartile	2.64	28.88	150.83	Lower Quartile	2.65	27.25	128.89
Upper Quartile	2.65	31.11	324.56	Upper Quartile	2.66	33.25	195.29
Interguartile Range	0.01	2.23	173.73	Interguartile Range	0.02	6.01	66.40
Standard Deviation	0.05	6.56	142.26	Standard Deviation	0.06	10.79	158.20
Skewness	2.42	-2.17	-0.43	Skewness	2.69	-2.03	0.13
Kurtosis	6.46	7.30	-0.90	Kurtosis	7.95	3.94	-0.53
Coefficient of Variation	0.02	0.22	0.52	Coefficient of Variation	0.02	0.38	0.71
Juwayl Formation				**Upper Dibsiyah Formation**			
N	5	5	5	N	22	22	22
Mean	2.69	25.74	245.86	Mean	2.69	31.93	262.51
Median	2.69	28.29	302.80	Median	2.66	30.40	231.74
Minimum	2.68	8.19	1.32	Minimum	2.62	25.99	44.97
Maximum	2.73	32.85	422.65	Maximum	2.89	43.05	548.31
Range	0.05	24.66	421.33	Range	0.27	17.06	503.34
Lower Quartile	2.68	17.93	57.03	Lower Quartile	2.65	28.39	143.49
Upper Quartile	2.69	28.29	302.80	Upper Quartile	2.66	30.40	231.74
Interguartile Range	0.01	10.36	245.76	Interguartile Range	0.01	2.01	88.24
Standard Deviation	0.02	10.05	182.16	Standard Deviation	0.06	4.84	146.01
Skewness	1.87	-1.97	-0.57	Skewness	1.86	1.02	0.20
Kurtosis	3.85	4.08	-1.98	Kurtosis	3.58	0.28	-1.16
Coefficient of Variation	0.01	0.39	0.74	Coefficient of Variation	0.02	0.15	0.56
Khussyayan Formation				**Lower Dibsiyah Formation**			
N	7	7	7	N	19	19	19
Mean	2.64	32.52	371.80	Mean	2.65	29.50	277.64
Median	2.64	33.26	359.08	Median	2.65	29.95	327.59
Minimum	2.63	29.11	319.36	Minimum	2.62	10.41	2.08
Maximum	2.66	34.55	430.12	Maximum	2.77	34.38	432.61
Range	0.03	5.44	110.76	Range	0.15	23.97	430.54
Lower Quartile	2.63	31.43	352.22	Lower Quartile	2.64	29.31	169.63
Upper Quartile	2.64	33.26	359.08	Upper Quartile	2.65	29.95	327.59
Interguartile Range	0.00	1.83	6.86	Interguartile Range	0.01	0.64	157.96
Standard Deviation	0.01	1.95	37.36	Standard Deviation	0.03	5.11	137.64
Skewness	2.31	-0.82	0.37	Skewness	3.42	-3.13	-0.97
Kurtosis	5.76	-0.07	-0.37	Kurtosis	13.45	11.68	-0.36
Coefficient of Variation	0.00	0.06	0.10	Coefficient of Variation	0.01	0.17	0.50

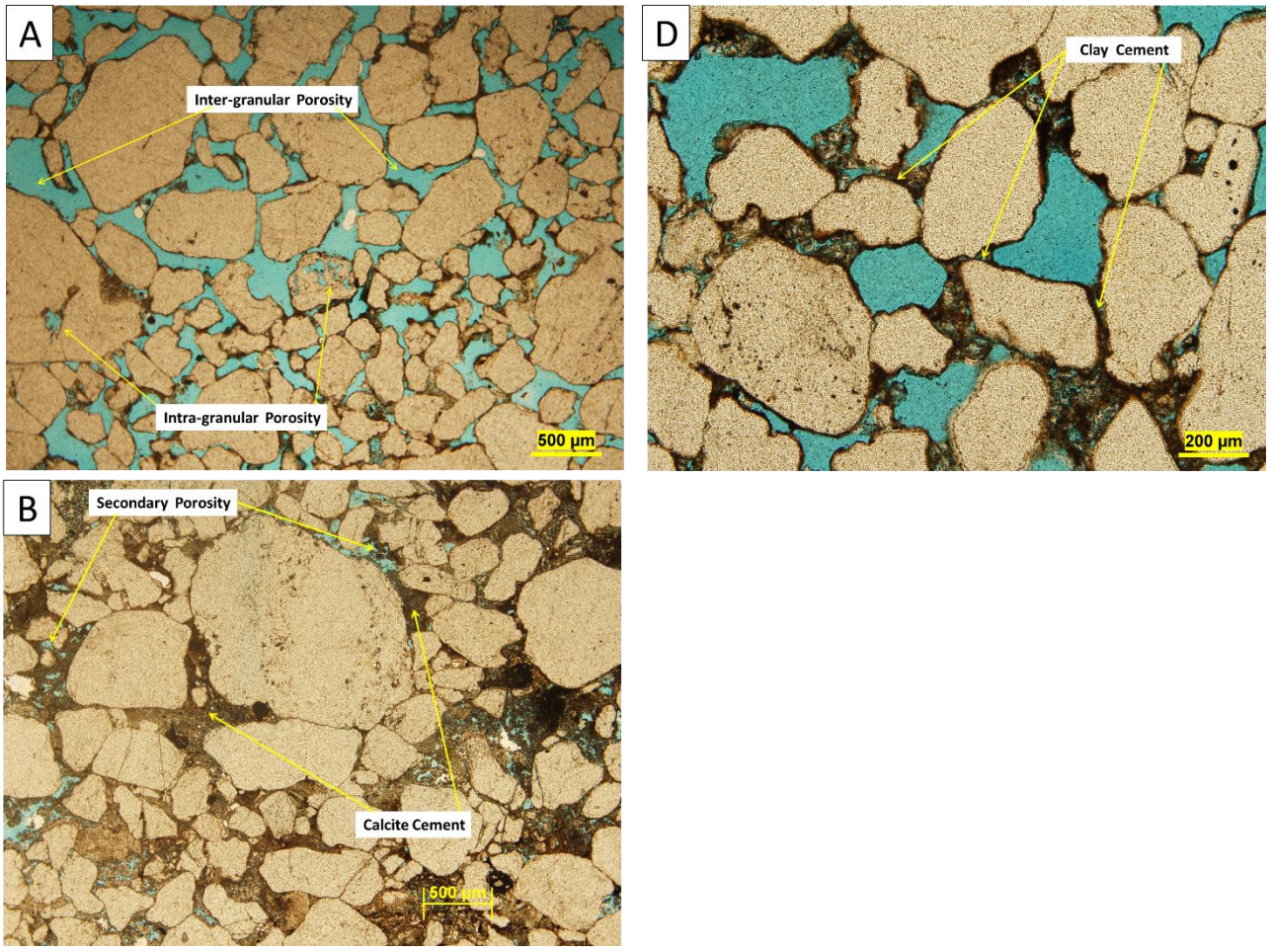

Figure 6.10: Microphotographs showing, A)inter-granular and intra-granular porosity (secondary porosity) porosity types of sandstone sample depleted from cement, B) secondary porosity within sandstone sample with high calcite cement and C) clay mineral blocking the pore throat between quartz grains.

6.3 Controls on Fracture Spacing

Distribution of the natural fractures in the sedimentary rock is mainly controlled by the fracture-hosting rock properties (included mineral composition, lithology (grain size), the degree of cementation and type of cement, porosity, and bed thickness)(Nelson, 2001). Thus, the rock properties can be used to predict the relative abundance of the natural fracture characteristics within the reservoir rocks (e.g. average fracture spacing). To study the relationship between fracture spacing and host rock properties, the entire succession of Wajid Group subdivided into fracture units based on the average fracture spacing values, and the average value of fracture spacing have been calculated for each fracture unit (Figure 6.11)(Table 6.6). Four geological factors include bed thickness, the degree of cementation and type of cement, lithofacies type, and porosity are observed controlling the average fracture spacing of Wajid Group outcrop.

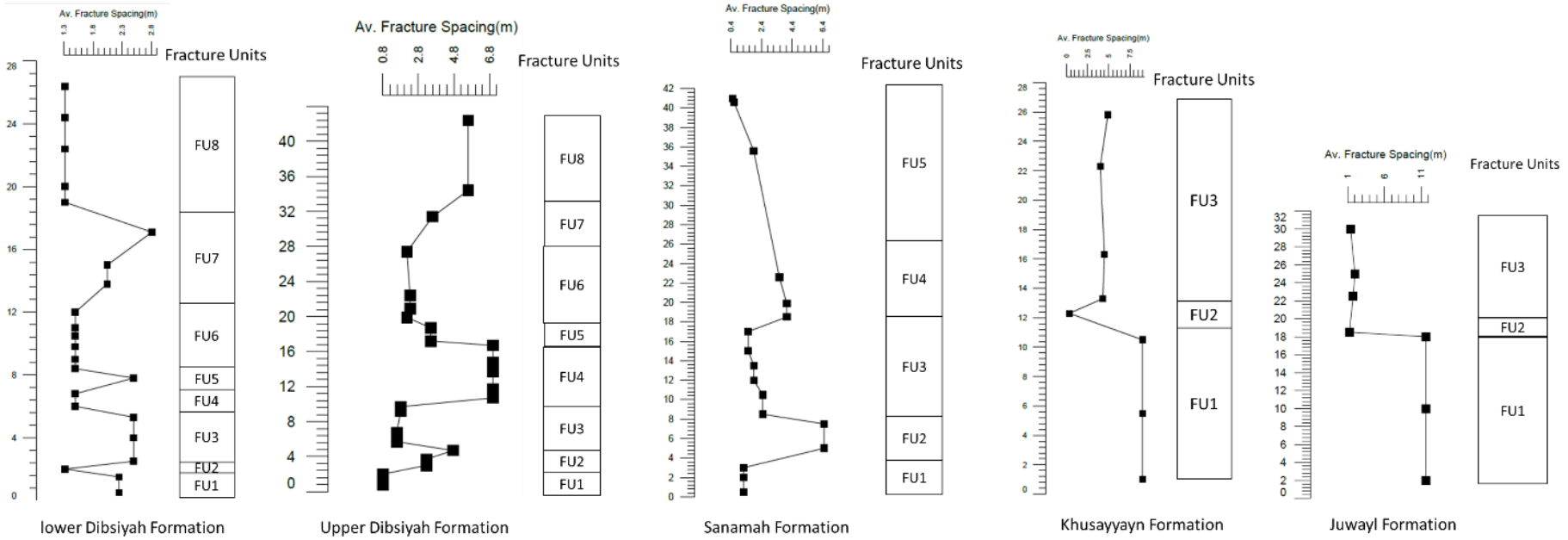

Figure 6.11: Fracture units of each formation of Wajid Group.

Table 6.6: Average fracture spacing, bed thickness and porosity values for each fracture unit.

Formation	Fracture Units	Average Fracture Spacing(m)	Bed Thickness(m)	Porosity(%)
Juwayl	FU3	1.72	4.33	24.24
	FU2	1.25	0.50	27.67
	FU1	11.67	18.00	28.29
Khusyyayn	FU3	4.43	3.38	32.67
	FU2	0.35	1.80	33.26
	FU1	9.00	5.25	31.83
Sanamah	FU5	1.00	6.17	19.37
	FU4	3.89	2.83	33.47
	FU3	1.97	3.17	34.07
	FU2	6.50	4.50	
	FU1	1.23	3.00	31.41
Upper Dibsiyah	FU8	5.60	12.00	27.66
	FU7	3.60	4.00	43.05
	FU6	2.24	2.80	27.76
	FU5	3.50	1.00	32.45
	FU4	7.00	5.00	32.80
	FU3	1.69	2.38	29.82
	FU2	3.75	1.80	37.27
	FU1	0.80	2.00	39.75
Lower Dibsiyah	FU8	1.32	3.98	26.48
	FU7	2.30	3.03	30.64
	FU6	1.50	2.25	31.24
	FU5	2.50	1.00	31.11
	FU4	1.50	1.50	30.75
	FU3	2.50	1.10	27.69
	FU2	1.32	0.50	26.01
	FU1	2.25	1.50	31.52

6.3.1 Bed thickness versus Average Fracture Spacing

A significant correlation is observed between the average fracture spacing and bed thickness for the entire Wajid Group succession, and the relationship between the average fracture spacing and bed thickness of Wajid Group sandstone is explained by the linear regression model with a coefficient of correlation (R) equal to 0.85 (Figure 6.12). This linear relationship between the average fracture spacing and bed thickness of sedimentary rocks documented by many researchers(Hobbs, 1967; Ladeira & Price, 1981; Narr & Suppe, 1991; Huang & Angelier, 1989; McQuillan, 1973; Gross, 1993; Wu and Pollard, 1995; Gross et al., 1995; Price, 1966; Ji & Saruwatari, 1998).

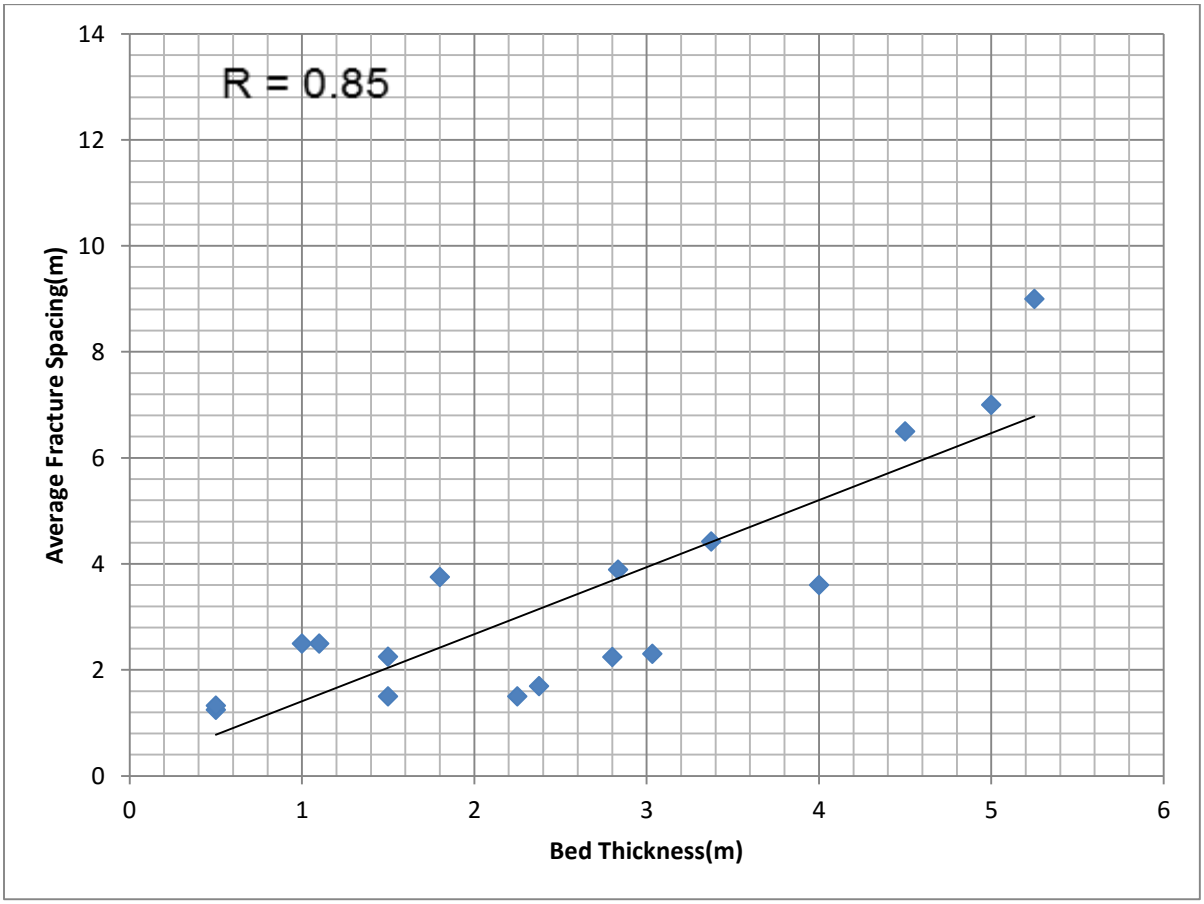

Figure 6.12: Scatterplot shows correlation between bed thickness and average fracture spacing.

6.3.2 Degree and Type of Cement versus Average Fracture Spacing

The influence of cement type and degree of cementation on the fracture distribution within sandstone reservoir documented by Sonntag et al., (2012). The well-cemented sandstone characterized by high strength, and then high fracture intensity; however, the poorly cemented sandstone showed low strength and then low fracture intensity. The strength of sandstone is controlled by the type of cement, where, the silica cement has great influence on the rock strength followed by carbonate cement, and the least effect is the clay cement.

The degree of cementation and type of cement of the Wajid Group sandstone units with thickness range from 1-3 m correlated to the average fracture spacing to evaluate the influence of the cementation degree and type on the fracture distribution within the studied sandstones (Figure 6.13)(Figure 6.14). The calcite-cemented sandstone displayed small average fracture spacing than clay cemented sandstone (Figure 6.13).

For the purpose of correlation between the degree of cementation and average fracture spacing, the degree of cementation grouped into three classes namely; low cement (<7.5%), moderate cement (>7.5% and <15%), and high cement (>15). As shown in Figure 6.14, the increasing in the degree of cementation corresponding with decreasing in the average fracture spacing, where, the highly cemented sandstone showed low values of average fracture spacing comparing to the poorly cemented sandstone.

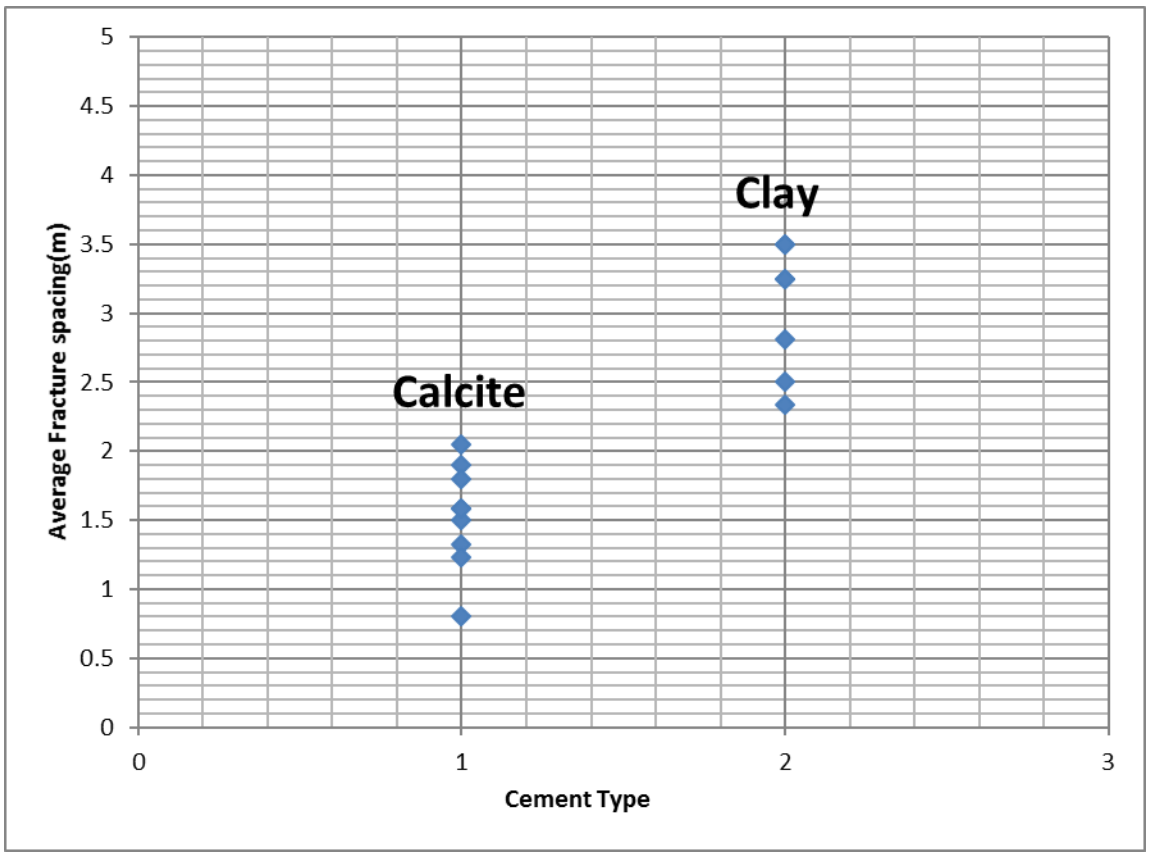

Figure 6.13: Scatterplot shows the average fracture spacing versus cement type. x-axis with value =1 represented the calcite cement with a mean of 1.52 m average fracture spacing, x-axis with value =2 represented clay cement with a mean of 3.02 m average fracture spacing.

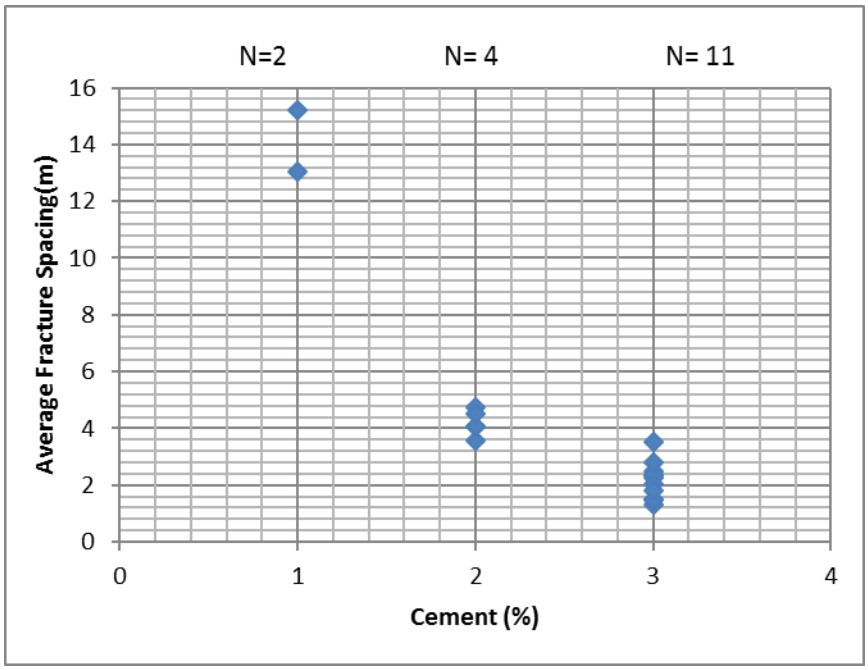

Figure 6.14: Scatterplot shows the degree of cementation versus the average fracture spacing. X axis value = 1 represented low cement content (< 7.5%), x axis value=2 represented moderate cement content (7.5%< cement >15%), x axis value=3 represented high cement content (> 15%).

6.3.3 Lithofacies versus Average Fracture Spacing

Six major sandstone lithofacies were defined for the entire succession of Wajid Group based on bed thickness, mean grain size, and sedimentary structures. They are 50-200 cm thick bed of fine to medium-grained cross-bedded sandstone lithofacies (L1), 50-200 cm thick beds of coarse-grained to pebbly cross-bedded sandstone lithofacies(L2), 50-200 cm thick bed of medium to coarse-grained bioturbated sandstone lithofacies(L3), >200 cm thick bed of fine to coarse-grained massive sandstone lithofacies(L4), >200 cm bed of fine to medium-grained cross-bedded sandstone lithofacies(L5), >200 cm bed of coarse-grained, pebbly to conglomeratic cross-bedded sandstone lithofacies (L6). The lithofacies of Wajid Group correlated with the average fracture spacing to investigate the influence of lithofacies type on the fracture distribution within the Wajid Group sandstones (Figure 6.15). Thin beds(50-200 cm) of medium to coarse-grained either cross-bedded or bioturbated sandstone lithofacies (L1,L2, and L3) display small average fracture spacing (1.77 m, 1.72 m, and 1.77 m respectively) than the thick beds(>200 cm) of medium to coarse, either cross-bedded or massive sandstone and conglomeratic sandstone lithofacies (L4, L5 and L6) (5.21 m, 3.1 m and 2.1 m respectively) (Figure 6.15).

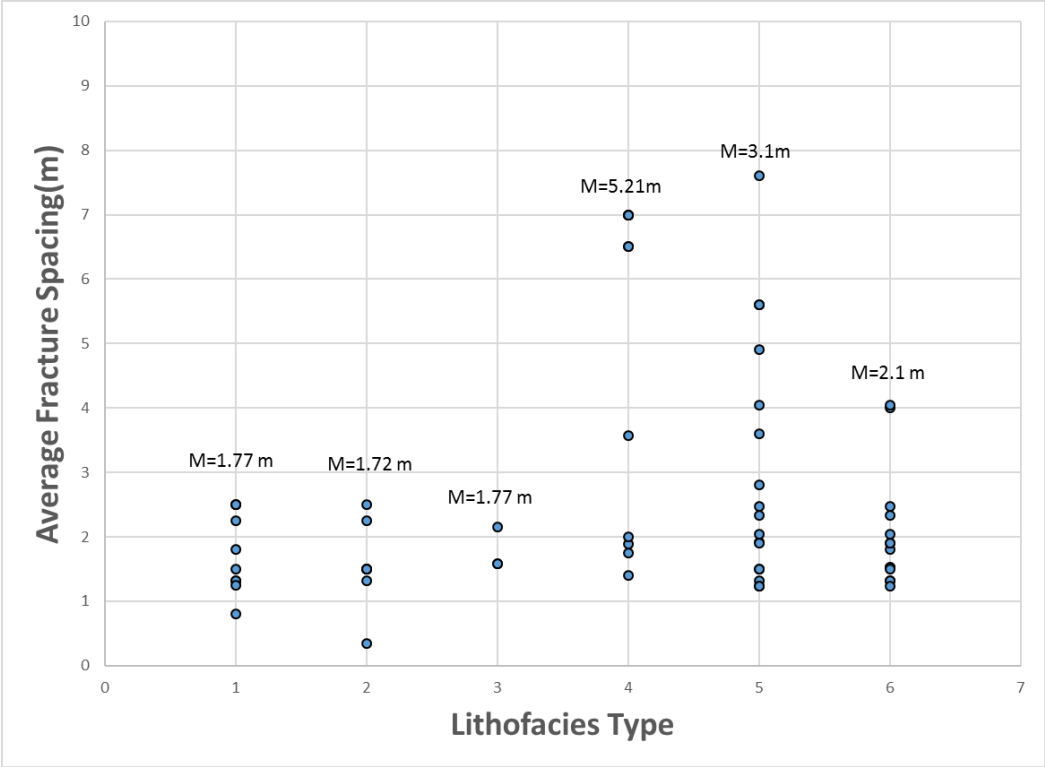

Figure 6.15: Scatterplot of average fracture spacing and sandstone lithofacies types of Wajid Group(M= mean). X axis value= 1 represented 50-200 cm thick beds of fine to medium-grained cross-bedded sandstone lithofacies (L1), x-axis value=2 represented 50-200 cm thick beds of coarse-grained to pebbly cross-bedded sandstone lithofacies(L2), x-axis value = 3 represented 50-200 cm thick beds of medium to coarse-grained Bioturbated sandstone lithofacies(L3), x-axis value = 4 represented >200 cm thick beds of fine to coarse-grained massive sandstone lithofacies(L4), x-axis value 5 represented >200 cm beds of fine to medium-grained cross-bedded sandstone lithofacies(L5), x-axis value = 6 represented >200 cm beds of coarse-grained, pebbly to conglomeratic cross-bedded sandstone lithofacies (L6).

6.3.4 Porosity versus Average Fracture Spacing

A significant and positive correlation observed between the average fracture spacing and matrix porosity for the entire Wajid Group succession (Figure 6.16). This correlation is fitted with exponential law distribution with a correlation of correlation(R) equal to 0.53. The highly porous sandstone units of Wajid Group associated with high values of average fracture spacing; however, the sandstone with low porosity displayed low average fracture spacing values (Figure 6.16).

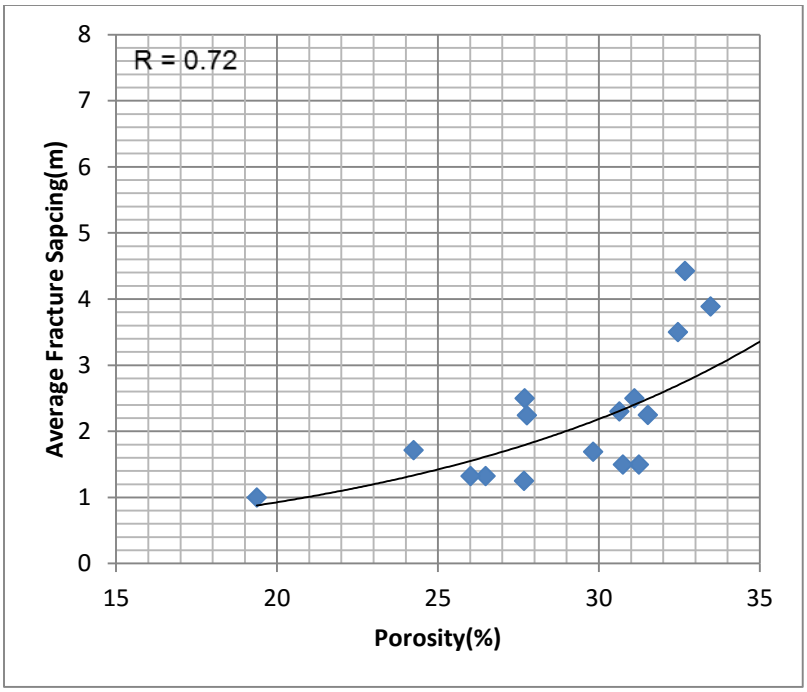

Figure 6.16: Scatterplot shows a correlation between porosity and average fracture spacing.

Chapter 7

Discussion, Conclusion, and Recommendation

7.1 Discussion

The lineament trends of Wajid Group include northerly, easterly, NW-SE and NE-SW are matching with the fracture trends at the outcrop and formation scales. This matching in lineament and fracture trends between the regional and outcrop and formation scale reveal that Wajid Group has a scale-independence fracture system. the northerly trend is predominant on the regional scale (lineament trace maps) and outcrop and formation scale. However, the NW-SE trend is predominant on the regional scale (lineament trace maps) than the outcrop and formation scale. On the contrary, the easterly trend is predominant at the outcrop and formation scale than the regional scale (lineament trace maps).

Zeeb et al., (2010) traced two main sets of the regional-scale fractures(lineaments) within Wajid Group outcrop in Wadi Al-Dawasir area included the N120^{o} At Uruq Khurb and N170^{o} at Jabal Al-Bara'im. In this study, the regional scale fracture(lineament)trends also included the N165^{o} and N135^{o} which are mostly matching with the fracture trends observed by Zeeb et al., (2010). Al-Ajmi et al., (2014) recognized four sets of fracture within Wajid Group in Wadi Al-Dawasir area included N170^{o}, N080^{o}, N020^{o}, and N120^{o}. Those fracture trends are matching with outcrop-scale fracture trends observed in this study included N165^{o}, N075^{o}, N015^{o}.

The regional-scale fracture(lineament) trends within Wajid Group compared with lineament and fracture trends present within the Cambro-Ordovician sedimentary succession (Saq Formation) in the northern part of Saudi Arabia. In the Tayma area, north of Saudi Arabia, Castaing et al., (1996) mapped and defined lineaments and fractures with NW-SE, WNW-ESE, and NE-SW trends. However, no observations of N-S, NNE-SSW, NNW-SSE and E-W trends of lineament traces and fractures were reported. Compared to the findings of this study, in southwestern Saudi Arabia, the N-S(000^{o}), NNE-SSW(015^{o}), NNW-SSE(165^{o}) and E-W(090^{o}) trends of lineament traces are also dominant. This variation in lineament trace trends within the Paleozoic sedimentary succession between the southern and northern parts of Saudi Arabia are most probably due to the dominant of the northerly and easterly trending structures in the southern part of the Arabian Shield compared to those of the north (Nehlig et al., 2002). The eastern part of the Wajid Group outcrops (From Wadi Al-Dawasir till Najran city) characterized by the abundance of NW-SE, and the northerly (Included N-S, NNE-SSW, NNW-SSE) trending regional scale fractures(lineaments); However, the NE-SW trending regional fracture(lineaments) observed as dominant trend in the western part of the Wajid Group outcrops (Abha area). This variation in the regional fractures(lineaments) trend between the eastern and western portions of the Wajid Group outcrop corresponding with the same variation in fracture zones trend within the Arabian Shield, where, the eastern portion of the Arabian Shield consisting very broadly of the NW-SE and N-S trending fracture zones; however, the western portion of the Arabian Shield consisting very broadly of the NE-SW (Nehlig et al., 2002; Stewart, 2016).

The trends of regional scale fracture(lineament) (detected from satellite images and the aeromagnetic anomaly map) are consistent with trends of aeromagnetic lineament traces in the southern part of the Arabian shield reported by Nehlig et al., (2002). They reported four main trends of aeromagnetic trends in the southern part of Arabian shield included the N135^{o}, N150^{o}, N-S, and E-W. Those trends also observed within Wajid Group sandstone in regional scale. Therefore, this reveals that the major lineaments trends within the Wajid Group outcrop may be inherited from basement structures and reflect their influence on the sedimentary cover in the studied area.

7.1.1 Relative age

The relative age of fractures observed in Wajid Group outcrop was determined using the crosscutting and termination relationships. The N165^{o} oriented fractures were observed cutting across the N075^{o} oriented fractures (Figure 7.1) which indicate that the N165^{o} oriented fractures are younger than the N075^{o}. The N165^{o} oriented fractures terminated against the N035^{o} oriented fractures, which indicate that the N035^{o} oriented fractures are older than the N165^{o} (Figure 7.1). The N135^{o} oriented fractures were observed displacing the N035^{0} and N165^{o} oriented fractures (Figure 7.1), then, this trend of fracture interpreted as the youngest fracture set in the studied outcrops. The cross-cutting and termination relationships between different fracture sets in Wajid Group indicate that the N165^{o}, N075^{o}, and N035^{o} oriented fractures are older than the N135^{o} oriented fractures. This conclusion is matching with the relative time of tectonic events of the Arabian-Nubian Shield(Edgell, 1992; Nehlig et al., 2002), where, the N-S, E-W, and NE-SW trending fractures and suture zones were formed during the Pan-African orogeny (accretion of the Arabian-Nubian shield); however, the NW-SE trending Najd fault

formed in the final stage of the accretion of the Arabian-Nubian Shield and dislocated the N-S trending Nabitah suture zone in the Arabian Shield (Al-Husseini, 2000; Nehlig et al., 2002; Stewart, 2016).

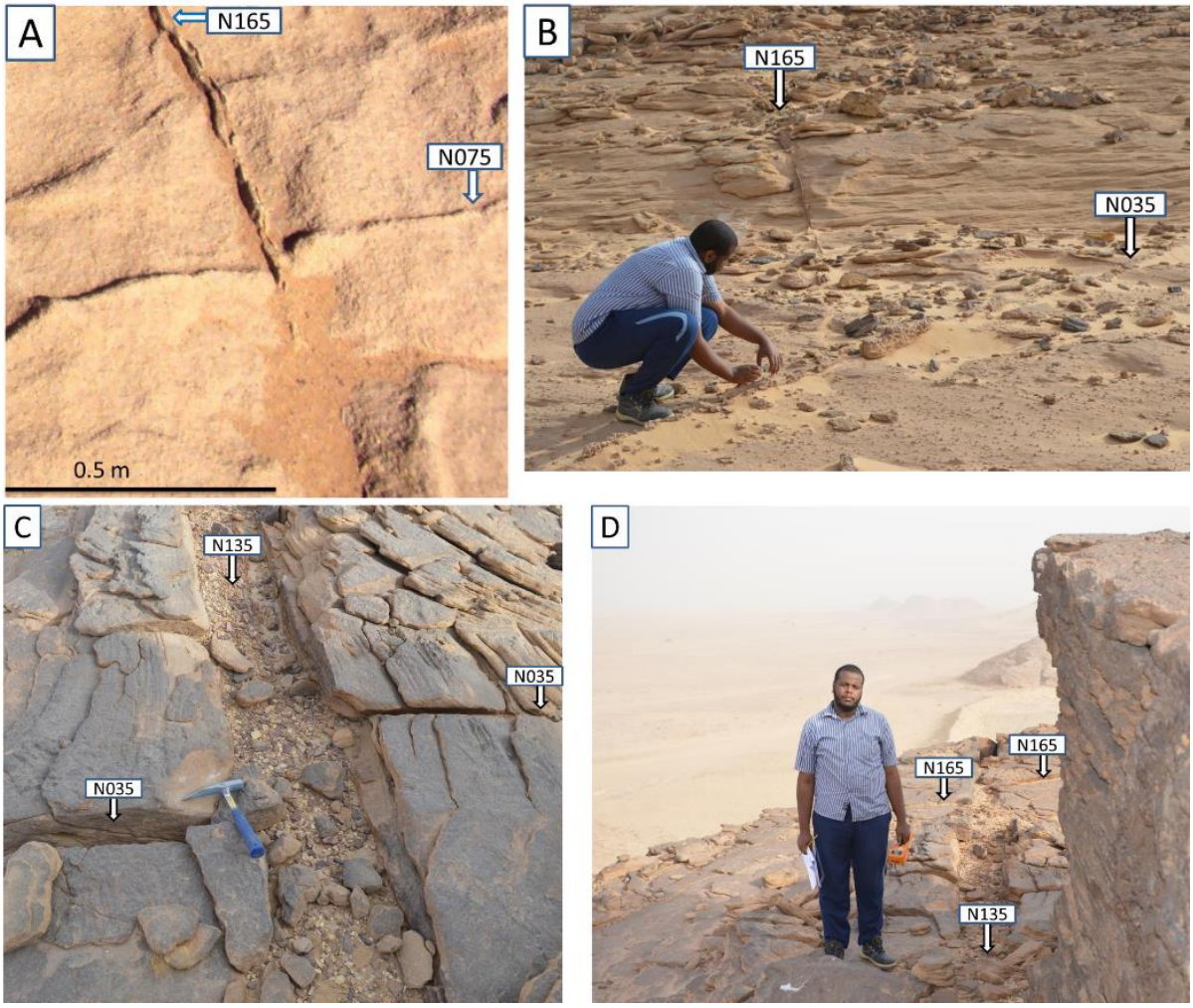

Figure 7.1: Outcrop photographs showing; A) N165º fracture cutting across the N075º. B) N165º fracture terminated against the N035º fracture. C) N135º fracture dislocated the N035º fracture. D) N135º fracture dislocated the N165º fracture.

7.1.2 Implication for Groundwater

Wheeler, (1978) suggested that the high-intensity fracture/lineament zones in the surface continue with depth, and Nur, (1978) suggested that the fractures/lineaments which are long in the map view (e.g. lineament trace map) continue deep through the section. Accordingly, the presence of two major lineament trends include NW-SE and northerly (including N-S, NNE-SSW, and NNW-SSE) with a kilometers scale and high frequency within the Wajid Group outcrop reveal that those lineaments most probably continue with depth and have influence on the groundwater and hydrocarbon flow in Wajid Graben and Rub' Al-Khali Basin, respectively. These lineaments most probably act as conduits for the fluid flow. Understanding the distribution of the lineaments within Wajid Group can help to predict the fluid flow behavior within either the groundwater fractured aquifers or fractured reservoirs. According to Zeeb et al., (2010) the direction of principal flow within Wajid aquifer is N147^{o} at Uruq Khurb, which is varied only by 12^{o} from N135^{o} and 3^{o} from the N150^{o} oriented large scale fracture (lineament) sets observed in this study. At Jabal Al-Bara'im in Wadi Al-Dawasir, the direction of principal flow is N158^{o} which differs only by 7^{o} from the N165^{o} and 8^{o} from the N150^{o} regional scale fracture(lineament) sets observed in this study. The NW-SE trend of regional scale fractures (lineaments) was observed as the highest frequent trend throughout the whole outcrop from Wadi Al-Dawasir until Najran area in multi-scale trace maps (1:1500000, 1:500000, and 1:200000) with length extend to 20 km. Therefore, the NW-SE trending regional fractures (lineaments) are most probably the pathways of groundwater flow in the Wajid Aquifers in the study area. The NNW-SSE trending lineaments which are occurred with length extend to 15 km and direction close to the direction of flow within

the Wajid Aquifers, are most probably have a major influence on the fluid flow in these aquifers.

7.1.3 Fracture Conceptual Models

Fracture systems within Wajid Group outcrops and their stratigraphic and lithological controls were summarized in hierarchal conceptual fracture models of two fracture sets. The first order model established to account for the regional scale lineament sets within Wajid Group outcrops (Figure 7.2). In this Model, the regional fracture (lineament) within Wajid Group extended from the Precambrian basement rock of the Arabian Shield, and cutting across the entire Wajid outcrops and not controlled by stratigraphic and lithological variations. This Model also showed that the lower part of Wajid Group exhibits high fracture intensity than the upper part, due to its proximity to the basement rock. The second order model with 100's meters scale established to account for two fracture sets observed at the outcrop scale (Figure 7.2). In this model, the fracture distribution controlled by lithological, stratigraphic and diagenetic variation, where, the lower Dibsiyah Formation which has small bed thickness comparing with other formations display high fracture density. However, the upper Dibsiyah, Sanamah, Khusayyayn and Juwayl Formations which have thick sandstone layers display low fracture density, except the uppermost part of the glacial origin sandstone of Sanamah and Juwayl Formations display high fracture density than the lower part of each formation due to diagenetic controls, where those sandstones are highly cemented by calcite or iron oxides.

The third order model with 10's meters' scale established for two fracture sets observed within at the outcrop scale. In this model, the variation in fracture density within each formation controlled by the variation in lithological, stratigraphic, and digenetic characteristics of sandstone units deposited within the same depositional environments.

10's meter scale models of the N165^{o} and N075^{o} fracture sets were established for Dibsiyah, Sanamah, Khusayyayn and Juwayl Formations (Figure 7.3). They showed that the fracture distribution is dependent on the stratigraphic boundaries (bedding plane), bed thickness and the lithological variation (e.g. grain size). The reported fracture spacing is large in the coarse-grained to conglomeratic sandstone than the fine-grained sandstone. Moreover, the fracture spacing is large in the poorly stratified sandstone than the well-stratified sandstone, and the degree of fracture termination at the bedding plane is large in the well-stratified sandstone. The fracture terminations were mainly concentrated on the bedding plane between fine and coarse-grained sandstone. These models also showed that the fracture spacing controlled by the thickness of the sandstone beds, and the degree of cementation where the fracture spacing are large in the poorly cemented thick sandstone beds than the highly cemented thinner ones.

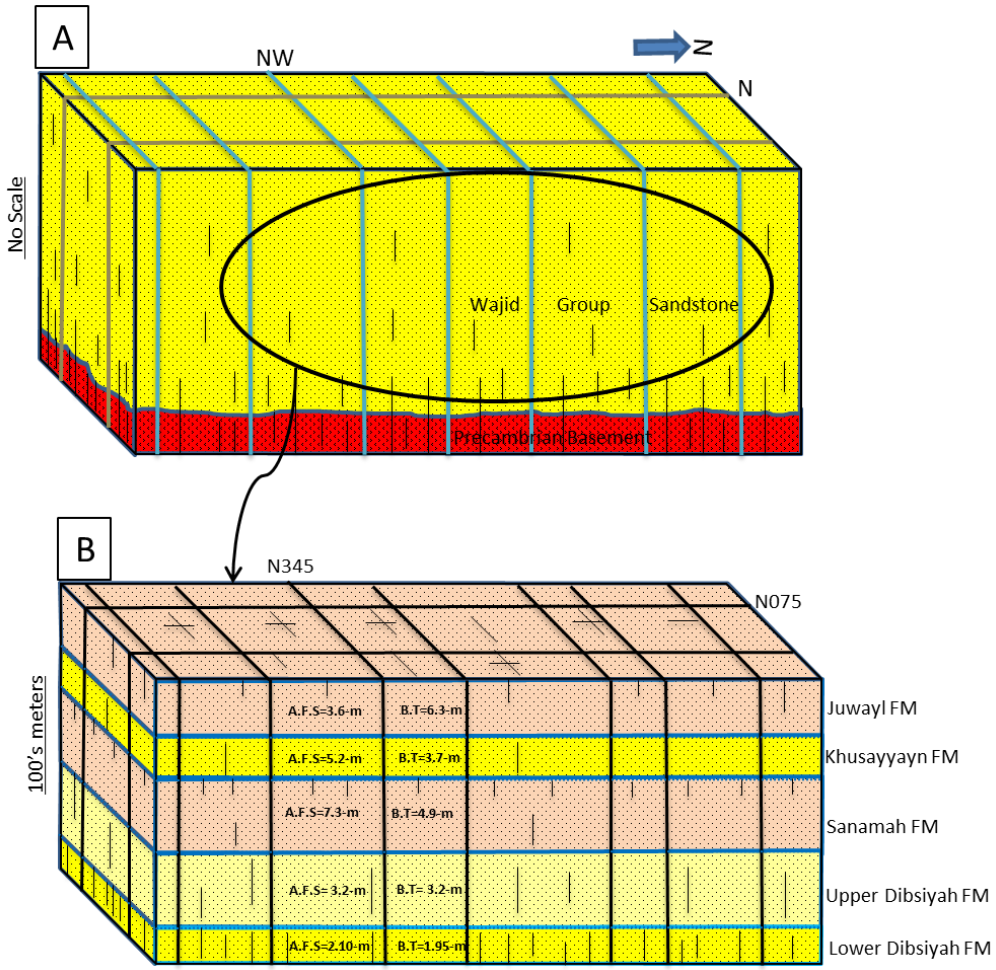

Figure 7.2: First and second order conceptual model of two fracture sets within Wajid Group. A) first order model, B)second order 100's meters scale model.

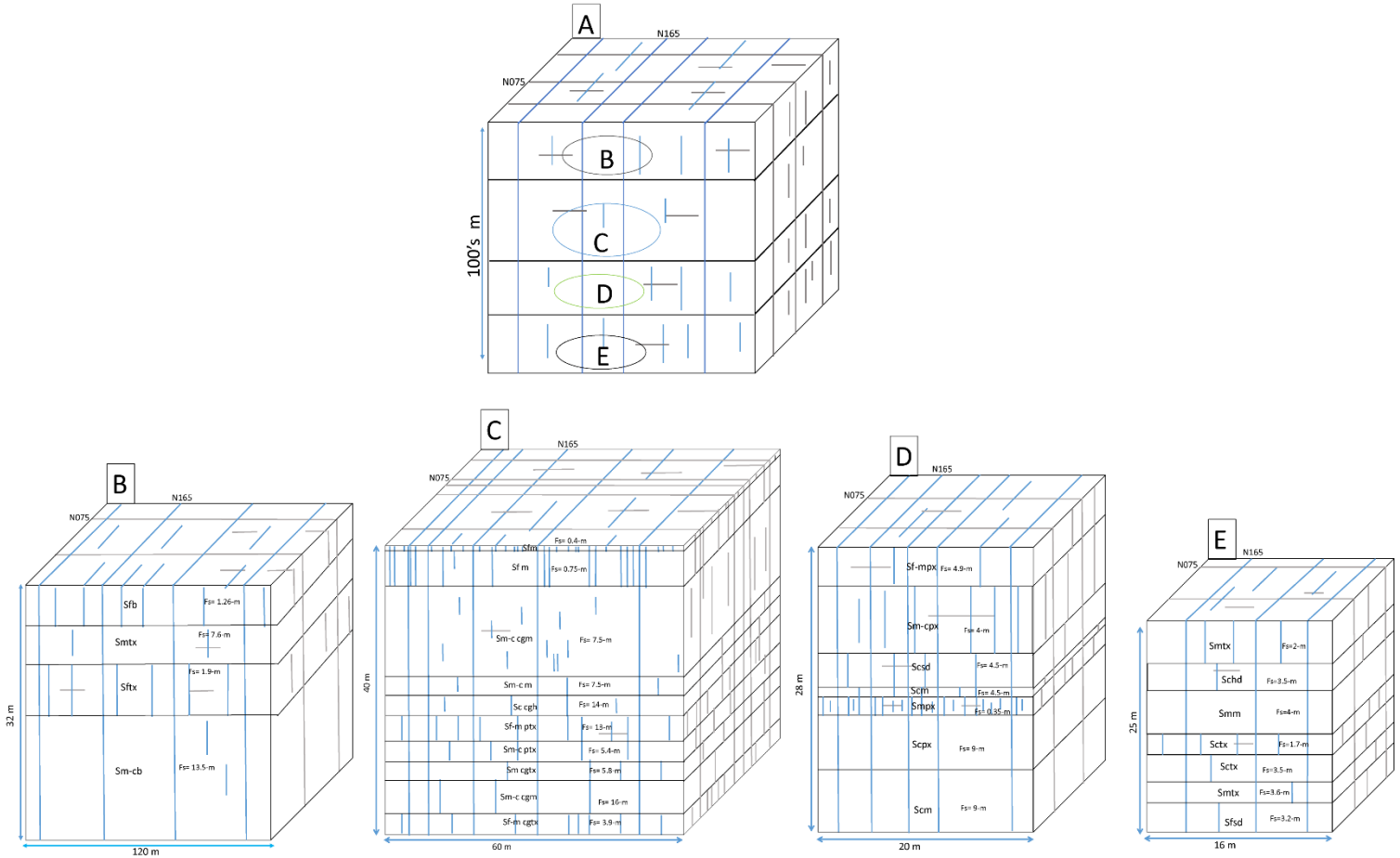

Figure 7.3: A Conceptual multi-scale model for the N165º and N075º fracture sets. A)100's meter scale model of the entire Wajid Group. B, C, D, and E are the 10's meter fracture models for Dibsiyah, Sanamah, Khusayyayn, and Juwayl Formation, respectively. Fs= average fracture spacing. Sm-cb = medium to coarse-grained burrowed sandstone, Sfb= fine-grained burrowed sandstone, Sftx=

fine-grained trough cross-bedded sandstone, Smtx= medium-grained trough cross-bedded sandstone. Sf-mcgtx = fine to medium-grained conglomeratic trough cross-bedded sandstone, Sm-ccgm= medium to coarse-grained conglomeratic massive sandstone, Smcgtx = medium-grained conglomeratic trough cross-bedded sandstone, Sm-c ptx = medium to coarse-grained pebbly trough cross-bedded sandstone, Sf-m ptx = fine to medium-grained pebbly trough cross-bedded sandstone, Sc cgh = coarse-grained conglomeratic horizontally bedded sandstone, Sm-c m = medium to coarse-grained massive sandstone, Sm cgm = medium-grained conglomeratic massive sandstone, Sf m = fine-grained massive sandstone. Scm= coarse-grained massive sandstone, Scpx= coarse-grained planar cross-bedded sandstone, Smpx = medium-grained planar cross-bedded sandstone, Scsd= coarse-grained soft deformed sandstone, Sm-cpx= medium to coarse-grained planar cross-bedded sandstone, and Sf-mpx= fine to medium-grained planar cross-bedded sandstone. Scsd= coarse-grained soft deformed sandstone. Smtx= medium-grained trough cross-bedded sandstone. Sf m = fine-grained massive sandstone. Schd = coarse-grained horizontal bedded sandstone.

7.1.4 Comparison with Subsurface Fracture System

Subsurface study on the reservoir completion and fracture simulation conducted on Sarah Formation in Rub' Al-Khali Basin by Bu-Khamseen et al. (2010) indicated that the Sarah Formation is a naturally fractured reservoir with dominant fracture trends of NE-SW, NW-SE, E-W, NNW-SSE, and WNW-ESE. The subsurface Sarah Formation is equivalent to Sanamah Formation of Wajid Group in term rock type, age, and depositional setting, where, both are Late Ordovician glacial to glaciofluvial siliciclastic (Vaslet, 1990; Stump & Van der Eem, 1995; Laboun, 2010). Those trends of fracture are also observed in Sanamah Formation of Wajid Group in the studied outcrop. Therefore, the fracture trends of Sanamah Formation in outcrop are comparable with the fracture trends of subsurface Sarah Formation in Rub' Al-Khali. This similarity may reveal the same regional stress regime, which is probably related to Precambrian basement tectonics. Accordingly, the fracture systems of Sanamah Formation of Wajid Group in the outcrop can be used as an analogue to characterize and model fracture systems in Sarah Formation of the Rub' Al-Khali Basin. Additionally, the results and information obtained from a study conducted on fracture systems of Sanamah Formation will help to enhance gas exploration and production from subsurface Sarah reservoir in Rub' Al-Khali Basin and as a guide for other areas of similar rock types, age and fracture trends in the region.

Based on regional magnetic and gravity data, and reflection seismic data, Stewart (2016), detected two trends of the Precambrian basement structure in west Rub' Al-Khali Basin include N-S and NW-SE (Figure 7.4). These trends are matching with the N-S and NW-SE trending lineaments within Wajid Group outcrop detected in this study. This matching

of fracture trends between Wajid Group outcrops and the west Rub' Al-Khali Basin indicate the same regional stress and most probably related to Pan-African orogeny.

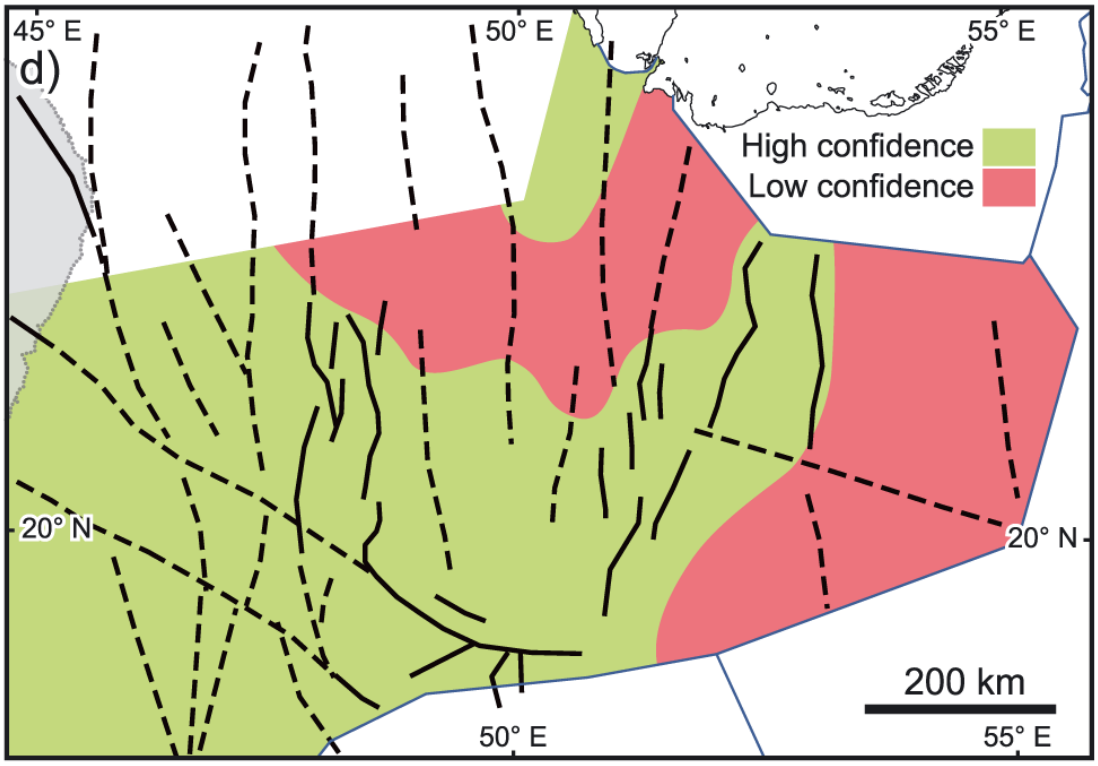

Figure 7.4: Basement structural trends in the Rub' Al-Khali Basin(after (Stewart, 2016).

7.1.5 Petrographic and Petrophysical Controls on the Geomechanical Properties

The influences of the petrographic and petrophysical properties (included: cement content, grain size, mineral composition, porosity, and permeability) on the geomechanical properties (included the uniaxial compressive strength(UCS) and static Young' modulus(E)) of sandstone documented by many researchers(Fahy and Guccione, 1979; Shakoor and Bonelli, 1991; Zorlu et al.,2004; Ulusay et al.,1994; Vutukuri et al., 1974; Gunsallus and Kulhawy, 1984; Bell, 1978; Vernik et al., 1993; Jizba, 1991). Increasing in the rock strength is mainly associated with increasing in cement content(Fahy, and Guccione, 1979; Shakoor and Bonelli, 1991; Zorlu et al.,2004; Ulusay et al.,1994), and Sandstone cemented by silica are strong followed by calcite, and ferrous minerals; however, sandstone cemented by clay minerals is the weakest (Vutukuri et al., 1974). In the Wajid Group sandstone, the cement content observed as a main control on the rock strength, where, highly cemented sandstone displayed high value of UCS values which indicate that the sandstone is strong. The silica and calcite-cemented sandstone showed UCS values higher than the clay-cemented sandstone.

Increasing in the quartz percentage within the compositional framework of the sandstone associated with increasing in sandstone strength(UCS) (Gunsallus and Kulhawy, 1984; Zorlu et al., 2004). This relationship was observed in Khusayyayn Formation of Wajid Group, where, sandstone with high quartz percentage displayed UCS values higher than the sandstone with a significant amount of feldspars minerals. Fahy and Guccione, (1979) found that the fine-grained sandstone showed high strength values than the coarse-grained sandstone. The influence of grain size on the UCS and E values of Wajid group

sandstone was observed, where, the increasing in grain size associated with decreasing of UCS and E values. Negative influence of porosity on the geomechanical properties of the sandstone rock was observed by many researchers(Bell, 1978; Vernik et al., 1993; Jizba, 1991), and this relationship was also observed in Wajid Group outcrop, where, the increasing of porosity values of the studied sandstone associated with decreasing in UCS and E values.

Moderate to strong correlation between the permeability and geomechanical properties (RN, UCS, and E) of glacial origin sandstone from Sanamah and Juwayl Formations. However, no significant correlation between the permeability and geomechanical properties (RN, UCS, and E) of the non-glacial origin sandstones from Dibsiyah and Khusayyayn Formations. In literature, no documentation of the relationship between the matrix permeability and the geomechanical properties (RN, UCS, and E) of sandstone reservoirs.

7.1.6 Geological Controls on the Fracture Distribution

Nelson, (2001) summarized some geologic controls on fracture intensity (fracture spacing is the inverse of fracture intensity), among them the texture (included grain size) and the bed thickness. Ortega et al., (2006) emphasized that the most important geological control on fracture intensity is the bed thickness (or they call it mechanical layer thickness). Bogdanov, (1947) documented that the fracture spacing in layered sedimentary rock is proportional to the bed thickness. This relationship was also concluded by other researchers (Price, 1966; McQuillan, 1973; Huang & Angelier, 1989; Narr & Suppe, 1991; Gross, 1993; Mandal et al., 1994; Wu and Pollard, 1995; Becker &

Gross, 1996; Narr, 1996; Pascal et al., 1997; Ji & Saruwatari, 1998; Bai & Pollard., 2000). The result of this study is in the same line with previous publications regarding the relationship between the fracture spacing and the bed thickness. The increasing in bed thickness of the studied sandstone associated with increasing in fracture spacing and a simple linear regression model account for this relationship. The increasing in the gain size of the studied sandstone associated with increasing in fracture spacing and this relationship is in the same line with what have been documented in the literature (Nelson, 2001; Sonntag et al., 2012; Lyu et al., 2016).

The relationship between the degree of cementation and the average fracture spacing within Wajid Group sandstone was investigated, where, the increasing in the degree of cementation associated with decreasing in fracture spacing. This relationship is in the same line with what Sonntag et al., (2012) reported from the Mesaverde Group sandstone, Uinta Basin, USA. The reported result of the relationship between the cement type and fracture spacing showed that the silica and calcite-cemented sandstone displayed small average fracture spacing comparing with the clay-cemented sandstone. This relationship also has been documented by Sonntag et al., (2012).

The rock strength is mainly decreased when the porosity increased and this influence of porosity on the rock strength documented by many researchers (Price, 1960; Bell, 1978; Shakoor & Bonelli, 1991; Dobereiner & De Freitas, 1986; Bell & Lindsay, 1999). The strong rock is mainly characterized by close-spacing fractures and has a low value of porosity. This relationship between matrix porosity of rocks and the average fracture spacing observed in the Wajid Group sandstone, where, the sandstone with low porosity values displayed small average fracture spacing.

lithofacies type was observed as primary control on the average fracture spacing of Wajid Group sandstone, where, the fine to medium-grained thinly bedded, small scale cross-bedded sandstone lithofacies of lower Dibsiyah Formation have small average fracture spacing (the highest fracture density) comparing with the coarse-grained pebbly thick bedded massive sandstone lithofacies of Sanamah and Juwayl Formation. Grain size, bed thickness, the scale of cross-bedding sedimentary structures, and degree of cementation and cement type influence the fracture spacing of different lithofacies. The influence of lithofacies type on the fracture distribution with the Mesaverde Group sandstone, Uinta Basin, USA studied by Sonntag et al., (2012). They reported that the thinly bedded fine to medium grained sandstone lithofacies has the highest fracture density (the lowest fracture spacing); however, the thickly bedded medium to coarse-grained sandstone lithofacies has the lowest fracture density (the highest fracture spacing).

7.2 Conclusions

The regional and outcrop-scaled fracture systems within Wajid Group outcrop were studied using multiscale approach. The regional-scaled fractures(lineaments) were studied by Integration of satellite images (Landsa-8 OLI/TIRS and Spot-5) with multiple resolutions, SRTM Digital Elevation Models (DEM), and magnetic anomaly map. Multiscale lineament trace maps (1:1500000, 1:500000, 1:200000, 1:125000, 1:12000, and 1:6000) were generated, and eight lineament trace trends were identified including NW-SE, NNW-SSE, N-S, NNE-SSW, NE-SW, ENE-WSW, E-W, and WNW-ESE. The NW-SE, NE-SW and the northerly (include N-S, NNE-SSW, and NNW-SSE) trending lineament were observed as the predominant trends. Seven trends of outcrop-scale fractures were directly delineated from outcrop included N-S, E-W, NNE-SSW, NE-SW, ENE-WSW, NNW-SSE, and NW-SE. The northerly (included NNW-SSE and NNE-SSW) and ENE-WSW trending fracture sets are the predominant at the outcrop scale. The fractures with Wajid Group are regional fractures and related to various tectonic events according to their orientation. The northerly, easterly, and the NE-SW trends of fractures are most probably inherited from the Precambrian basement structures which formed during the Pan-African orogeny. The NW-SE trending fractures are most probably related to the NW-SE trending left-lateral Najd fault system which formed in the late stage of Pan-African orogeny. Those trends are matching with the structure and fracture zones trends observed in the Arabian Shield (Nehlig et al., 2002; Whitehouse et al., 2001). The Precambrian basement structures most probably reactivated during the Phanerozoic Era and formed the fracture system of Wajid Group outcrop, where, Arabian Shield extends beneath the Phanerozoic sedimentary rocks in Saudi Arabia. Compatible

trends between the regional and outcrop-scaled fractures within Wajid Group outcrop; however, the easterly (E-W, ENE-WSW, and WNW-ESE) trending fractures are more pronounced at the outcrop scale than regional scale. The fluid flow in the fractured aquifers and reservoirs in Wajid Basin Rub' Al-Khali Basin, respectively, is excepted to be controlled by regional-scaled fracture trends included the northerly (N-S, NNE-SSW, and NNW-SSE), NW-SE, and NE-SW.

The entire outcrop of Wajid Group in the study area is fractured by vertical to sub-vertical, open, mode I (joints) fractures; however, in some places, the joints were infilled by either iron oxides or calcite minerals. N015^{o} oriented fracture swarms were also observed in Khusayyayn Formation outcrops in the southern part of Wadi Al-Dawasir area. The lengths of the regional scale fractures (lineaments) distributed according to negative exponential distribution. The average spacing of the outcrop-scale fractures varied vertically from bed to bed and from one formation to another. Fine-grained thin sandstone layers displayed small average fracture spacing than the coarse-grained thick sandstone layers. Thus, the bed thickness and sandstone texture (mainly grain size) observed as the main controls on the average fracture spacing in the studied sandstone. The distribution of fracture systems within Wajid Group outcrops and their stratigraphic and lithological controls represented in hierarchal outcrop conceptual models. The models showed that the regional scale fractures (lineaments) are not controlled by stratigraphic and lithological variations; however, the outcrop-scale fractures are mainly controlled by the stratigraphic and lithological properties of the fracture-hosting sandstones.

The Geomechanical properties of the Wajid Group sandstone controlled by its petrographic and petrophysical properties (included: cement content, grain size, mineral composition, porosity, and permeability). Cement content and type of the studied sandstone observed as main control on the uniaxial compressive strength(UCS) and static Young' Modulus(E), where, the increasing in the cement content associated with increasing in the uniaxial compressive strength(UCS) and static Young' Modulus(E) of the studied sandstone which indicate that the sandstone is dense and more brittle. The calcite-cemented sandstone showed strength values greater than mixed (calcite, silica and clay and iron oxides), and clay minerals cemented sandstone. The quartz percentage of mineral composition observed as a main control on the geomechanical properties of Khusayyayn Formation sandstone. The main grain size of Wajid Group sandstone observed controlling its geomechanical properties. The increasing in the mean grain size associated with decreasing in the uniaxial compressive strength(UCS) and static Young' Modulus(E) of studied sandstone. Matrix porosity of the studied sandstone observed controlling on its geomechanical properties. The increasing in the matrix porosity associated with decreasing in the uniaxial compressive strength (UCS) and static Young' Modulus(E) of studied sandstone.

Generally, the main factors controlled the geomechanical behavior of Wajid Group sandstone are texture (mean grain size), mineral composition, cement content and type, and the matrix porosity and matrix permeability. These factors have a different magnitude of influence on the geomechanical behavior of such sandstone, however, the grain size, cement content and type, matrix porosity, and permeability observed as the

major factors for all studied sandstone except Khusayyayn Formation, where, the mineral composition has also influence on the mechanical behavior.

The variation of fracture characteristics (e.g. average fracture spacing) within Wajid Group sandstone in the outcrop associated with variation in the sandstone properties included sedimentological, stratigraphic and petrophysical properties. The bed thickness observed as a main control on the fracture spacing of the studied sandstone, where, the thick sandstone beds associated with large fracture spacing; however, the thin beds display small fracture spacing. Among the four formations of Wajid Group, the lower Dibsiyah Formation which has sandstone beds thinner than other formation showed the lowest average fracture spacing. Diagenetic features (cementation) observed as main controls on the fracture spacing of the studied sandstone, where, the highly cemented sandstone display small values average fracture spacing than the low cemented sandstone. On the contrary, the dissolution of calcite cement and feldspar grains enhanced the secondary porosity and associated with large values of average fracture spacing (high fracture density). Lithofacies type(lithology) observed as main controls on the fracture spacing of the studied sandstone, where, the fine to medium-grained thinly bedded sandstone lithofacies display average fracture spacing smaller than the coarse-grained pebbly or conglomeratic thickly bedded sandstone lithofacies. The matrix porosity of the studied sandstone plays a key role on the fracture spacing, where, the high porosity sandstone units display values of average fracture spacing higher than low-porosity sandstone. No significant influence of the mineral composition and texture of studied sandstone on the fracture spacing.

7.3 Recommendations

1- Conducting a study on the fracture system of the Wajid Group sandstone in the subsurface of Wajid Graben and Rub' Al-Khali Basins to understand its control on fluid flow and storage space within the aquifers and reservoirs.

2- Use this study outcome of fracture distribution and characteristics as a guide for study the fracture system of similar sandstone in central and northern Saudi Arabia.

3- Conducting a near surface geophysical investigation to study the extension of fracture system observed within Wajid Group sandstone at the surface.

4- conducting a detailed study on the fracture system of Sarah Formation in the subsurface using image logs, core, and thin section to assist the effect of fracture system on the fluid flow and storage space, and combine the result with the results of this study to build a fracture network model.

References

Abdulkadir, I. T. (2007). Sedimentology and reservoir characteristics of paleozoic Dibsiyah Member(Wajid sandstone), southwestern Saudi Arabia. King Fahd University of Petroleum and Minerals.

Abdulkadir, I. T., & Abdullatif, O. M. (2013). Facies, Depositional Environments, Reservoir Potential and Palaeogeography of the Cambro-Ordovician Dibsiyah Formation, Wajid Outcrop Belt, Saudi Arabia. Arabian Journal for Science and Engineering, 38(7), 1785–1806. https://doi.org/10.1007/s13369-012-0388-x

Abdulkadir, I. T., Sahin, A., & Abdullatif, O. M. (2010). Distribution of petrophysical parameters in the cambro-ordovician dibsiyah member of the wajid sandstone, Sw Saudi Arabia. Journal of Petroleum Geology, 33(3), 269–280. https://doi.org/10.1111/j.1747-5457.2010.00478.x

Abu-Ali, M., & Littke, R. (2005). Paleozoic petroleum systems of Saudi Arabia: a basin modeling approach. GeoArabia, 10(3), 131–168.

Agar, R. A. (1987). The Najd fault system revisited; a two-way strike-slip orogen in the Saudi Arabian Shield. Journal of Structural Geology, 9(1), 41–48.

Al-Ajmi, H. F., Keller, M., Hinderer, M., & Filomena, C. M. (2015). Lithofacies, depositional environments and stratigraphic architecture of the Wajid Group outcrops in southern Saudi Arabia. GeoArabia, 20(1), 49–94.

Al-Husseini, M. (2004). Pre-Unayzah unconformity, Saudi Arabia. In M.I. Al-Husseini (Ed.), Carboniferous,Permian and Early Triassic Arabian Stratigraphy. GeoArabia Special Publication 3, 15–59. Retrieved from G. article library

Al-Husseini, M. I. (2000). Origin of the Arabian plate structures: Amar Collision and Najd Rift. GeoArabia, 5(4), 527–542.

Al-Mahmoud, M. J., & Al-Ghamdi, I. (2010). An Overview of Tight Gas Reservoirs in Saudi Arabia. In In Second EAGE Middle East Tight Gas Reservoirs Workshop.

Al Ajmi, H. (2013). Sedimentology, stratigraphy and reservoir quality of the Paleozoic Wajid Sandstone in SW Saudi Arabia (Doctoral dissertation). Technische Universität.

Al Ajmi, H., Hinderer, M., Rausch, R., Hornung, J., Bassis, A., Keller, M., & Schüth, C. (2014). Matrix versus fracture permeability in a regional sandstone aquifer (Wajid sandstone, SW Saudi Arabia). Grundwasser, 19(2), 151–157. https://doi.org/10.1007/s00767-014-0258-4

Al Alawi, J., & Abdulrazzak, M. (1994). Water in the Arabian Peninsula: problems and perspectives, Chapter 7. Water in the Arab World: Perspectives and Prognoses, Harvard University Press, USA, 171–252.

Alabouvette, B., & Villemur, J. (1973). Reconnaissance survey of the Wajid Sandstone. French Bureau. Recherches Geologie Ministres Open-File Report, 70.

Alsharhan, A. S., & Nairn, A. E. M. (1997). Sedimentary basins and petroleum geology of the Middle East. Elsevier.

Alsharhan, A. S., Nairn, A. E. M., & Mohammed, A. A. (1993). Late Palaeozoic glacial sediments of the southern Arabian Peninsula: their lithofacies and hydrocarbon potential. Marine and Petroleum Geology, 10(1), 71–78.

Alsharhan, A. S., Nairn, A. E. M., & Shegewi, O. (1991). The Paleozoic sandstones of the Rub A1 Khali Basin, Arabia: a review. Palaeogeography, Palaeoclimatology, Palaeoecology, 85(3–4), 161–168. https://doi.org/10.1016/0031-0182(91)90156-L

Babalola, L. O. (1999). Depositional environments and provenance of the Wajid Sandstone, Abha-Khamis Mushayt Area, southwestern Saudi Arabia. MSc Thesis. King Fahd University of Petroleum and Minerals.

Bai, T., & Pollard., D. D. (2000). Fracture spacing in layered rocks: A new explanation based on the stress transition. Journal of Structural Geology, 22(1), 43–57.

Becker, A., & Gross, M. R. (1996). Mechanisms for joint saturation in mechanically layered rocks— An example from southern Israel. Tectonophysics, 257, 223– 237.

Bell, F. G. (1978). The physical and mechanical properties of the Fell Sandstones, Northumberland, England. Engineering Geology, 12, 1–29.

Bell, F. G., & Lindsay, P. (1999). The petrographic and geomechanical properties of some sandstones from the Newspaper Member of the Natal Group near Durban, South Africa. Engineering Geology, 53(1), 57–81. https://doi.org/10.1016/S0013-7952(98)00081-7

Bertotti, G., Hardebol, N., Taal-van Kroppen, J. K., & Luthi, S. M. (2007). Toward a quantitative definition of mechanical units: New techniques and results from an outcropping deep-water turbidite succession (Tanqua-Karoo Basin, South Africa). AAPG Bulletin, 91(8), 1085–1098. https://doi.org/10.1306/03060706074

Beydoun, Z. R. (1991). Arabian plate hydrocarbon geology and potential. Tulsa, OK (United States); American Association of Petroleum Geologists.

Bogdanov, A. A. (1947). The intensity of cleavage as related to the thickness of beds. Soviet Geology, 16, 102–104.

Bosworth, W., Huchon, P., & McClay, K. (2005). The Red Sea and Gulf of Aden Basins. Journal of African Earth Sciences, 43(1), 334–378.

Brown, G. E., Schmidt, D. L., & Huffman Jr, A. C. (1989). Geology of the Arabian Peninsula; shield area of western Saudi Arabia.(No. 560-A). U.S. Geological Survey Professional Paper.

Brown, G. F. (1972). Tectonic map of the Arabian Peninsula.US Geological Survey.

Brown, G. F., & Jackson, R. O. (1960). The Arabian Shield. Proceedings of the 21st International Geological Congress, Copenhagen, Section, 9, 69–77.

Bu-Khamseen, R. H., Khakimov, A., Sierra, L., Machala, M. S., & Young, D. A. (2010). First Successful Selective Tight Gas Reservoir Completion and Fracture Stimulation in Sarah Formation, Rub Al-Khali Empty Quarter of Saudi Arabia. In In SPE Russian Oil and Gas Conference and Exhibition. Society of Petroleum Engineers. https://doi.org/10.2118/136038-MS

Castaing, C., Halawani, M. A., Gervais, F., Chilès, J. P., Genter, A., Bourgine, B., … Janjou, D. (1996). Scaling relationships in intraplate fracture systems related to Red Sea rifting. Tectonophysics, 261(4), 291–314. https://doi.org/10.1016/0040-1951(95)00177-8

Cepeda, J. C. (1994). Fracture orientation and distribution on the Kaibab Plateau of Northern Arizona. The Mountain Geologist, Rocky Mountain Asso. of Geologists, 31(3), 77–83.

Dabbagh, M. E., & Rogers, J. J. W. (1983). Depositional environments and tectonic significance of the Wajid Sandstone of southern Saudi Arabia. Journal of African Earth Sciences, (1), 47–57.

Davies, F. B. (1984). Strain analysis of wrench faults and collision tectonics of the Arabian-Nubian Shield. The Journal of Geology, 82, 37–53.

Dobereiner L, & De Freitas, M. (1986). Geotechnical properties of weak sandstone. Geotechnique, 36(1), 79–94.

Dyer, R. A. R., & Husseini, M. (1991). The Western Rub'Al-Khali Infracambrian Graben System. Middle East Oil Show, SPE 21396, 2139. Retrieved from https://www.onepetro.org/conference-paper/SPE-21396-MS

Edgell, H. S. (1992). Basement tectonics of Saudi Arabia as related to oil field structures. Basement Tectonics, 9, 169–193.

Edgell, H. S. (1997). Aquifers of Saudi Arabia and their geological framework. Arabian Journal for Science and Engineering, 22(1 C), 3–31.

Evans, D. S., Lathon, A. B., Senalp, M., & Connally, T. C. (1991). Stratigraphy of the Wajid Sandstone of Southwestern Saudi Arabia. In the 7th Society of Petroleum Engineers Middle East Oil Show. (SPE 21449).

Fahy, M., & Guccione, M. (1979). Estimating strength of sandstones using petrographic thin-section data. Bulletin of the Association of Engineering Geologists, 16(4), 467–485.

Fall, A., Eichhubl, P., Bodnar, R. J., Laubach, S. E., & Davis, J. S. (2015). Natural hydraulic fracturing of tight-gas sandstone reservoirs , Piceance Basin , Colorado, 127(1–2), 61–75. https://doi.org/10.1130/B31021.1

Faqira, M., Rademakers, M., & Afifi, A. M. (2009). New Insights into the Hercynian Orogeny, and their Implications for the Paleozoic Hydrocarbon System in The Arabian Plate. GeoArabia, 14(3), 199–228.

Gross, M.R., Fischer, M.P., Engelder, T., Greenfield, R. J. (1995). Factors controlling joint spacing in interbedded sedimentary rocks: integrating numerical models with field observations from the Monterey Formation, USA. Geological Society Special Publication, 92, 215–233.

Gross, R. (1993). The origin and spacing of cross joints: examples from the Monterey Formation, Santa Barbara Coastline, California. Journal of Structural Geology, 15(6), 737–751.

GTZ/DCo. (2009). Detailed water resources studies of Wajid and overlying aquifers. Final report for the Ministry of Water and Electricity, Kingdom of Saudi Arabia.

Guiton, M. L. E., Sassi, W., Leroy, Y. M., & Gauthier, B. D. M. (2003). Mechanical constraints on the chronology of fracture activation in folded Devonian sandstone of the western Moroccan Anti-Atlas, 25, 1317–1330.

Gunsallus, K., & Kulhawy, F. (1984). A comparative evaluation of rock strength measures. International Journal of Rock Mechanics and Mining Sciences, 21(5), 233–248.

Hadley, D., & Schmidt, D. L. (1975). Nonglacial origin for conglomerate beds in the Wajid Sandstone of Saudi Arabia(No. 74-21). US Geological Survey.

Hariri, M. M. (2008). Implications of lineaments trends from Ghawar field and adjacent areas. In GEO 2008.

Hatcher, R. D. (1995). Structural geology: Principles, concepts, and problems. Macmillan Publishing Company.

Hennings, P., Olson, J. E., & Thompson, L. B. (2000). Combining Outcrop Data and Three- Dimensional Structural Models to Characterize Fractured Reservoirs : An example from Wyoming. AAPG Bulletin, 84, 830–849. https://doi.org/10.1306/A967340A-1738-11D7-8645000102C1865D

Hobbs, D. W. (1967). The Formation of Tension Joints in Sedimentary Rocks: An Explanation. Geological Magazine, 104(6), 550–556. https://doi.org/10.1017/S0016756800050226

Hooker, J. N., Gale, J. F. W., Gomez, L. A., Laubach, S. E., Marrett, R., & Reed, R. M. (2009). Aperture-size scaling variations in a low-strain opening-mode fracture set , Cozzette Sandstone , Colorado. Journal of Structural Geology, 31(7), 707–718. https://doi.org/10.1016/j.jsg.2009.04.001

Hooker, J. N., Larson, T. E., Eakin, A., Laubach, S. E., Eichhubl, P., Fall, A., & Marrett, R. (2015). Fracturing and fluid flow in a sub-décollement sandstone; or, a leak in the basement. Journal of the Geological Society, 172(4), 428–442. https://doi.org/10.1144/jgs2014-128

Hooker, J. N., Laubach, S. E., & Marrett, R. (2014). A universal power-law scaling exponent for fracture apertures in sandstones. Geological Society of America Bulletin, 126(9–10), 1340–1362. https://doi.org/10.1130/B30945.1

Huang, Q., & Angelier, J. (1989). Fracture spacing and its relation to bed thickness. Geological Magazine, 126(4), 355–362. https://doi.org/10.1017/S0016756800006555

Hussain, M., Babalola, L. O., & Hariri, M. M. (2004). Heavy minerals in the Wajid Sandstone from Abha-Khamis Mushayt area, southwestern Saudi Arabia: Implications on provenance and regional tectonic setting. GeoArabia, 9(4), 77–102.

Husseini, M. I. (1988). The Arabian infracambrian extensional system. Tectonophysics, 148(1–2), 93–103.

Husseini, M. I. (2000). The Arabian lnfracambrian extensional system. Tectonophysics,

148(1988), 93–103.

Jackson, R. O., Bogue, R. G., Brown, G. F., & Gierhart, R. D. (1963). Geologic map of the southern Najd quadrangle, Kingdom of Saudi Arabia.

Ji, S., & Saruwatari, K. (1998). A revised model for the relationship between joint spacing and layer thickness. Journal of Structural Geology, 20(11), 1495–1508.

Jizba, D. (1991). Mechanical and Acoustical Properties of Sandstones and Shales. PhD Thesis, Stanford University.

Johnson, P. R. (1998). Tectonic map of Saudi Arabia and adjacent areas, scale 1: 4000 000 (Vol. 3).

Johnson, P. R. (2003). Post-amalgamation basins of the NE Arabian shield and implications for Neoproterozoic III tectonism in the northern East African Orogen. Precambrian Research, 123(2–4), 321–337. https://doi.org/10.1016/S0301-9268(03)00074-3

Johnson, P. R., & Stewart, I. C. F. (1995). Magnetically inferred basement structure in central Saudi Arabia. Tectonophysics, 245(1–2), 37–52. https://doi.org/10.1016/0040-1951(94)00179-D

Keller, M., Hinderer, M., Al-Ajmi, H., & Rausch, R. (2011). Palaeozoic glacial depositional environments of SW Saudi Arabia: process and product. Geological Society, London, Special Publications, 354(1), 129–152.

Kellogg, K. S., Fourniguet, J., Janjou, J., & Minoux, L. (1986). Geologic map of the Wadi Tathlith quadrangle. Sheet-20G, Saudi Arabian Deputy Ministry for Mineral Resources, Map GM-103 A, Scale (1:250000).

Knox, R. W., Franks, S. G., & Cocker, J. D. (2007). Stratigraphic evolution of heavy-mineral provenance signatures in the sandstones of the Wajid group (Cambrian to Permian), southwestern Saudi Arabia. GeoArabia, 12(4), 65–96.

Koike, K., Nagano, S., & Kawaba, K. (1998). Construction and analysis of interpreted

fracture planes through combination of satellite-image derived lineaments and digital elevation model data. Computers & Geosciences, 24(6), 573–583.

Konert, G., Afifi, A. M., Al-Hajri, S. A., & Droste, H. J. (2001). Paleozoic stratigraphy and hydrocarbon habitat of the Arabian plate. GeoArabia, 6(3), 407–442.

Laboun, A. A. (2010). Paleozoic tectono-stratigraphic framework of the Arabian Peninsula. Journal of King Saud University - Science, 22(1), 41–50. https://doi.org/10.1016/j.jksus.2009.12.007

Ladeira, F. L., & Price, N. J. (1981). Relationship between fracture spacing and bed thickness. Journal of Structural Geology, 3(2), 179–183.

Lange, S. (2006). Structural Evolution of the Wajid Area, Western Rub Al-Khali Basin, Saudi Arabia. GEO 2006 Conference Abstracts, GeoArabia, 12(2), 190.

Laubach, S. E., Olson, J. E., & Cross, M. R. (2009). Mechanical and fracture stratigraphy. AAPG Bulletin, 93(11), 1413–1426. https://doi.org/10.1306/07270909094

Laubach, S. E., & Ward, M. E. (2006). Diagenesis in porosity evolution of opening-mode fractures, Middle Triassic to Lower Jurassic La Boca formation, NE Mexico. Tectonophysics, 419(1), 75–97.

Lyu, W., Zeng, L., Liu, Z., Liu, G., & Zu, K. (2016). Fracture responses of conventional logs in tight-oil sandstones: A case study of the Upper Triassic Yanchang Formation in southwest Ordos Basin, China. AAPG Bulletin, 100(9), 1399–1417. https://doi.org/10.1306/04041615129

Mahgoub, I. (2007). Geological and Statistical Reservoir Characteristics of the Late Carboniferous-Permian Juwayl Member (Wajid Sandstone), Southwestern Saudi Arabia. King Fahd University of Petroleum and Minerals.

Mandal, N., Deb, S. K., & Khan, D. (1994). Evidence for a nonlinear relationship between fracture spacing and layer thickness. Journal of Structural Geology, 16(9), 1275–1281.

Mandl, G. (2005). Rock joints. Berlin: Springer.

McClure, H. A. (1980). Permian-Carboniferous glaciation in the Arabian peninsula. Geological Society of America Bulletin, 91(12), 707–712.

McClure, H. A., Hussey, E., & Kaill, I. (1988). Permian-Carboniferous glacial deposits in southern Saudi Arabia. Geologisches Jahrbuch, 3–31.

McGillivray, J. G., & Husseini, M. I. (1992). The Paleozoic Petroleum Geology of Central Arabia. AAPG Bulletin, 76(10), 1473–1490.

McQuillan, H. (1973). Small-Scale Fracture Density in Asmari Formation of Southwest Iran and its Relation to Bed Thickness and Structural Setting. AAPG Bulletin, 57, 2367–2385.

Mogren, S., Al-Amri, A. M., Al-Damegh, K., Fairhead, D., Jassim, S., & Algamdi, A. (2008). Sub-surface geometry of Ar Rika and Ruwah faults from gravity and magnetic surveys. Arabian Journal of Geosciences, 1(1), 33–47.

Moore, J. M., & Al-Shanti, A. M. (1979). Structure and mineralization in the Najd fault system, Saudi Arabia. In: S.Talhoun (Editor), Evolution and Mineralization of the Arabian-Nubian shield, 2. Pergamon, New York, N.Y., 17-28. (Vol. 2).

Moshrif, M. A., & El-Hiti, A. (1989). Lithofacies and petrography of Wajid sandstone (Cambrian-Ordovician) Saudi Arabia. Journal of African Earth Sciences, 9(3–4), 401–412. https://doi.org/10.1016/0899-5362(89)90024-9

Narr, W. (1996). Estimating average fracture spacing in subsurface rock. AAPG Bulletin, 80(10), 1565–1586.

Narr, W., & Suppe, J. (1991). Joint spacing in sedimentary rocks. Journal of Structural Geology, 13(9), 1037–1048. https://doi.org/10.1016/0191-8141(91)90055-N

Nehlig, P., Genna, A., & Asfirane, F. (2002). A review of the Pan-African evolution of the Arabian shield. GeoArabia, 7(1), 103–124.

Nelson, R. . (2001). Geologic Analysis of Naturally Fractured Reservoirs (second).

Houston: Gulf Professional Publishing. https://doi.org/10.1016/B978-088415317-7/50005-1

O'leary, D. W., Friedman, J. D., & Pohn, H. A. (1976). Lineament, linear, lineation: some proposed new standards for old terms. Geological Society of America Bulletin, 87(10), 1463–1469.

Odling, N. E. (1997). Scaling and connectivity of joint systems in sandstones from western Norway. Journal of Structural Geology, 19(10), 1257–1271.

Odling, N. E., Gillespie, P., Bourgine, B., Castaing, C., Chiles, J. P., Christensen, N. P., … Watterson, J. (1999). Variations in fracture system geometry and their implications for fluid flow in fractures hydrocarbon reservoirs. Petroleum Geoscience, 5(4), 373–384. https://doi.org/10.1144/petgeo.5.4.373

Olson, J. E., Laubach, S. E., & Lander, R. H. (2009). Natural fracture characterization in tight gas sandstones: Integrating mechanics and diagenesis. AAPG Bulletin, 93(11), 1535–1549. https://doi.org/10.1306/08110909100

Ortega, O. J., Marrett, R. A., & Laubach, S. E. (2006). A scale-independent approach to fracture intensity and average spacing measurement. AAPG Bulletin, 90(2), 193–208. https://doi.org/10.1306/08250505059

Pallister, J. S. (1982). Reconnaissance geology of Jabal Al-Ilman quadrangle, sheet 18/44A. Saudi Arabian Deputy Ministry for Mineral Resources, Open File Report USGS-OF-02-90.

Pascal, C., Angelier, J., Cacas, M., & Hancock, P. L. (1997). Distribution of joints: Probabilistic modeling and case study near Cardiff (Wales, U.K.). Journal of Structural Geology, 19, 1273– 1284.

Peacock, D. C. P. (2001). The temporal relationship between joints and faults. Journal of Structural Geology, 23(2), 329–341.

Pollastro, R. M. (2003). Total Petroleum Systems of the Paleozoic and Jurassic, Greater Ghawar Uplift and Adjoining Provinces of Central Saudi Arabia and Northern

Arabian-Persian Gulf. U.S. Geological Survey Bulletin, 2202–H, 52.

Powers, R. W., Ramirez, L. F., Redmond, C. D., & Elberg, E. L. J. (1966). Geology of the Arabian Peninsula Sedimentary Geology of Saudi Arabia. U.S. Geological Survey Professional Paper, 560–D, 154.

Price, N. J. (1960). The compressive strength of coal measures rocks. Colliery Engineering, 37, 283–292.

Price, N. J. (1966). Fault and Joint Development in Brittle and Semi- Brittle Rocks. Pergamon Press, Oxford.

Quick, J. E. (1991). Late Proterozoic transpression on the Nabitah fault system—implications for the assembly of the Arabian Shield. Precambrian Research, 53(1), 119–147. https://doi.org/http://dx.doi.org/10.1016/0301-9268(91)90008-X

Rickman, R. (2008). A practical use of shale petrophysics for stimulation design optimization: All shale plays are not clones of the Barnett shale, SPE Annual Technical Conference and Exhibition, 21-24 September 2008, Denver, Colorado, USA, SPE 115258.

Ross, A. L., & Frohlich, R. K. (1993). Fracture trace analysis with a geographic information system "GIS." Bulletin of the Association of Engineering Geologists, 30(1), 87–98.

Roy, D. W., Schmitt, L., Woussen, G., & DuBerger, R. (1993). Lineaments from airborne SAR images and the 1988 Saguenay earthquake, Quebec, Canada. Photogrammetric Engineering and Remote Sensing;(United States), 59(8).

Sabin, F. (1997). Remote Sensing: Principles and Interpretation. Waveland Press.

Shakoor, A., & Bonelli, R. (1991). Relationship between petrographic characteristics, engineering index properties, and mechanical properties of selected sandstones. Bulletin of the International Association of Engineering Geology, 28(1), 55–71.

Sharland, P. R., Archer, R., Casey, D. M., Davies, R. B., Hall, S. H., Heward, A. P., …

Simmons, M. D. (2001). Arabian Plate Sequence Stratigraphy: GeoArabia, Special Publication 2, 371. Retrieved from http://www.gulfpetrolink.com/geoarabia/index.php/ga/article/view/14

Siddiqi, S. A. T. A. (2007). Depositional Environments and Facies Reservoir Properties of the khusayyayan Member, Wajid Sandstone, Saudi Arabia. MSc Thesis. King Fahd University of Petroleum and Minerals.

Sonntag, R., Evans, J. P., La Pointe, P., Deraps, M., Sisley, H., & Richey, D. (2012). Sedimentological controls on the fracture distribution and network development in Mesaverde Group sandstone lithofacies, Uinta Basin, Utah, USA. Geological Society, London, Special Publications, 374(1), 23–50. https://doi.org/10.1144/SP374.4

Stewart, S. . (2016). Structural geology of the Rub' Al-Khali Basin, Saudi Arabia. Tectonics, 35, 2417–2438.

Stoeser, D., & Camp, V. (1985). Pan Afraican microplate accretion of the Arabian Shield. Geological Society of America Bulletin, 96(7), 817–826.

Strijker, G., Bertotti, G., & Luthi, S. M. (2012). Multi-scale fracture network analysis from an outcrop analogue: A case study from the Cambro-Ordovician clastic succession in Petra, Jordan. Marine and Petroleum Geology, 38(1), 104–116. https://doi.org/10.1016/j.marpetgeo.2012.07.003

Stump, T. E., & Van der Eem, J. G. (1995). The stratigraphy, depositional environments and periods of deformation of the Wajid outcrop belt, southwestern Saudi Arabia. Journal of African Earth Sciences, 21(3), 421–441. https://doi.org/10.1016/0899-5362(95)00099-F

Ulusay, R., Tureli, K., & Ider, M. (1994). Prediction of engineering properties of a selected litharenite sandstone from its petrographic characteristics using correlation and multivariate statistical techniques. Engineering Geology, 38(1–2), 135–157.

Vaslet, D. (1990). Upper Ordovician Glacial Deposits in Saudi-Arabia. Episodes, 13(3),

147–161.

Vernik, L., Bruno, M., & Bovberg, C. (1993). Empirical relations between compressive strength and porosity of siliciclastic rocks. International Journal of Rock Mechanics and Mining Sciences, 30(7), 677–680.

Vutukuri, V., Lama, R., & Saluja, S. (1974). Handbook on Mechanical Properties of Rocks. Trans Tech Publications Clausthal, Germany.

Wanas, H. A., & Abdel-Maguid, N. M. (2006). Petrography and geochemistry of the Cambro-Ordovician Wajid Sandstone, southwest Saudi Arabia: Implications for provenance and tectonic setting. Journal of Asian Earth Sciences, 27(4), 416–429. https://doi.org/10.1016/j.jseaes.2005.05.002

Whitehouse, M. J., Windley, B. F., Stoeser, D. B., Al-Khirbash, S., Ba-Bttat, M. A. O., & Haider, A. (2001). Precambrian basement character of Yemen and correlations with Saudi Arabia and Somalia. Precambrian Research, 105(2–4), 357–369. https://doi.org/http://dx.doi.org/10.1016/S0301-9268(00)00120-0

Windley, B. F., Whitehouse, M. J., & Ba-Bttat, M. A. (1996). Early Precambrian gneiss terranes and Pan-African island arcs in Yemen: crustal accretion of the eastern Arabian Shield. Geology, 24(2), 131–134.

Wu, H., & Pollard, D. (1995). An experimental study of the relationship between joint spacing and layer thickness. Journal of Structural Geology, 17(6), 887–905.

Yassin, M. A., & Abdullatif, O. M. (2017). Chemostratigraphic and sedimentologic evolution of Wajid Group (Wajid Sandstone): An outcrop analog study from the Cambrian to Permian, {SW} Saudi Arabia. Journal of African Earth Sciences, 126, 159–175. https://doi.org/http://dx.doi.org/10.1016/j.jafrearsci.2016.11.029

Zahm, C. K., & Hennings, P. H. (2009). Complex fracture development related to stratigraphic architecture: Challenges for structural deformation prediction, Tensleep Sandstone at the Alcova anticline, Wyoming. AAPG Bulletin, 93(11), 1427–1446. https://doi.org/10.1306/08040909110

Zeeb, C., Göckus, D., Bons, P., Al Ajmi, H., Rausch, R., & Blum, P. (2010). Fracture flow modeling based on satellite images of the Wajid Sandstone, Saudi Arabia. Hydrogeology Journal, 18(7), 1699–1712.

Zorlu, K., Ulusay, R., Ocakoglu, F., Gokceoglu, C., & Sonmez, H. (2004). Predicting intact rock properties of selected sandstones using petrographic thin-section data. International Journal of Rock Mechanics and Mining Sciences, 41(1), 93–98.

Vitae

Name	: Mohammed Hasan Barran Benaafi.
Nationality	: Yemeni.
Date of Birth	: 20/03/1978.
Email	: Benaafi1978@gmail.com
Address	: KFUPM, Al- Dhahran, Saudi Arabia
	: Hadramout, Yemen.

Academic Background

Education 1	
Qualification 1:	Bachelor
Specialization :	Oil management
Institute :	Oil and Minerals Collage, Aden University
Year:	2001
Education 2	
Qualification 1:	Master Degree
Specialization :	Petroleum Geology
Institute :	College of Science, King Saud university, Riyadh, Saudi Arabia
Year:	2011.
Education 3	
Qualification 1:	Ph.D
Specialization :	Geology
Institute :	Geosciences Department, College of Petroleum Engineering and Geosciences, King Fahd University of Petroleum and Minerals
Year:	**30/05/ 2017.**

Work Experience

- **Ph.D. student (Lecturer-B),** King Fahd University of Petroleum & Minerals, from 2012 –present.
- **Assistant researcher,** King Saud University, October

2007-2012.

- **Administrator,** Hawk company, November 2005 – August 2007
- **Assistant Researcher,** Aden University, August 2002 - September 2005.

Participation

- Participating in the 9th Meeting of the Saudi Society for Geosciences. Riyadh. **2011**.

- Participating in the 10th Middle East geosciences conference and exhibition **(GEO 2012)** and the student short courses organized by AAPG, in Bahrain on **March 4-8, 2012**.

- Participating in the 10th Meeting of the Saudi Society for Geosciences. Dhahran.**2013**.

- Participating in the SPE Kingdom of Saudi Arabia Annual Technical Symposium and Exhibition. Society of Petroleum Engineers. **Dhahran. 2016.**

- Participating in the EAGE/SPE Workshop on Integrated Geomechanics in Exploration and Production. **Abu-Dhabi, UAE, 2016.**

- Participating in the 12th Middle East Geosciences Conference & Exhibition (GEO 2016), Manama, Bahrain, **March 7-10, 2016.**

- Participating in **summer field geology trip** (35 days) in Midyan Basin, Northwestern of Saudi Arabia, 2009. King Saud University.

- Participating in **summer field geology trip** (35 days) in Abha and Khamis Musheet area, Saudi Arabia, 2010,2011,2012. King Saud University.

- Participating in **summer field geology trip** (35 days) in Abha and Khamis Musheet area, Saudi Arabia, 2016. King Fahd University of Petroleum & Minerals.

- Participating in **teaching geology courses** 2012- 2017. King Fahd University of Petroleum & Minerals.

Extra Experience

- Describing the rock samples in **thin sections** using petrographic microscopy.
- Conducting the **X-Ray diffraction analysis** to identify the mineral composition of rock samples.
- Conducting the petrophysics analyses included Autopore IV, Helium porosimeter, and Mini-permeameter.
- Conducting the **SEM-EDX analysis** of rock samples and interpret the dataset.
- Conducting the **geochemical analysis (XRF)** of rock samples.
- Working with **the geochemical data(ICP-MS) (included major oxides, trace, and rare earth elements)** of rock samples.
- Conducting the **geomechanical analysis (unconfined compression test (UCS))** of rock samples.
- Conducting the **heavy minerals analysis**, and describe the heavy minerals using petrographic microscopy.
- Working with Halliburton company in Al-Dhahran technovalley on the **characterization of Saudi Arabia sand** from November 2015 to November 2016.

Publications

1. Al-Laboun, A., Al-Quraishi, A., Zaman, H., & **Benaafi**, M. (**2014**). Reservoir characterization of the Burqan Formation sandstone from Midyan Basin, northwestern Saudi Arabia. Turkish Journal of Earth Sciences, 23(2), 204-214.

2. **Benaafi**, M., & Abdullatif, O. (**2015**). Sedimentological, mineralogical, and geochemical characterization of sand dunes in Saudi Arabia. Arabian Journal of Geosciences, 8(12), 11073-11092.

3. **Benaafi**, M., Hariri, M., Abdullatif, O., Makkawi, M., & Al-Shaibani, A. (**2017**). Analysis of lineaments within the Wajid Group, SW Saudi Arabia, and their tectonic significance. Arabian Journal of Geosciences, 10(5), 106.

4. **Benaafi**, M., Hariri, M., Bertotti, G., Al-Shaibani, A., Makkawi, M. and Abdullatif, O. (**2017**). Characterization of Natural Fractures System within the Combro-Permian Wajid Group, SW Saudi Arabia. Marine and Petroleum Geology. (**Under Review**)

5. **Benaafi** M., Hariri, M. (**2017**). Integrated Geomechanical, Petrographical and Petrophysical study of Wajid Group sandstone, SW Saudi Arabia. Journal of African Earth Sciences. (**Under Review**).

6. **Benaafi**, M., Hariri, M. (**2015**). Nature and geometric properties of the natural fracture system within the Wajid sandstone group, SW Saudi Arabia. 11th International Conference for Geosciences, At Riyadh, KSA.

7. **Benaafi**, M., Hariri, M. (**2015**). Fractures System Within Brum Granitic Rocks, an Extend of Subsurface Fractured Basement Reservoir, Sabatyan Basin, Yemen. GEO India 2015, New Delhi, India.

8. **Benaafi**, M., Hariri, M., Abdullatif, O., Al-Shaibani, A., & Makkawi, M. (**2016**, October). Integrative Study of Sedimentological and Geomechanical Properties of Wajid Group Sandstone, SW Saudi Arabia. In EAGE/SPE Workshop on Integrated Geomechanics in Exploration and Production.

9. **Benaafi**, M., Abdullatif, O., Razzaq, W. A., & Zoghbi, B. (**2016**, April). Geological Characterization of Saudi Arabia Sand for Oilfield Applications. In SPE Kingdom of Saudi Arabia Annual Technical Symposium and Exhibition. Society of Petroleum Engineers.

10. **Benaafi**, M., Hariri, M., Abdullatif, O., Makkawi, M., & Korvin, G. (**2016**, April). Sedimentological and

Stratigraphic Controls on Natural Fracture Distribution in Wajid Group, SW Saudi Arabia. In EGU General Assembly Conference Abstracts (Vol. 18, p. 7262).

11. **Benaafi**, M., Hariri, M., Abdullatif, O., Makkawi, M and Korvin, G.(**2016**). Characterization of natural fractures network within Khusayyayn formation, SW Saudi Arabia: An implication for groundwater and hydrocarbon potentiality. 2nd International Conference on Geology.

12. **Benaafi**, M., & Alfaif, H. (**2016**). Heavy Minerals Stratigraphy (HMS) of the Sand-rich Member of the Burqan Formation, Midyan Basin, N.W. Saudi Arabia. 12th Middle East Geosciences Conference and Exhibition - GEO 2016.

13. **Benaafi**, M., Hariri, M. (**Accepted**)(**2017**). Compatibility Between the Fracture Trends of Subsurface Sarah Formation, Rub' Al-Khali Basin with The Fracture Trends Associated with Sanamah Formation Outcrop, SW Saudi Arabia. AAPG Siliciclastic Reservoirs of the Middle East Workshop, Amman, Jordan.